MAGNETOHYDRODYNAMIC INSTABILITIES IN LIQUID MERCURY

by

DAVID S. WILEY

SUBMITTED IN PARTIAL FULFILLMENT
OF THE REQUIREMENTS FOR THE
DEGREE OF MASTER OF SCIENCE IN PHYSICS
AND FOR THE
DEGREE OF BACHELOR OF SCIENCE
AT THE
MASSACHUSETTS INSTITUTE OF TECHNOLOGY

June, 1961

Signature of Author _____
Department of Physics, May 22, 1961

Certified by _____
Thesis Supervisor

Accepted by _____
Chairman, Departmental Committee on Theses

Magnetohydrodynamic Instabilities in Liquid Mercury

by

David S. Wiley

Submitted to the Department of Physics on May 22, 1961 in partial fulfillment of the requirements for the degree of Master of Science in Physics and for the degree of Bachelor of Science.

ABSTRACT

The purpose of the experiment is to investigate the instability of a stream of mercury with circular cross section and with current passing through it which falls freely in an external magnetic field in the direction of current and fall. Currents used were between 0-450 amps; magnetic field, 0-3000 gauss; stream radius, 1.5-3 mm; and initial speed of the stream, 40-120 cm/sec.

We photographed at 250 frames/sec the development in time of at least four types of instabilities: the "sausage" pinch, the side or "kink" pinch, the spiral instability, and a new branching instability in which the stream splits, both halves then being unstable. Qualitative and quantitative data are exhibited on which generalizations are made about the dependence of the instabilities on current, magnetic field, and stream radius. In general the instabilities are nonlinearly more violent for higher currents and fields, and thinner streams.

A theory is developed which attempts to explain qualitatively and somewhat quantitatively the phenomena observed. Suggestions are made for further and more detailed work.

Thesis Supervisor: Uno Ingard
Title: Associate Professor of Physics

Table of Contents

Introduction

We wish to investigate both theoretically and experimentally two types of instabilities which result from the motion of a fluid, conducting medium (through which current passes) in an external magnetic field. The instabilities arise from (1) the self-fields of the current distribution and (2) the external field interacting with the current distribution. As described in a recent paper by Lehnert,[1] interaction (1) gives rise to the so-called "pinch effect." In general, the "pinch" arises when the forces resulting from the self-fields of a medium support a perturbation of its mass distribution rather than to restore the medium to some initial equilibrium distribution. The "pinch" was first observed, recorded, and named by Carl Hering at the turn of the century in relation to the heating of molten metals by electric conduction.[2] He found that a crucible of molten metal through which current was flowing tended to "pinch" in half (similarly to the manner in which one might imagine the parting of the waters of the Red Sea in Biblical references). E. E. Northrup analyzed the phenomenon several years later.[3]

The pinch is an often observed phenomenon and has become important in recent years because of the physical limitations the "pinch" places on certain experiments in plasma dynamics[4]

and in solid state in relation to the exploding wire phenomenon.[5] Alfven's theory of the origin of the solar system depends on an understanding of the "pinch."[6]

The "spiral instability" arises when the direction of the current flow is exactly in the direction of an external magnetic field and then the direction is perturbed slightly. Rather than restoring its motion parallel to the external field, the $\vec{J} \times \vec{B}$ body force causes the fluid conductor to assume some type of helical motion about the direction of the external magnetic field.

In particular, in this paper cylindrically symmetric fluid conductors (where the axis of symmetry is along the direction of flow) will be considered. Possibly the fundamental results of our theory may give us insight into the general case of unidirectional conducting fluid flows. Even by having such symmetry, the general magnetohydrodynamic equations are impossible to solve, but we will be able to obtain reasonable first and second order approximations by reducing the problem to a very simplified model -- that of liquid mercury (with current passing through it in the direction of flow) exiting from a circular orifice and falling freely in a uniform magnetic field B_o along the direction of flow. Mercury is ideal for such an experiment because as a liquid conductor it (1) exhibits the fluid properties of a plasma, but (2) has a well-defined boundary and is incompressible, which facilitate the solution of the general problem.

From Lehnert's discussion we may predict that due to any inhomogeneities in the mercury, beads (like "sausages") will form along (and move with) the mercury flow. The inhomogeneities may be (1) temperature gradients in the mercury (local density changes), (2) impurities (local current and magnetic properties change), and a non-perfect orifice through which the mercury exits (slight imperfections in the boundary of the mercury) -- plus externally induced perturbations of the same general types above. From Lehnert's work we also may predict that if we place the stream of mercury (with current) such that the direction of flow (and current) is along a uniform magnetic field $\vec{B}_o$ and perturb the direction a few degrees, then the mercury will spiral around B_o in a helical path of radius on the order of the dimensions of the apparatus rather than remaining a small deflection. Clearly, the mercury would spiral if $\vec{B}_o$ were perpendicular to the flow.

Because magnetohydrodynamic instabilities have been relatively unsystematically explored, the purpose of the present work is to do initial groundwork -- which hopefully will lead to further systematic experiment. Therefore, we have not attempted to obtain precise quantitative results by inducing precisely known perturbations and measuring the effects. Indeed, our perturbations result by not having a carefully ground outlet nozzle for the mercury stream and by having the mercury stream disaligned from $\vec{B}_o$ by a small

amount; we show, though, that the initial perturbations are smaller than the eye can detect.

Our work consisted of designing and setting up equipment, developing suitable photographic techniques of observation, and predicting theoretically the nature of the instabilities. From our results we made suggestions for new and improved experiments to systematize our understanding of the pinch and spiral instabilities.

We observed, recorded, and were able to reproduce the pinch and spiral instabilities. In fact, we found a new type of instability in which the mercury stream splits into two halves, both parts then spiraling around each other (the bifurcation instability). From the results of our data, we were able to make generalizations on the dependence of the instabilities on the current through the stream I_o, the external magnetic field B_o, the radius of the stream R_o, and the exit speed from the nozzle v_o.

For increasing fields (B_o), we have a quicker, more violent field-current interaction which results in more loops in the spiral and larger spirals. We found that the violent reaction cuts off the current; for higher fields, the current actually flows less than 10% of the time. The current cut-off phenomenon results in a periodic variation of the spiral instability. For very high fields and currents we obtained the new bifurcation instability which we mentioned before.

For increasing currents through the mercury (I_o), we found that the pinches pinch faster and there are more of them along the stream, and that the spirals grow faster and contain more loops.

For slower stream speeds (v_o), we have more pinches and more violent pinches. By varying v_o we are able to compute an approximate time for the mercury stream to pinch in two.

For smaller stream radii (R_o), the spiral instabilities are larger and contain more loops.

The report contains charts of quantitative data from which the above generalizations were taken.

A theory was developed which to first order qualitatively predicts the phenomena which were observed.

Theory

As stated in the introduction, our problem is to describe the motion of a circular stream of Hg with current through it, falling freely in a region which has a constant magnetic field $\vec{B}_o$ along the direction of flow and current. We wish to derive the theoretical result that such a stream is unstable with respect both to its diameter (the pinch effect) and with respect to its direction along $\vec{B}_o$ (the spiral instability).

We may ask for the motion of each volume element of the Hg as a function of $\vec{x}$ and t or we may look for a macro-description, asking only for the functional dependence of the boundary surface of the Hg, not caring what goes on within the volume. The former approach implies a complete solution of the MHD equations. The latter, the approach we shall take, lends itself more readily to approximate and heuristic arguments.

The Pinch (No External Magnetic Field)

I. To first order we shall neglect viscosity and heat conduction (joule heating in the Hg). The forces on the Hg stream are due to (1) magnetic forces -- the interaction of the self-field with its current distribution, (2) surface tension, (3) gravity, and (4) air pressure (which we assume to be uniform).

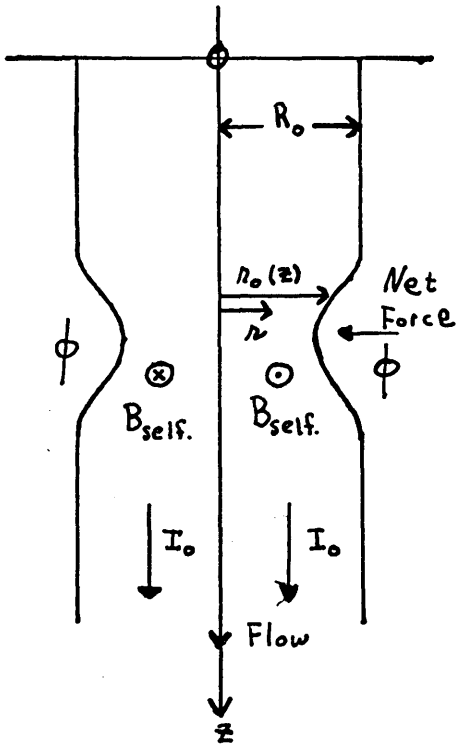

Fig. a

(1) Magnetic forces

Consider the symmetrical stream of Hg in Fig. a (Hg flowing downward with a perturbation ϕ on the surface moving with the stream).

$$\vec{B}_{self}(r,z) = \frac{2\mu I_o r}{r_o^2(z)} \vec{e}_\vartheta$$

from Ampere's Circuital Law. (We shall use c.g.s. electromagnetic units.) Therefore, the net volume force $\vec{f} = -\frac{I_o^2}{\pi r_o^4} 2\mu r \vec{e}_r$.

We note that $\vec{f}$ acts inwardly on the stream. We can consider the average pressure on the surface of the stream given by

$$\int_o^{r_o} f dr \equiv P_{I_o}(r_o(z)) = \frac{I_o^2 \mu}{\pi r_o^2} .$$

If the average radius of the stream is R_o and $r_o(z) < R_o$ then $P_{I_o}(R_o) < P_{I_o}(r_o)$. Therefore, heuristically the inward perturbation ϕ tends to grow and eventually will pinch off.

In the above arguments, we made two assumptions; (a) the current density has only a z-component, and (b) the circuital law holds in the region of the perturbation.

(a) It is clear that the current at the surface of the Hg is approximately parallel to the tangent of the surface and that the current at r = 0 is along the z-axis. We can guess

$$\vec{j} = \frac{I_o}{\pi r_o^2} \left[\frac{(\frac{\partial r_o}{\partial z}) f(r) \vec{e}_r + \vec{k}}{\left(1 + f^2 (\frac{\partial r_o}{\partial z})^2\right)^{1/2}} \right].$$

Setting $\vec{\nabla} \cdot \vec{j} = 0$, solving for $f(r)$ such that $f(0) = 0$, and dropping terms of order $f^2(\partial r_o/\partial z)^2 << 1$, we have $f(r) = (\frac{r}{r_o})$.

$$\vec{j} = \frac{I_o}{\pi r_o^2} \left[\left(\frac{\partial r_o}{\partial z}\right) \frac{r}{r_o} \vec{e}_r + \vec{k} \right].$$

We shall use this value of $\vec{j}(r,z)$ for future calculations.

(b) How valid is the circuital law in our calculations?

If we set up the vector potential $\vec{A}(\vec{x}) = \int \frac{\vec{j}(\vec{x}')d^3x'}{|\vec{x}-\vec{x}'|}$, regardless of the functional form of $\vec{j}(\vec{x}')$, by symmetry $A_\theta = 0$ and A_r, A_z are functions only of r and z. $\therefore B_\theta$ is the only component. Therefore, the circuital law is exact (for our symmetry) with respect to direction, but is correct only to an additive quantity given by $\frac{\partial A_r}{\partial z}$. If we assume a perturbation of the form $r_o(z) = R_o + \alpha e^{-\beta z^2}$ $\quad \alpha << R_o$

$$A_r \cong 2 \frac{I_o}{\pi} \int_{-\infty}^{\infty} dz' \int_0^{R_o + \alpha e^{-\beta z'^2}} dr' \int_0^{2\pi} d\theta' \cdot \frac{r'}{r_o^3(z')} \frac{\partial r_o(z')}{\partial z'} \frac{1}{\left[(z-z')^2 + (r^2 - 2rr'\cos\theta' + r'^2)\right]^{1/2}}$$

$$B_1 \equiv \frac{\partial A_r}{\partial z} \simeq \frac{2I_o}{\pi} \frac{\alpha\beta e^{-\beta z^2}}{R_o^3} \int_{-\infty}^{\infty} e^{-\beta y^2} y^2 dy \left\{ \frac{1}{\left(y^2 + r^2 + R_o^2\right)^{1/2}} - \frac{1}{\left(y^2 + r^2\right)^{1/2}} \right\}.$$

We note that B_1 is proportional to α and is therefore small; also it goes as $e^{-\beta z^2}$. Because of its analytical complexity, and smallness, we shall neglect it (though in more exact calculations we must include it because if the stream pinches off $\alpha \simeq R_o$, and the term becomes important).

II. Using our value of $\vec{j}(r,z)$ and the discussion of the circuital law, we can now derive more precisely the force on the Hg surface.

$$\vec{P}_{I_o} = \int_o^{r_o} (\vec{j} \times \vec{B}_{self}) dr = - \vec{e}_r \frac{I_o^2 \mu}{\pi r_o^2} + \vec{k} \frac{I_o^2 \mu}{\pi r_o^2} \frac{4}{3} \left(\frac{\partial r_o}{\partial z} \right) .$$

Clearly, the magnetic forces must have a z-component, since in the region of the perturbation, we have current in the $\vec{e}_r$ direction. From the form of $\vec{P}_{I_o}$ it is clear that the z-component of $\vec{P}_{I_o}$ tends to stretch the pinch by a factor $1/r_o^2$ which $\longrightarrow \infty$ as $r_o \longrightarrow 0$. The average magnetic volume force is then given by

$$\vec{f} = - \frac{\vec{e}_r I_o^2 \mu}{\pi r_o^3} + \vec{k} \frac{4}{3} \frac{I_o^2 \mu}{\pi r_o^3} \left(\frac{\partial r_o}{\partial z} \right) \qquad (1)$$

Equation (1) could have been approximately obtained by taking the gradient of the P_{I_o} obtained in section I, part (1).

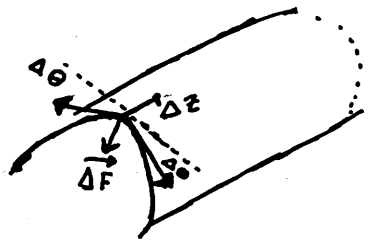

Fig. b

(2) Surface tension

Given a tube of Hg (see fig. b)

$$\vec{\Delta F} = Tdz\Big|_{\theta=\Delta\theta} - Tdz\Big|_{\theta=-\Delta\theta}$$

$$= 2Tdz\Delta\theta$$

$$\text{Pressure} = \frac{2Tdz}{2\Delta\theta r_o dz} = \frac{T}{r_o} \equiv P_T$$

and clearly acts inwardly.

The volume force due to surface tension $= -\vec{e}_r \frac{T}{r_o^2} + \vec{e}_z \frac{T}{r_o^2}\left(\frac{\partial r_o}{\partial z}\right)$. (2)

III. In order to discuss instabilities due to self-interactions of the current distribution, we must know the conditions under which the stream will not pinch with no current. We must also discuss a smooth stream flow (with no perturbations) in order to discover what type of steady state the perturbations are superimposed upon.

(a) If $I_o = 0$, $T = 0$ then $r_o^2\left(v_o^2 + 2gz\right)^{1/2} \cong R_o^2 v_o$, where R_o is the radius and v_o the velocity at $z = 0$. If $v_o = 120$ cm/sec, $z = 5$ cm, $R_o = .25$ cm, then $r_o = .215$ cm, i.e., $\approx 14\%$ contraction -- i.e., no pinch.

(b) If $I_o \neq 0$, $T \neq 0$ then conservation of momentum requires:

$$\rho\left\{\frac{\partial(\pi r_o^2 v)}{\partial t} + \overset{\times}{\textcircled{v}}\frac{\partial(\pi r_o^2 v^2)}{\partial z}\right\} = \rho g \pi r_o^2 + \pi r_o^2\left\{\frac{a}{r_o^3} + \frac{b}{r_o^2}\right\}\left(\frac{\partial r_o}{\partial z}\right)$$

$$a \equiv \frac{4}{3}\frac{I_o^2\mu}{\pi} \qquad b \equiv T$$

and conversation of mass:

$$\frac{\partial}{\partial z}(\pi r_o^2 v) = -\frac{\partial}{\partial t}(\pi r_o^2)$$

where v is the velocity of the stream in the z-direction, $r_o = r_o(z,t)$.

We obtain:

$$\text{(i)} \qquad \frac{\partial v}{\partial t} = g + \frac{1}{\rho}\left\{\frac{a}{r_o^3} + \frac{b}{r_o^2}\right\}\left(\frac{\partial r_o}{\partial z}\right)$$

$$\text{(ii)} \qquad v\frac{\partial r_o}{\partial z} + \frac{r_o}{2}\frac{\partial v}{\partial z} + \frac{\partial r_o}{\partial t} = 0$$

We shall linearize the equations by assuming $r_o = R_o + r$ where $r \ll R_o$.

We obtain:

$$\frac{\partial v}{\partial t} = g + A\frac{\partial r}{\partial z} - Br\frac{\partial r}{\partial z} \qquad (3)$$

$$A \equiv \frac{1}{\rho}\left\{\frac{a}{R_o^3} + \frac{b}{R_o^2}\right\}$$

$$v\frac{\partial r}{\partial z} + R_o\frac{\partial v}{\partial z} + \frac{\partial r}{\partial t} = 0 \qquad (4)$$

$$B \equiv \frac{1}{\rho}\left\{\frac{3a}{R_o^4} + \frac{2b}{R_o^3}\right\}$$

If we drop the nonlinear terms,

$$\frac{\partial v}{\partial t} = g + A\frac{\partial r}{\partial z}; \qquad R_o\frac{\partial v}{\partial z} = -\frac{\partial r}{\partial t}.$$

$$\gamma^2\frac{\partial^2 r}{\partial z^2} = -\frac{\partial^2 r}{\partial t^2} \qquad \gamma = (AR_o)^{1/2}$$

which gives a solution of the type:

$$f(\omega)e^{\omega(i\gamma t-z)} \quad \underline{\text{and}} \quad g(\omega)e^{\omega(-it\gamma-z)}$$

$$\therefore \quad r(z,t) \equiv \int_o^\infty f(\omega)e^{i\omega\gamma t}e^{-\omega z}d\omega + \int_o^\infty g(\omega)e^{-i\omega\gamma t}e^{-\omega z}d\omega$$

In order to solve for $r(z,t)$ we need a linear approximation to the initial stream size with no perturbations. We use the approximation that $\partial r/\partial t \approx 0$. In this case,

$$\rho \frac{\partial v}{\partial t} = \left\{\frac{a}{r_o^3} + \frac{b}{r_o^2}\right\}\left(\frac{\partial r_o}{\partial z}\right) + \rho g$$

$$r_o^2 v = R_o^2 v_o \qquad\qquad v = \dot{z}$$

$$\frac{\partial r_o}{\partial z} \cong \frac{-\rho g}{\left\{\frac{2\rho R_o^4 v_o^2}{r_o^5} + \frac{a}{r_o^3} + \frac{b}{r_o^2}\right\}}$$

Solving and linearizing, we find:

$$r = \frac{-R_o\rho g z}{\left\{2\rho v_o^2 + \frac{a}{R_o^2} + \frac{b}{R_o}\right\}} \equiv -R_o\nu z$$

We shall use as initial conditions

$$r(z,0) = \alpha e^{-\beta z^2} - R_o\nu z = \int_o^\infty (fe^{-\omega z} + ge^{-\omega z})dz$$

$$\frac{\partial r(z,t)}{\partial t}\bigg|_{t=o} = 0 = \int_o^\infty \omega(f - g)e^{-\omega z}d\omega$$

where $\alpha e^{-\beta z^2}$ is an induced perturbation. We see $f = g$.

Taking the Laplace transform of both sides, and solving for f, we see

$$r(z,t) = \mathrm{Re}\left\{\alpha e^{-\beta z_1^2} - R_o v z_1\right\}_{z_1=(z-it\gamma)}$$

$$r(z,t) = \alpha e^{-\beta\left(z^2-t^2\gamma^2\right)} \cos 2\beta z t\gamma - R_o v z \ . \qquad (5)$$

γ acts like the propagation velocity of the perturbation.

For $t\gamma > z$, the pulse begins to grow, which is exactly what we would expect. However, we would expect $\gamma \approx v_o$. This is <u>not</u> the case -- the reason being that we neglected the $v\frac{\partial r}{\partial z}$ term in equation (4). Thus, we expect that r(z,t) is incorrect for our particular problem. We submit it because it is approximately the solution for an incompressible plasma whose $v_o \approx 0$ (thus justifying our neglecting of the $v\frac{\partial r}{\partial z}$ term). We predict that the pinches are unstable in the plasma and move with velocity γ. The fact that plasmas are compressible may invalidate the value of the propagation velocity. We also must keep in mind that equation (5) is strictly valid only for $r << R_o$. For the case of Hg moving with v_o initially, the above solution may be correct if we make the physically intuitive assumption that the correct γ_1 is given approximately by $\gamma_1^2 = \gamma^2 + v_o^2$ -- a guess which may correct for our neglecting the $v\frac{\partial r}{\partial z}$ term in equation (4). The cos $2\beta z t\gamma$ factor oscillates extremely fast (for a given z), which indicates that the perturbation (except for $z \approx 0$)

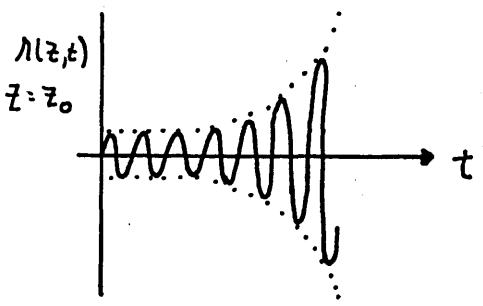

is very unstable. A more physical interpretation would lead us to conclude that the contour of the above packet represents the perturbation. Our solution is valid only in the limit as $z \to 0$.

The information obtained above neglecting the $v\frac{\partial r}{\partial z}$ term will now yield the general solutions of our linearized perturbations on the stream of Hg. Letting $v = v_o + v_1$, equations (3) and (4) become $v_1 << v_o$

$$\frac{\partial v_1}{\partial t} = g + A\frac{\partial r}{\partial z} \tag{6}$$

and

$$(v_o + v_1)\frac{\partial r}{\partial z} + R_o\frac{\partial v_1}{\partial z} + \frac{\partial r}{\partial t} = 0, \tag{7}$$

which give:

$$v_o\frac{\partial^2 v_1}{\partial t\partial z} - g\frac{\partial v_1}{\partial z} + \gamma^2\frac{\partial^2 v_1}{\partial z^2} = -\frac{\partial^2 v_1}{\partial t^2}.$$

Let $v_1 = Ve^{i\omega t}e^{-kz}$,

which implies $\quad -v_o\omega ki + gk + \gamma^2k^2 = \omega^2$

$$k = \frac{-g}{2\gamma^2} + \frac{v_o i\omega}{2\gamma^2} \pm \left(\frac{\omega^2}{\gamma^2} + \frac{g^2}{4\gamma^4} - \frac{v_o^2\omega^2}{4\gamma^4} - \frac{gv_o\omega i}{2\gamma^4}\right)^{1/2}$$

$$k \cong \frac{-g}{2\gamma^2} + \frac{v_o i\omega}{2\gamma^2} \pm \left(\frac{\omega}{\gamma}\sigma - \frac{gv_o}{2\gamma^3\sigma}i\right) \qquad f(\omega) = 0 \text{ as } \omega \to 0$$

$$\sigma \cong \left(1 - \frac{v_o^2}{4\gamma^2}\right)^{1/2}$$

$$\lambda_1 \equiv \frac{-g}{2\gamma^2} - \frac{gv_o}{2\gamma^3\sigma}i \equiv -M - Ni$$

$$\lambda_2 \equiv \frac{-g}{2\gamma^2} + \frac{gv_o}{2\gamma^3\sigma}i \equiv -M + Ni$$

$$\frac{1}{\tau_1} \equiv \frac{v_o i}{2\gamma^2} + \frac{\sigma}{\gamma}$$

$$\frac{1}{\tau_2} \equiv \frac{v_o i}{2\gamma^2} - \frac{\sigma}{\gamma}$$

$$k = -\lambda_1 + \frac{i\omega}{\tau_1} \quad \text{and} \quad \lambda_2 + \frac{i\omega}{\tau_2} .$$

$$r(z,t) \equiv \int_o^\infty (f(\omega)e^{i\omega t\tau_1}e^{-\omega z}e^{-\lambda_1 z}d\omega + g(\omega)e^{i\omega\tau_2}e^{-\omega z}e^{-\lambda_2 z}d\omega).$$

Using our linear approximation as before, and starting with a perturbation of form $\alpha e^{-\beta z^2}$ at $t = 0$

$$r(z,0) = -R_o\nu z + \alpha e^{-\beta z^2} \equiv F(z)$$

$$\frac{\partial r}{\partial t}\Big|_{t=0} = 2R_o v_o \nu^2 z - R_o \nu v_o - 2\nu v_o R_o \alpha + \nu^2 z^2 2\beta\alpha v_o e^{-\beta z^2} \equiv G(z)$$ by satisfying equation (4).

$$F(z) = -R_o\nu z + \alpha e^{-\beta z^2} = e^{-\lambda_1 z}\int_o^\infty f e^{-\omega z}d\omega + e^{-\lambda_2 z}\int_o^\infty g e^{-\omega t}d\omega$$

$$G(z) = i\tau_1 e^{-\lambda_1 z}\int_o^\infty \omega f e^{-\omega z}d\omega + i\tau_2 e^{-\lambda_2 z}\int_o^\infty \omega g e^{-\omega z}d\omega$$

By taking Laplace transforms, solving for f,g and solving for r(z,t), and using the same approximation we made earlier that $f(\omega) = 0$ as $\omega \to 0$, which enables us to linearize to obtain the Laplace integrals, we find

$$r(z,t) = \frac{1}{(\tau_2-\tau_1)} e^{Mz} e^{-Nt\tau_1}\left\{\tau_2 F(z')e^{-Mz'} + i\int_{z'}^{\infty} Ge^{-Mz}dz\right\}_{z'=z-it\tau_1}$$

$$- \frac{1}{(\tau_2-\tau_1)} e^{Mz} e^{+Nt\tau_2}\left\{\tau_1 F(z')e^{-Mz'} + i\int_{z'}^{\infty} Ge^{-Mz}dz\right\}_{z'=z-it\tau_2}$$

The terms involving G are impossible to integrate exactly; however, since they depend on $\frac{\partial r}{\partial t}\Big|_{t=0}$ they are small. The physically important part of our solution will come from the terms involving F. We shall denote this part of r(z,t) by r'(z,t), calling $\tau_1 \equiv P - iQ$ $\quad$ $\tau_2 \equiv -P - iQ$

$$r'(z,t) = \alpha e^{t(MQ-NP)} e^{-\beta\left[(z-tQ)^2 - t^2P^2\right]}\left(\cos Xt - \frac{Q}{P}\sin Xt\right)$$

$$X \equiv NQ + MP + 2\beta P(z - tQ)$$

where

$$P = \sigma\gamma \qquad\qquad Q = \frac{v_o}{2}$$

Noting $Q \approx v_o$, i.e., we now have the proper group velocity. Clearly, for $(z - tQ)^2 < t^2P^2$ we have an exponential increase of the pulse.

The terms depending on G(z) can be integrated numerically, but will add no new information as far as obtaining the approximate size of the pinch. We may plot r'(z,t) as follows: Let $R_o = .15$ cm, $I_o = 400^a$. $v_o = 80$ cm/sec; then $\gamma = 46$ cm/sec, at $\beta \approx 3$, $\sigma = .33$, $M = .23$, $N = 1.20$, $P = 15$, $Q = 40$, which yields (at $z = 4$ cm) a pulse which looks like

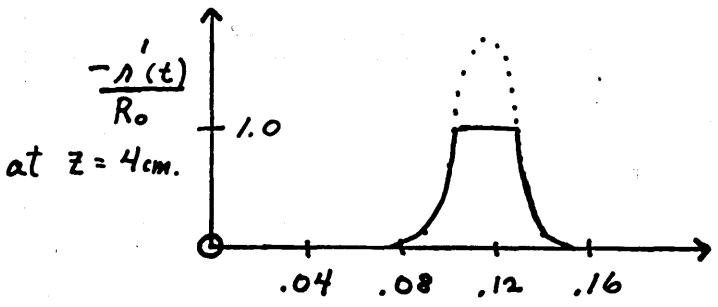

Let $-\frac{\alpha}{R_o} = .002$

$\beta = 3$ $\quad v_o = 80$ cm/sec.

$\gamma = 46$ cm/sec.

i.e., our linear approximations clearly indicate that the stream should pinch off (α is negative). We also note that the group velocity of the disturbance now depends on v_o and is approximately v_o. However, the equation does not yield the experimentally observed results as yet (for example, it predicts pinching too close to the nozzle). We do have a general form -- possibly we can <u>choose</u> the constants P, Q, M, N, σ, ... to fit the experimental results. Further analysis of the present solution will be deferred to a later paper.

If $\frac{v_o^2}{4\gamma^2} > 1$, i.e., I_o and $T_o \longrightarrow 0$, then

$$\sigma \longrightarrow i\sigma \qquad P \longrightarrow iP \qquad N \longrightarrow iN$$

$$r'(z,t) \longrightarrow -\alpha e^{-t(NQ + MP - NP)} e^{-\beta[z - tQ + tP]^2} \sin tMP,$$

which has a completely different functional dependence: the strongest term goes as $\alpha e^{-\beta\,(z-Qt+Pt)^2}\, e^{-t(PM+QN-NP)}$, which decays to zero. Perturbations clearly do not grow in this case. Further investigation should be done on the cutoff value $\frac{v_o}{2\gamma} = 1$.

IV. We have seen that we obtain a reasonable estimate of the pinch by considering the motion of the stream as functions of z and t. However, in order to obtain the result we were required to linearize the force and the equations of motion. In doing this we lost the physical result that the forces due to I_o and T go as $1/r_o^n$, n = 3 and 2 respectively, i.e., the forces approach infinity as $r_o \longrightarrow 0$. Therefore, to avoid this difficulty, we shall use a more physical argument to determine the shape of a pinch as a function of time by linearizing <u>just</u> the equations of motion and by making certain assumptions about the nature of a pinch.

We shall move with the stream and consider z, the displacement of the "wall" of a pinch from its initial position as $f(z_o,t)$.

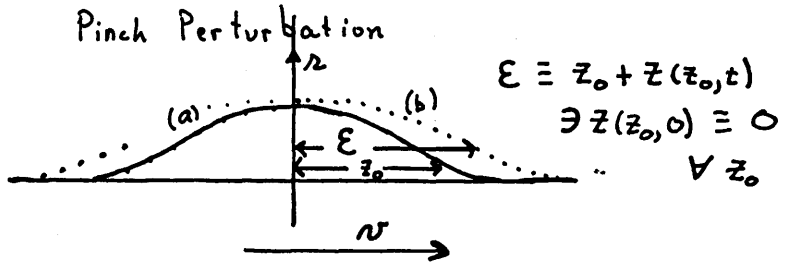

(a) solid line : perturbation at $t=0$ $r_o = r_o(z_o)$
(b) dotted line : at t : perturbation displaced along the direction of flow by $z(z_o,t)$

Analogously to what has been done previously:

$$\rho \frac{\partial^2 z}{\partial t^2} = \left\{ \frac{a}{r_o^3} + \frac{b}{r_o^2} \right\} \left(\frac{\partial r_o}{\partial z} \right). \qquad (8)$$

We will not consider the possibility of generating surface waves (as we did in the previous calculation), which would contribute significantly to the energy. We will use only a first order approximation to $\partial r_o/\partial t$ since the energy contribution from $\partial r_o/\partial t$ is small. Therefore, as before, we write the conservation of mass equation as

$$v_o \frac{\partial r_o}{\partial z} + \frac{r_o}{2} \frac{\partial v}{\partial z} + \frac{\partial r_o}{\partial t} = 0. \tag{9}$$

The physical assumption being made through equation (9) coupled with equation (8) is that the elongation of a pinch increases the velocity of the mercury which in turn decreases the radius of the stream. We are justified by the physical observation that pinches elongate as they "grow." The physical nature of r_o and $z(z_o,t)$ leads us to guess a functional dependence of the type:

$$r_o(z_o,t) = f(z_o + z(z_o,t),\ t),$$

where $f(z_o,0)$ describes the initial perturbation and $z(z_o,0) = 0$ for all z_o.

$$r(z_o,t) \approx f_o + \frac{\partial f_o}{\partial z_o} z(z_o,t) + tG(z_o),$$

where we have taken the first terms in the Taylor's expansion of $r(z_o,t)$.

$$f_o \equiv f(z_o,0) = R_o + \alpha e^{-\beta z_o^2}$$

$$r(z_o,t) \equiv f_o + Y$$

$$\frac{\partial^2 z}{\partial t^2} = \frac{\partial^2 Y/\partial t^2}{(\partial f_o/\partial z_o)}$$

$$\rho \frac{\partial^2 Y}{\partial t^2} = \left\{ \frac{a}{(f_o + Y)^3} + \frac{b}{(f_o + Y)^2} \right\} \left(\frac{\partial f_o}{\partial z_o} \right)^2$$

$$C \equiv 2 \left(\frac{\partial f_o}{\partial z_o} \right)^2 \frac{(a + bf_o)}{\rho} \qquad D \equiv \frac{2b}{\rho} \left(\frac{\partial f_o}{\partial z_o} \right)^2$$

$$\frac{d\dot{Y}^2}{dY} = \frac{(C + DY)}{(f_o + Y)^2}$$

$$\dot{Y}^2 - \dot{Y}_o^2 = - \frac{(E + 2DY)}{2(Y + f_o)^2} + \frac{E}{2f_o^2} ;$$

where $E = C + Df_o$

and $\dot{Y}_o = G(z_o)$.

From equation (9):

$$v_o \frac{\partial f_o}{\partial z_o} + v_o \frac{\partial^2 f_o}{\partial z^2} z(z_o, t) + \frac{(f_o + Y)g}{(v_o^2 + 2gz_1)^{1/2}} = - \frac{\partial f_o}{\partial z_o} \frac{\partial z}{\partial t} - G ,$$

evaluated at $t = 0$, gives

$$G = - \left\{ v_o \frac{\partial f_o}{\partial z_o} + \frac{f_o g}{(v_o^2 + 2gz_1)^{1/2}} \right\}$$

z_1 = height of fall of the Hg stream when $t = 0$, i.e., when the stream is perturbed.

$$t = \int_{o}^{Y} - \frac{dY}{\dot{Y}} = \int_{f_o}^{Y+f_o} + \frac{dY\sqrt{2}\, f_o Y}{\left(Y^2(2G^2f_o^2+E) - 2DYf_o^2 + (-Cf_o^2 + Df_o^3)\right)^{1/2}}$$

Such an integral is trivial, but yields a transcendental equation which must be solved numerically to obtain $Y(z_o,t)$ from which we can get $z(z_o,t)$. Therefore, since we have an estimate on $G(z_o)$ we know $r(z_o,t)$. Although the above equation utilizes the exact nature of the force dependence, we again had to linearize the functional dependence. Thus, a more correct solution is probably a synthesis of the two methods we have presented. A more complete analysis (for example, plotting $Y(z_o,t)$) has not as yet been completed. We note, though, that the pole of $1/\dot{Y}$ should give enough divergence so as to require the mercury to pinch off.

V. The methods of Section III and IV do not lend themselves to obtain easily the time it takes for a perturbation to collapse (pinch off). From Section III we may approximate it as $\sim 1/12$ sec, a value which is too large by a factor of 2. We may <u>estimate</u> it as follows:

$$\rho \frac{\partial^2 r_o}{\partial t^2} = - \frac{a'}{r_o^3} = \frac{\rho}{2} \frac{\partial \dot{r}_o^2}{\partial r_o} ,$$

which implies

$$\dot{r}_o = + \frac{a'}{\rho} \left\{ \frac{1}{r_o^2} - \frac{1}{R_o^2} \right\} \qquad a' = \frac{2\mu I_o^2}{\pi}$$

$$\tau \simeq \frac{\rho}{a'} \int_0^{R_o} \frac{R_o r_o dr_o}{\left(R_o^2 - r_o^2\right)^{1/2}} = R_o^2 \sqrt{\frac{\rho}{a'}}$$

Let $R_o = .25$ cm, $I_o = 300^a$, $\tau \approx .01$ sec, which is the right order of magnitude. The experimental value is $\approx .04$ sec, i.e., ρ should be sixteen times as large.

This gives us some approximation to the "effective" mass being displaced.

VI. One might ask if the mercury always pinches off -- such a question being brought up because as $r_o \longrightarrow 0$, the resistance R of the circuit approaches infinity and $I_o \longrightarrow 0$.

$$R \simeq R_o + \frac{x_o}{\pi r_o^2 \sigma}$$

where $R_o \approx .02\,\Omega$

and x_o length of pinch $\approx$ 1 cm.

$R_o = x_o/\pi r_o^2 \sigma$ for $r_o \simeq .2$ mm, i.e., the current cuts in half when $r_o = .2$ mm. If we set up the equations for the pinch but use $\dfrac{V}{R_o + \dfrac{x_o}{\pi r_o^2 \sigma}}$ instead of I_o, we find that r_o should oscillate about some small value, with the current oscillating accordingly. However, if we compute the temperature rise of the part of the mercury comprising the pinch, we find that the temperature change, given by

$$T = -\int_0^{r_o} \frac{V^2}{\left(R_o + \frac{x_o}{\pi r_o^2 \sigma}\right)^2} x_o \frac{r_o}{\left(\frac{\partial r_o}{\partial t}\right) \pi r_o^2 \sigma c_V \rho \pi r_o^2 x_o}$$

is approximately 5600°_{A} for the conditions of V, i.e., when the radius becomes small enough, the last filament is vaporized, rather than being "pinched" off by the magnetic forces.

VII. If the stream of mercury is placed in a weak external magnetic field parallel to the direction of flow and current, then due to the slope of a pinch, we may predict a net torque on the stream. (See Fig. f.) From Fig. f we see that the top half of the pinch has a net torque τ_1 which is equal and opposite to that τ_2 on the bottom half, i.e., the pinch should tend to twist off:

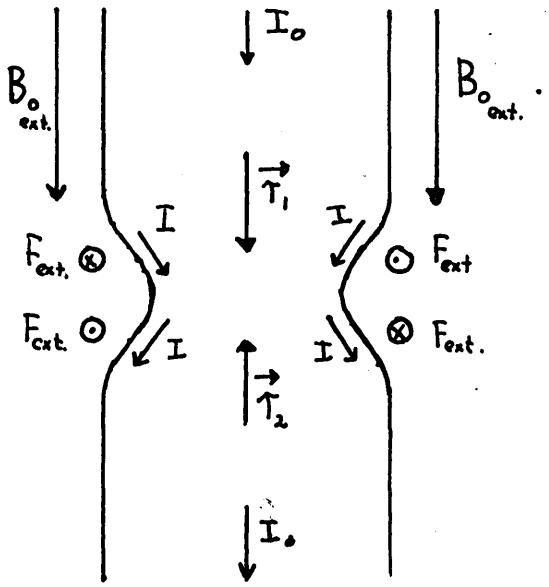

fig. f

Force/volume = $jB \sin \theta$ ext.

$$j \cong \left(\frac{\partial r_o}{\partial z}\right) \frac{I_o}{\pi r_o^2} \frac{2r}{r_o}$$

$$B = B_o$$

$$\sin \theta \cong \left(\frac{\partial r_o}{\partial z}\right) \frac{r}{r_o}$$

The net average torque/length as a function of z

$$\text{equals} \left(\frac{\partial r_o}{\partial z}\right)^2 \frac{I_o}{\pi r_o^2} 2\pi r_o \frac{B_o}{r_o^2} \int_o^{r_o} 2r^3 dr$$

$$= \left(\frac{\partial r_o}{\partial z}\right)^2 I_o r_o B_o \ .$$

If we assume a pinch of the type $r_o(z) = R_o + \alpha e^{-\beta z^2}$ the net torque

$$\tau_1 = I_o B_o 4\alpha^2\beta^2 \int_o^{\infty} z^2 e^{-2\beta z^2} (R_o + \alpha e^{-\beta z^2})$$

$$= B_o I_o \alpha^2 \beta^2 \left[R_o \sqrt{\frac{\pi}{8\beta^3}} + \alpha \sqrt{\frac{\pi}{27\beta^3}} \right]$$

If we want to find an approximate angle of rotation:

$$\tau_1 \approx \frac{R_o^2}{2} \rho \pi r_o^2 \ell \frac{d^2\theta}{dt^2}$$

let the pinch form linearly, i.e.,

$$\alpha = - \frac{R_o t}{t_o} \qquad t_o \approx 1/25 \text{ sec}$$

$$\theta \approx \frac{2B_o I_o \sqrt{\beta\pi}}{\pi R_o^4 \rho \ell} \left\{ \frac{R_o^3 t_o^4}{\sqrt{8}\ t_o^2\ 3\cdot 4} - \frac{R_o^3 t_o^5}{\sqrt{27}\ t_o^3\ 4\cdot 5} \right\}$$

$$\theta \approx \frac{B_o I_o}{\rho R_o} \sqrt{\frac{\beta}{\pi}} \frac{t_o^2}{\ell\ 12} \left\{ \frac{\sqrt{2}}{4} - \frac{1}{5\sqrt{3}} \right\}$$

If $B_o = 2000$, $I_o = 300^a$, $R_o = .25$ cm, $t_o = 1/25$ sec, $\ell \approx 2$cm, and $\beta \approx 10$, then $\theta \approx 60^o$. ℓ is greater than the length of the pinch because surface tension and viscosity will couple the torque to the rest of the stream. The above calculation suggests an experiment to measure the rotation. The important result, though, is that we have found the stream to be unstable with respect to rotations about the axis of symmetry!

VIII. Thus far our considerations have concentrated on cylindrically symmetric perturbations. It is clear that many perturbations will be local fluctuations rather than symmetrically distributed,

i.e., of the type 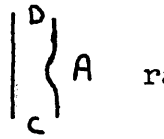

rather than 

It is clear that the pressure at A is greater than that at B. Therefore, we might expect not only that the pinch at A grows, but also that the whole stream is displaced to the left (with C and D moving appropriately so that the center of mass stays fixed). Therefore, we might predict a pinch sequence of the type:

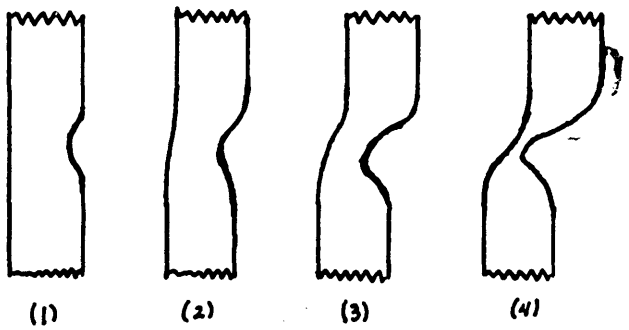

The analysis of the above type of pinch is complicated by the appearance of B_r and B_z self-field components. Our analysis will therefore stop at the above physical prediction.

Spiral Instability

In discussing the spiral instability, we wish to (1) show analytically that a spiral of some sort should develop, and (2) demonstrate using physical and geometrical arguments to conclude that the spiral will become large in comparison with an initial, small perturbation.

IX. The motion of a straight flow of mercury with current, falling in a magnetic field which is in the same direction as the flow and which is perturbed, looks (for small perturbation) like a perturbed string of tension T with a side thrust due to the current field interaction. To first order in $\partial x/\partial z$, $\partial y/\partial z$, the equations of motion are:

$$\rho\pi r_o^2(z)\frac{\partial^2 x}{\partial t^2} = I_o B_o \frac{\partial y}{\partial z} + \frac{\partial}{\partial z}\left(2\pi T r_o(z)\frac{\partial x}{\partial z}\right) \qquad (10)$$

and

$$\rho\pi r_o^2(z)\frac{\partial^2 y}{\partial t^2} = -I_o B_o \frac{\partial x}{\partial z} + \frac{\partial}{\partial z}\left(2\pi T r_o(z)\frac{\partial y}{\partial z}\right). \qquad (11)$$

If r_o = constant, then

$$\frac{\partial^2 x}{\partial t^2} = A\frac{\partial y}{\partial z} + B\frac{\partial^2 x}{\partial z^2}\ ;\ \frac{\partial^2 y}{\partial t^2} = -A\frac{\partial y}{\partial z} + B\frac{\partial^2 y}{\partial z^2}$$

$$A(r_o) \equiv \frac{I_o B_o}{\rho\pi r_o^2} \qquad B(r_o) \equiv \frac{2T}{\rho r_o}$$

which has the normal mode solution

$$\left.\begin{matrix} x = x_o \\ y = y_o \end{matrix}\right\} e^{i\omega t} e^{ikz} \; ; \; k = \pm \frac{A}{2B} \pm \mp \left(\left(\frac{A}{2B}\right)^2 + \frac{\omega^2}{B} \right)^{1/2}$$

i.e., purely undamped waves on the string. Therefore, we conclude that any instabilities must arise from the variation of $r_o(z)$ with z. From previous results we shall approximate

$$r_o(z) = R_o - R_o \nu z \tag{12}$$

Inserting (12) into (11) and (10) and linearizing we find:

$$\frac{\partial^2 x}{\partial t^2} = A\frac{\partial y}{\partial z} + B\frac{\partial^2 x}{\partial z^2} - \nu\frac{\partial x}{\partial z} \tag{13}$$

$$\frac{\partial^2 y}{\partial t^2} = - A\frac{\partial x}{\partial z} + B\frac{\partial^2 y}{\partial z^2} - \nu\frac{\partial y}{\partial z} \tag{14}$$

with A, B evaluated at $r_o = R_o$.

Trying solutions of the type $e^{i\omega t} e^{ikz}$ we find

$$k = \pm \frac{A}{2B} - \frac{i\nu}{2B} \pm \mp \left(\left(\frac{A}{2B}\right)^2 + \frac{\omega^2}{B} - \frac{\nu^2}{4B^2} \pm \frac{A\nu i}{2B^2} \right)^{1/2}$$

$A >> B$ and $A >> \nu$. Therefore, the only growing exponential term is $e^{\nu z/2B}$ <u>but</u> $\nu/2B << 1$, i.e., we cannot assume that this is the only result which predicts that the mercury will spiral -- it is independent of I_o and B_o.

X. There are two physical considerations which we have not considered in the above arguments. (1) The field of the magnet is not 100% homogeneous. Consider the presence of a cross field B_y (where we know $B_y < .02\ B_o$). The force resulting from B_y is the order of magnitude of $A\partial y/\partial z$ and therefore for $B_y < .02\ B_o$, it would not be strong enough to give us the deflection we seek. However, certainly the cross field inhomogeneity does help the instability, a problem which we cannot look into in further detail because of lack of detailed information about the character of the magnetic field.

(2) The second factor we did not consider in equations (10) and (11) is the effect due to perturbations resulting from pinch. For example, a side pinch of the type sketched

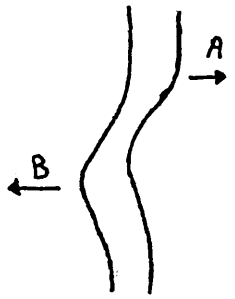

has a large horizontal component of current and therefore the points A and B tend to move outward due to the force resulting (1) from the $\vec{j} \times \vec{B}$ volume force which causes the mercury to rotate and (2) from the centrifugal force of the velocity of the stream. The only restoring force is due to surface tension, which we have seen is very small in comparison with the magnetic forces. The pitch of the spirals is determined somewhat by the number of pinch instabilities along the stream. As the mercury spirals outward, it must become thinner, which, as we have seen, causes the spiral to become larger exponentially by the

factor $e^{(\frac{\partial r_o}{\partial s})z/2B}$, thus increasing the instability even more. (s is the arc length along the stream.) As the stream spirals outward, the $\vec{j} \times \vec{B}$ force is even greater (because $\vec{j}$ is more nearly perpendicular to $\vec{B}_o$). If we consider the stream as a rod of length R rotating about an end, and compute the torque and moment of inertia of it:

$$\frac{\text{Torque}}{\text{Moment of inertia}} = \frac{IB\hat{\beta}}{2\rho r_o^2 R} = \text{const.}$$

Since $\pi r_o^2 R \sim$ const. to conserve mercury

$$\frac{d^2\theta}{dt^2} = \text{constant}$$

$$\frac{d\theta}{dt} = \omega = kt,$$

which means the angular velocity increases, i.e., the spiral takes off for infinity. The sum total of all the above effects leads us to conclude that the mercury stream is unstable with respect to its motion in an external magnetic field. The physical limitations on the spiralling are that (1) if the radius becomes too great, the stream becomes thin enough so that surface tension and the pinch effect tend to break the stream into droplets, which cuts the current off. The spiral then simply falls until electrical contact is re-established. From equations (11) and (10) and our above arguments, we can predict that the spiralling will be more violent for higher I_o

and B_o, and lower stream radius r_o. However, purely analytical predictions cannot be made at the present time. (1) We have seen that if we have an initial perturbation it will grow as $e^{\alpha z}$, while at the same time the $\vec{j} \times \vec{B}$ force causes the perturbation to rotate about the direction of B_o while the centrifugal force due to the initial velocity v_o causes the stream to move outward. (2) Also the pinch effect leads to instabilities which cause the stream to spiral. (3) The high nonlinearity and coupling in (1) and (2) lead us to conclude that the spiralling is limited only by the stream breaking into droplets and hence cutting off the current.

XI. We note that the velocity of the stream is not necessarily the velocity of fall of the spiral. In general, if the stream has an initial velocity v_o, and the magnetic force is so strong that the plane of the spiral is almost horizontal, then the plane of the spiral falls at $\approx$ gt cm/sec. If $v_o >$ gt and the radius of the spiral is small, then the stream radius may thicken, thus giving rise to globs of mercury spiralling. If such a globule were elliptically shaped and perturbed near the center (such that an end

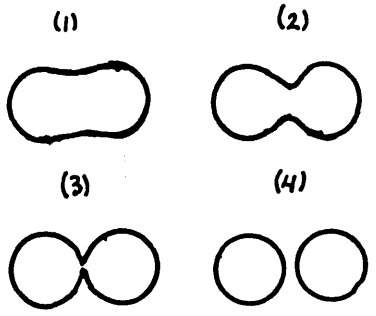

fig. 9

view of the stream would look like Fig. g), then due to the pinch effect and the inertial forces due to its rotation, we might expect that the globule of mercury would divide in half, thus giving rise to two streams (the sequence (i) → (n)) -- which would then spiral around each other. Such a phenomenon has been observed -- and we submit it here as a third type of instability, the "bifurcation instability."

XII. Now that we have qualitatively and somewhat quantitatively analyzed the pinch and spiral instabilities, it might be worth while to propose the general solution to the problem, by looking at the MHD equations. We may summarize them as follows:

Assuming ρ = constant and $\vec{\nabla}\cdot\vec{v} = 0$, $\frac{D}{Dt} \equiv \frac{\partial}{\partial t} + (\vec{v}\cdot\vec{\nabla})$.

We have

$$\vec{\nabla}\cdot\vec{B} = 0 \tag{15}$$

$$\frac{D\rho}{Dt} = 0 \tag{16}$$

$$\rho\frac{D\vec{v}}{Dt} = -\vec{\nabla}p + \eta\nabla^2\vec{v} + \rho\vec{g} - \vec{\nabla}\left(\frac{B^2}{2\mu}\right) + \frac{(\vec{B}\cdot\vec{\nabla})\vec{B}}{\mu} \tag{17}$$

$$\rho\frac{D}{Dt}\left(C_V T + \frac{1}{2}v^2\right) = -\vec{v}\cdot\vec{\nabla}p + \frac{\vec{j}^2}{\sigma} + \vec{v}\cdot(\vec{j}\times\vec{B}) + K\nabla^2 T + \rho\vec{g}\cdot\vec{v} + \eta\left[-\vec{v}\cdot\nabla^2\vec{v} - (\vec{\nabla}\times\vec{\omega})^2 + \nabla^2 v^2\right] \tag{18}$$

$$\frac{D\vec{B}}{Dt} = (\vec{B}\cdot\vec{\nabla})\vec{v} + \frac{1}{\mu\sigma}\nabla^2\vec{B} \tag{19}$$

$$\vec{j} = \frac{1}{\mu}(\vec{\nabla}\times\vec{B}) \tag{20}$$

where ρ = density

$\vec{v}$ = velocity

η = viscosity

C_V = specific heat

σ = conductivity (electrical)

K = thermal conductivity

μ = permeability

$\vec{j}$ = current density

Dot equation (17) with $\vec{v}$ and subtract (18). We find:

$$\rho C_V\left(\frac{\partial T}{\partial t} + (\vec{v}\cdot\vec{\nabla})T\right) - k\nabla^2 T = \frac{1}{\mu^2\sigma}(\vec{\nabla}\times\vec{B})^2 + \eta\left[\frac{\partial v_i}{\partial x_j}\frac{\partial v_i}{\partial x_j} + \frac{\partial v_i}{\partial x_j}\frac{\partial v_j}{\partial x_i}\right]$$

Thus, we can isolate the temperature dependence from the calculations, that is, we can find $T(\vec{x},t)$ once we know $\vec{B}(\vec{x},t)$ and $\vec{v}(\vec{x},t)$. We wish to solve:

$$\rho\frac{\partial\vec{v}}{\partial t} + \rho(\vec{v}\cdot\vec{\nabla})\vec{v} = -\vec{\nabla}p + \eta\nabla^2 v + \rho\vec{g} - \vec{\nabla}\left(\frac{\vec{B}^2}{2\mu}\right) + \frac{(\vec{B}\cdot\vec{\nabla})\vec{B}}{\mu}$$

and

$$\frac{\partial\vec{B}}{\partial t} + (\vec{v}\cdot\vec{\nabla})\vec{B} = (\vec{B}\cdot\vec{\nabla})\vec{v} + \frac{1}{\mu\sigma}\nabla^2\vec{B}$$

such that

$$\vec{\nabla}\cdot\vec{B} = \vec{\nabla}\cdot\vec{v} = 0$$

Call $P_o = \frac{p}{\rho} + \frac{\vec{B}^2}{2\mu\rho}$. This represents the pressure on the stream due to surface tension and magnetic forces. The procedure is as follows: From our analysis of the pinch, we know P_o fairly accurately at $t = 0$. We can then solve

the general MHD equations using this value, which gives us $\vec{v}$ and $\vec{B}$. $0 \leq t \leq \Delta t$. At Δt we can recompute P_o and repeat the procedure, ad infinitum. Let us solve for $\vec{v}$ and $\vec{B}$ in general. Let $\vec{H} \equiv \vec{B}/\sqrt{\mu\rho}$ and let $\vec{H} = \vec{H}_o + \vec{H}_1$, $\vec{v} = \vec{v}_o + \vec{v}_1$. $|\vec{H}_1| < < |\vec{H}_o|$ $|\vec{v}_1| < < |\vec{v}_o|$. $\vec{H}_o$, $\vec{v}_o$ are constants, i.e., the initial stream velocity and external magnetic field are much larger than the local fields and velocities caused by the currents and perturbations. This is justified in our experiment for $v_o > 100$ cm/sec. $B_o > 1000$ gauss. Linearizing the equations we find:

$$\frac{\partial \vec{v}_1}{\partial t} + (\vec{v}_o \cdot \vec{\nabla})\vec{v}_1 = \delta \nabla^2 \vec{v}_1 + \vec{g} - \vec{\nabla} P_o + (\vec{H}_o \cdot \vec{\nabla})\vec{H}_1$$

and

$$\frac{\partial \vec{H}_1}{\partial t} + (\vec{v}_o \cdot \vec{\nabla})\vec{H}_1 = (\vec{H}_o \cdot \vec{\nabla})\vec{v}_1 + \lambda \nabla^2 \vec{H}_1$$

where

$$\delta \equiv \frac{\eta}{\rho} \qquad \lambda \equiv \frac{1}{\mu\sigma}$$

Letting

$$\vec{v}_1 = \iint e^{-i\vec{k}\cdot\vec{x}} e^{-i\omega t} \vec{A}(\vec{k},\omega) d^3k dt$$

$$\vec{H}_1 = \iint e^{-i\vec{k}\cdot\vec{x}} e^{-i\omega t} \vec{B}(\vec{k},\omega) d^3k dt$$

$F_T \equiv$ Fourier transform:

$$F_T \vec{g} \equiv \vec{G}(\vec{k},\omega)$$

$$F_T \vec{\nabla} P_o \equiv \vec{M}(\vec{k},\omega)$$

We find:

$$\vec{A} = \frac{(\vec{G} - \vec{M})\left(i\omega + i(\vec{v}_o \cdot \vec{k}) - \lambda k^2\right)}{\left[\left(i\omega + i(\vec{v}_o \cdot \vec{k}) - \lambda k^2\right)\left(- i\omega - i(\vec{k} \cdot \vec{v}_o) + \delta k^2\right) + (\vec{H}_o \cdot \vec{k})^2\right]}$$

$$\vec{B} = \frac{i(\vec{H}_o \cdot \vec{k})\vec{A}}{\left[i\omega + i(\vec{v}_o \cdot \vec{k}) - \lambda k^2\right]}$$

Since we know $\vec{G}$ and $\vec{M}$, we <u>know</u> $\vec{A}$ and $\vec{B}$ and can solve for $\vec{v}_1$ and $\vec{H}_1$ and find the new P_o at Δt, ... Such a program could be accomplished on a computer to find the general motion of the mercury stream, given the initial perturbations.

The Experiment

Refer to Fig. 4 on the next page. The experiment consists of letting mercury fall freely from reservoir A to reservoir B through the circular hole (with a 2-inch spout) at C. Steel wool in the funnel-shaped nozzle prevents vortices from forming in the exit stream. Current flows through the mercury and makes contact via copper electrodes at the top and bottom. Current is supplied from a bank of submarine batteries ranging from 0-52^{V} in 2^{V} steps. A .09Ω steel tube (water-cooled) resistor, capable of dissipating 25 kw, is available in order to keep the current I_o through the mercury column approximately constant. The resistor, however, can be removed in order to decrease the open circuit voltage across the mercury stream (to minimize sparking).

The current through the mercury was measured using a 50 ma shunt connected both to a Sanborn two-channel recorder and a voltmeter (to calibrate the Sanborn recorder). Since reservoir A empties during a run, the exit velocity v_o is a function of time. The velocity was measured as a function of time by filling the reservoir with known quantities of mercury, and measuring the time it takes for the reservoir to empty. A pump circuit was designed and built to cycle the mercury back to reservoir A after a run. A 10-pancake coil, water-cooled magnet, homogeneous to 2% and with a hole

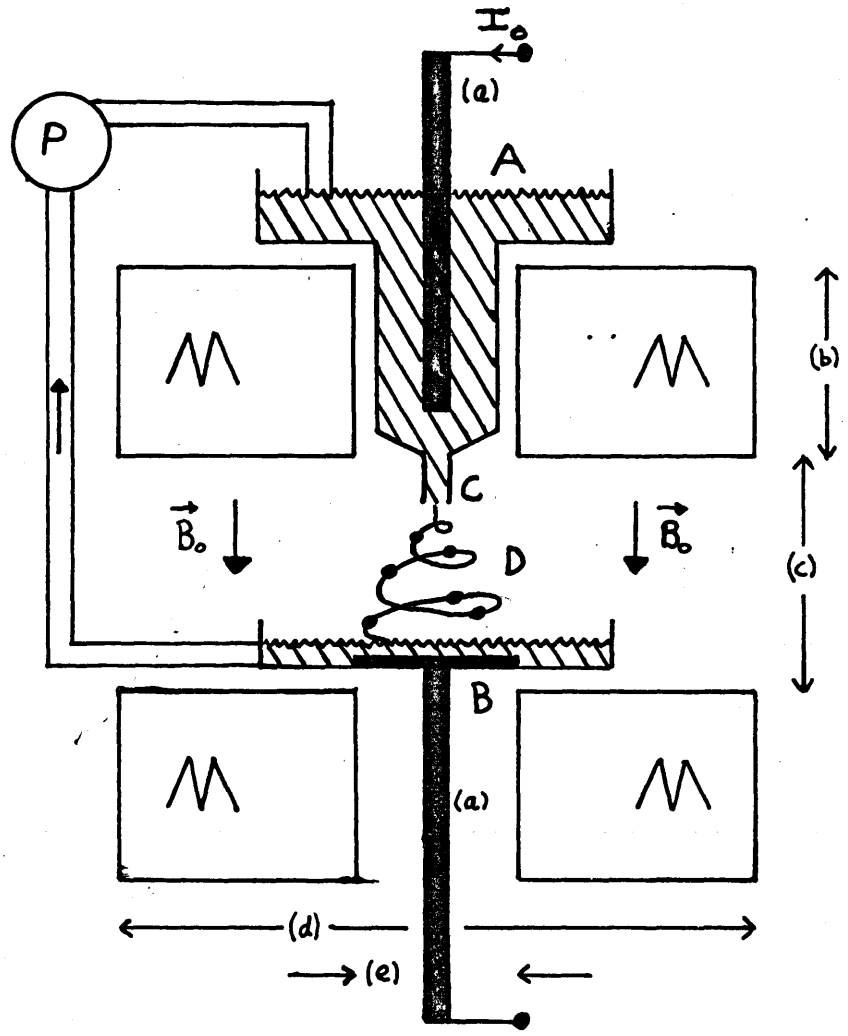

Fig. h

(a) $\frac{1}{2}$ inch copper electrode; (b) 35 cm.; (c) h_o, 4-6 inches; (d) 3 feet; (e) 5 cm.; (A) supply reservoir filled with Hg; (B) receiving reservoir for the falling Hg; (C) outlet nozzle with a diameter which can be varied from 2-6 mm.; (D) falling Hg stream with spiral and pinches; (M) annular shaped magnet; (P) pump assembly to recycle the Hg.

through both pole faces (in which we built reservoirs A and B) was used. The magnetic field was calibrated to 2% both in magnitude and direction.

Observations of the mercury stream were made using a General Radio motor-driven camera capable of 550 frames/sec (we ran at 250 frames/sec) using Kodak Plus-X 35 mm film. The lighting came from a Strobotac (GR stroboscope) with a flash rate from 100-25,000 rpm and a pulse approximately 4×10^{-6} sec long. We ran at 15,000 rpm. We used a special reflecting screen for shadow photography. Experiments on direct and indirect lighting were run; these were unsatisfactory because of specular reflection from the mercury stream. We tried using a Leica manually-controlled camera but found we could not take pictures nearly fast enough to see the instabilities forming. We tried various filters with limited success. Pan-Atomic X film was tried, but found not sensitive enough.

It was not clear at the start of the experiment that we were obtaining spirals and pinches. A great deal of guess work was required until we finally hit on the combination that gave us the desired results.

In addition to doing the experiment many precautions were taken because of the health hazard of an over-exposure to mercury vapor.

The parameters of the system that we were able to vary were:

(1) Magnetic field, 0-4000 gauss

(2) Current, 0-500[a]

(3) Hole size of the orifice at C, .1-.3 cm radius

(4) Initial velocity of the stream, v_o, 40-140 cm/sec

(5) Height of fall (distance between the magnets, 4-6 inches).

The experimental procedure consisted of setting the above parameters and then taking approximately 14 feet of film (2 sec) of the mercury stream. Although much more work is yet to be done, enough film has been taken at the present time to obtain some feeling for the phenomena involved and in order to suggest further experiments.

Presentation of Data and Results

We systematically varied the parameters of our apparatus. These are:

(1) The current I_o through the mercury stream,

(2) The initial exit speed v_o from the nozzle of reservoir A,

(3) The initial stream radius R_o,

(4) The external magnetic field B_o, and

(5) The height of fall h_o.

The mercury stream under the given conditions was then photographed. The photographs and tabulation of results follow.

Test 1

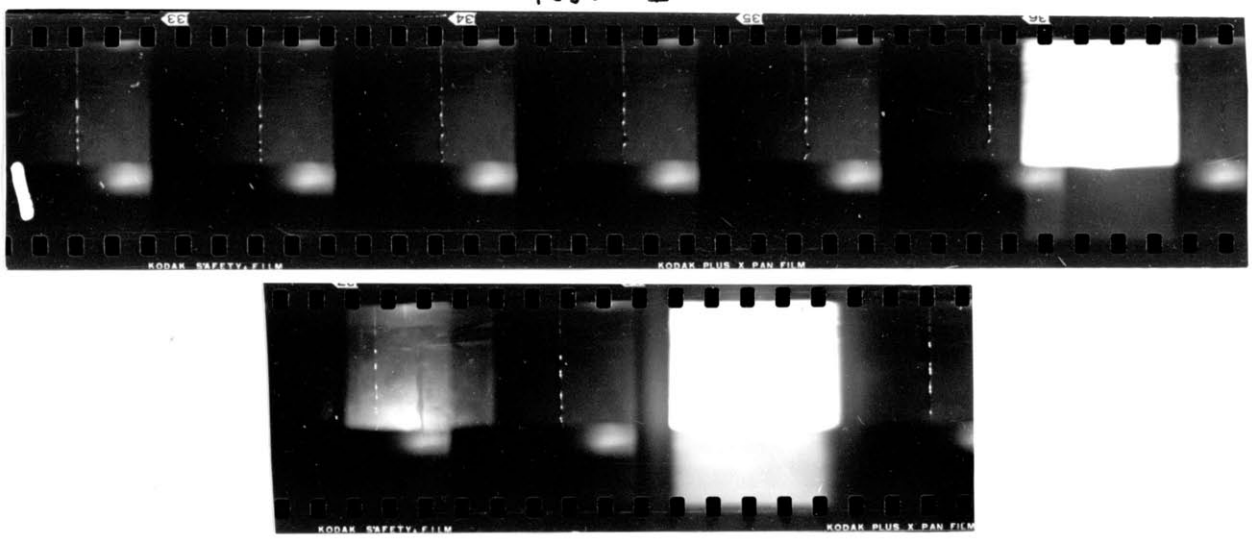

Test 2B

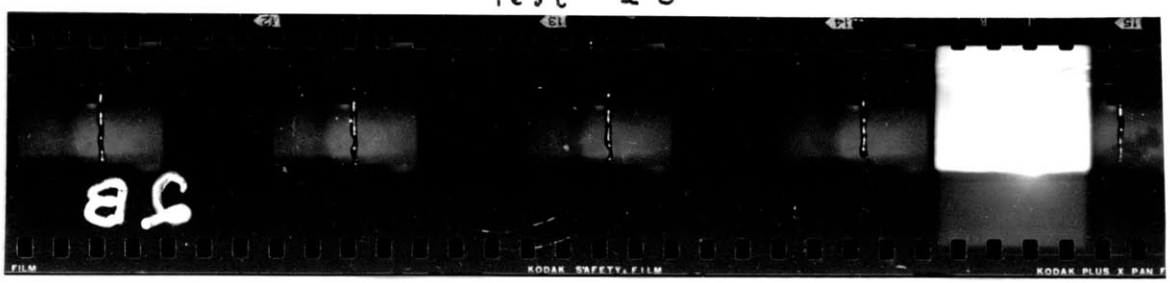

Test 2A

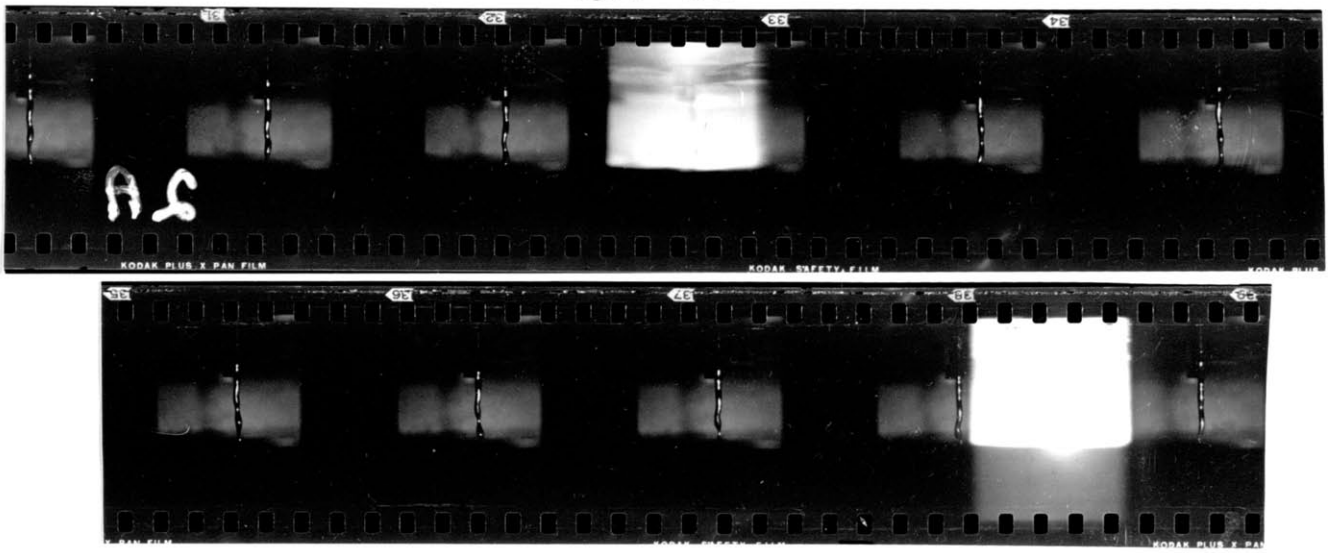

Test 3

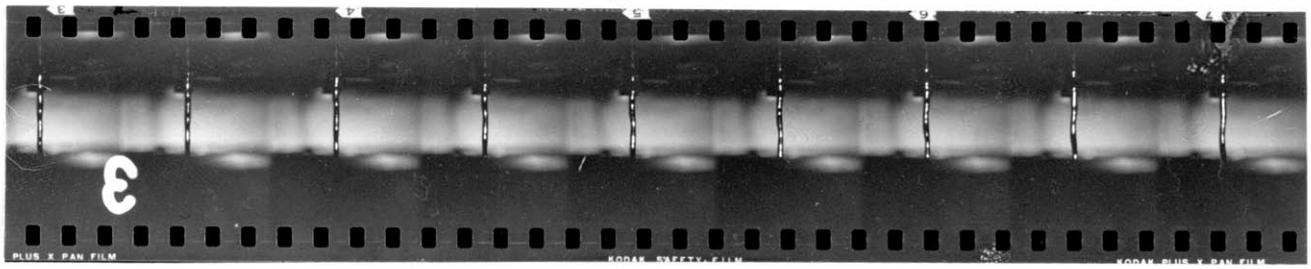

Test 4

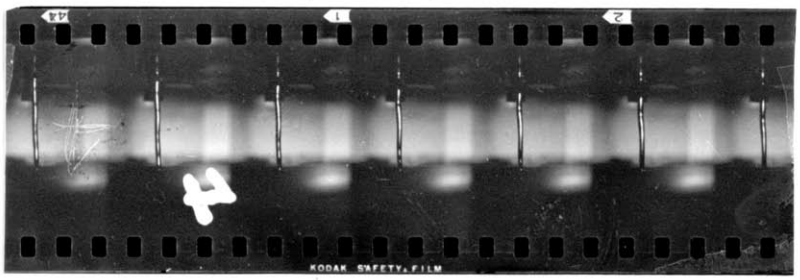

Test 5

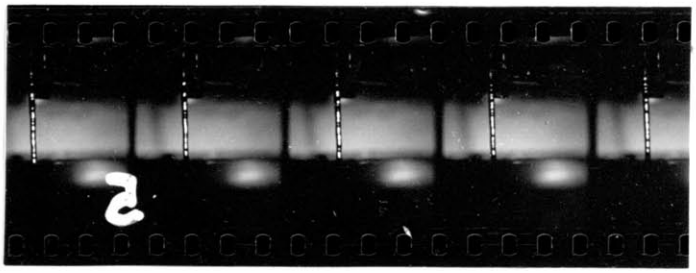

Test 6

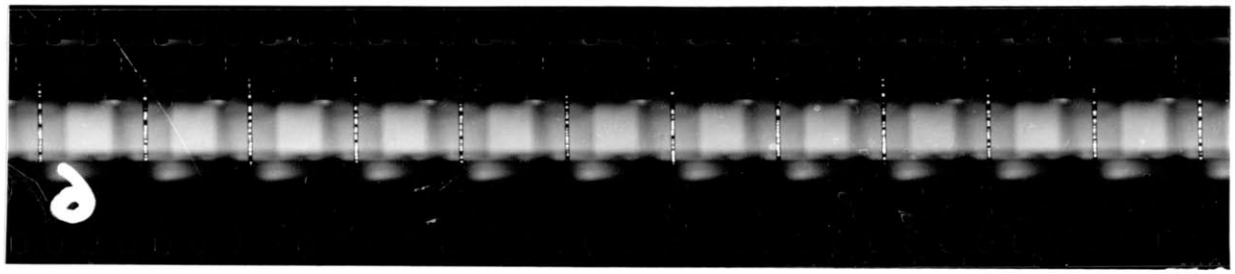

Test 7A

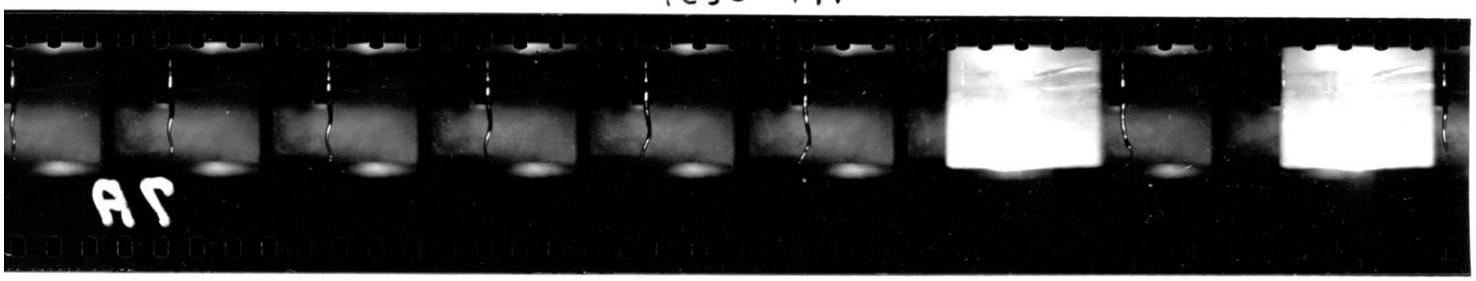

Test 7B

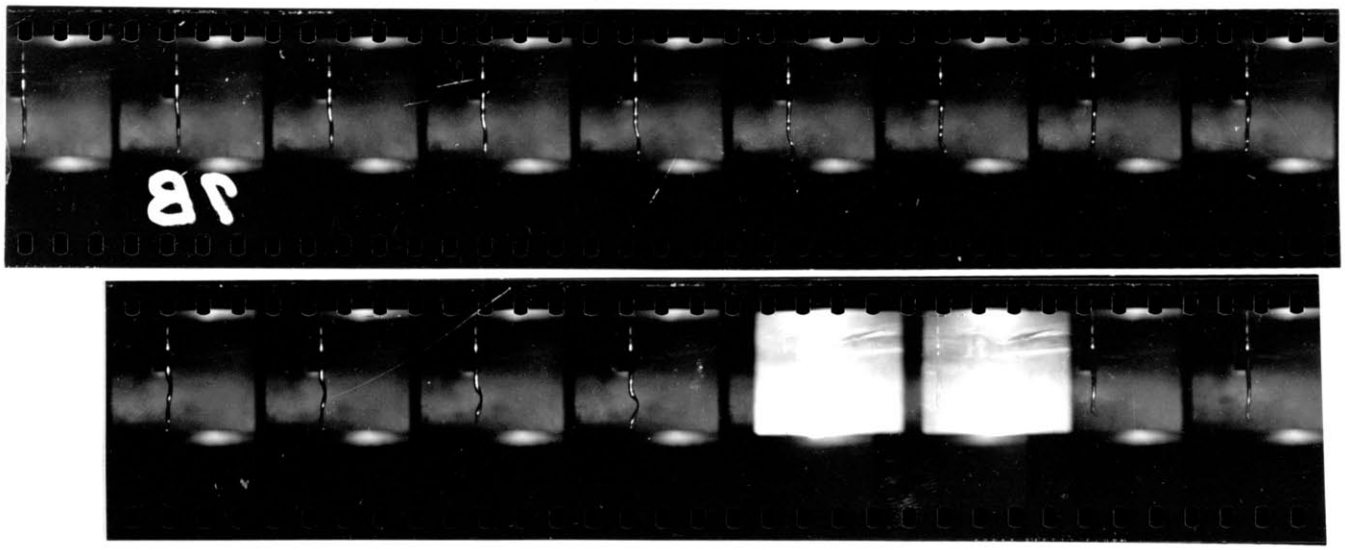

Test 8

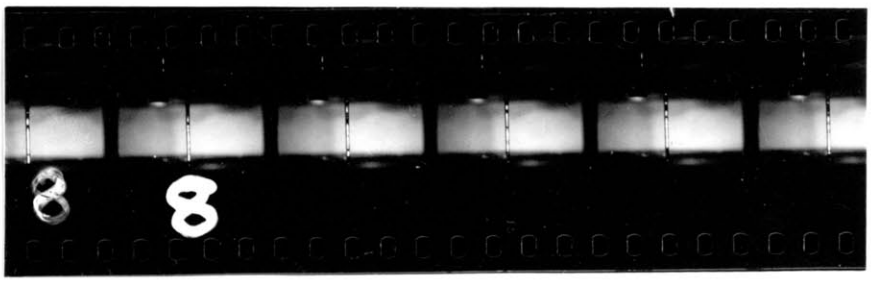

Test 9B

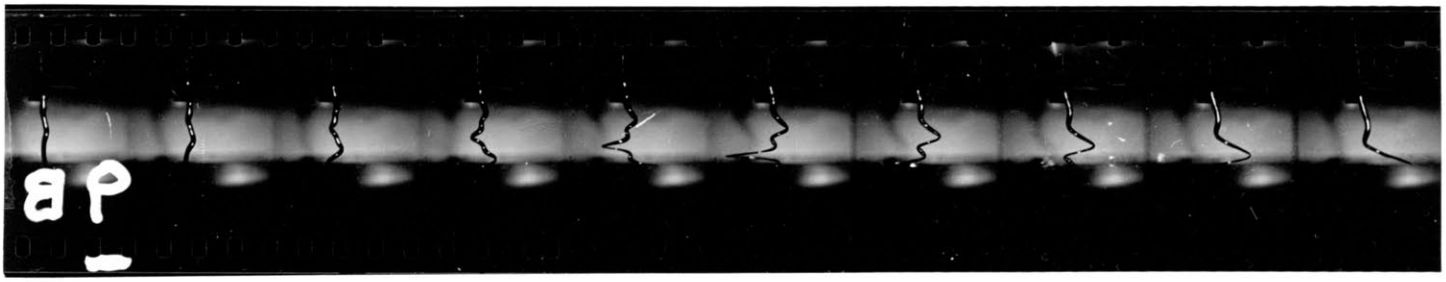

Test 9C

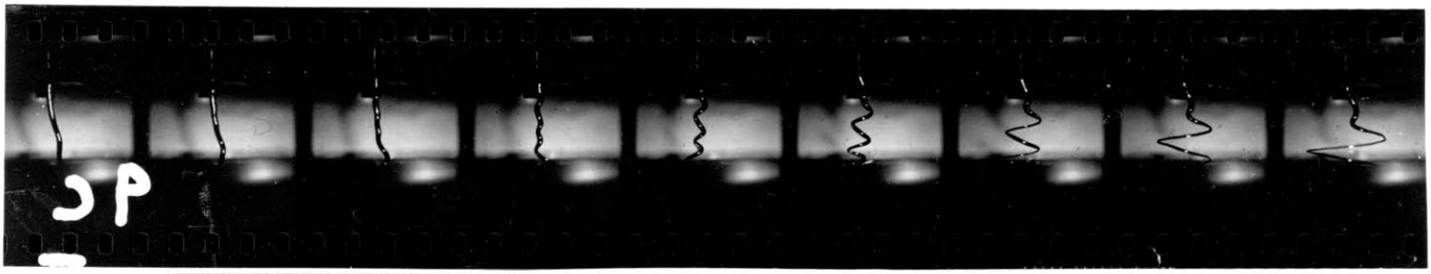

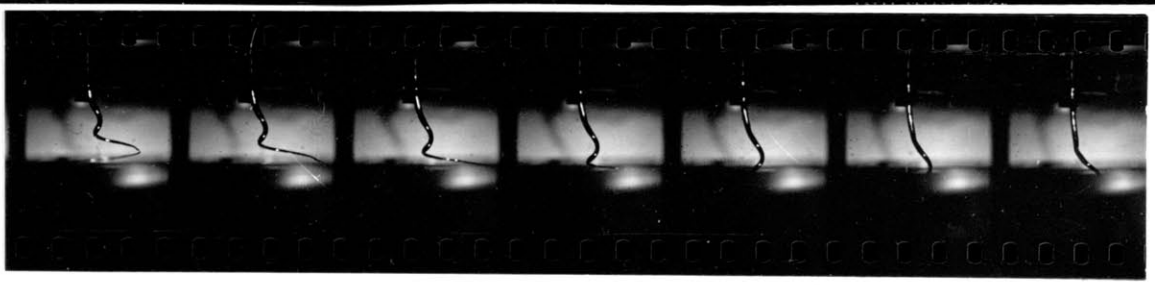

Test 10A

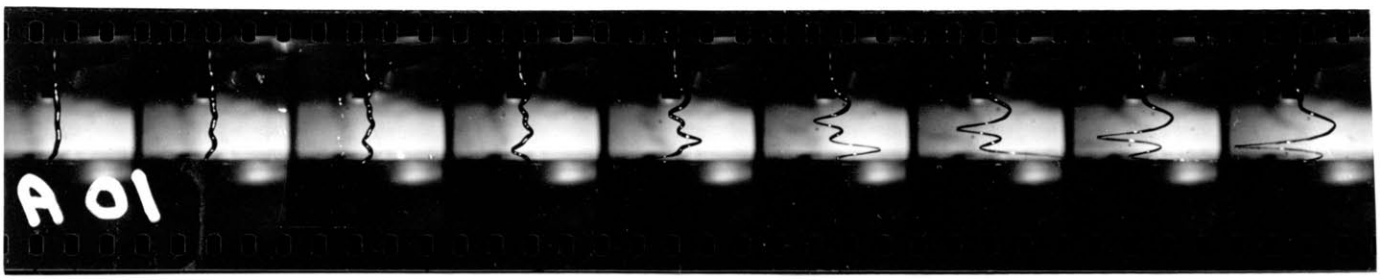

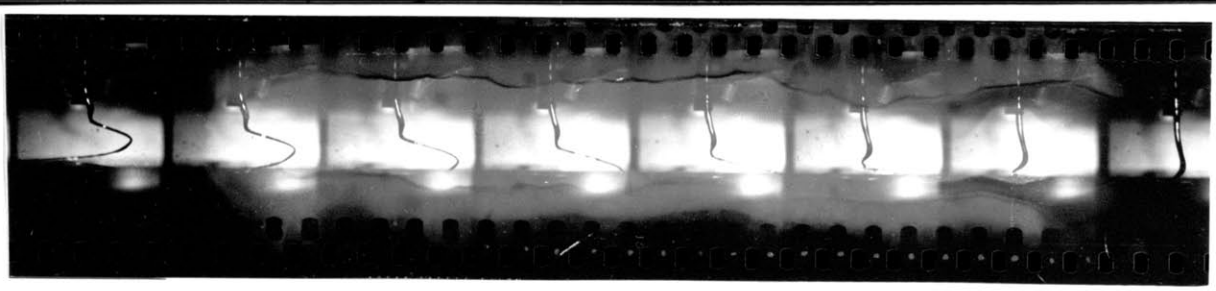

Test 10 B

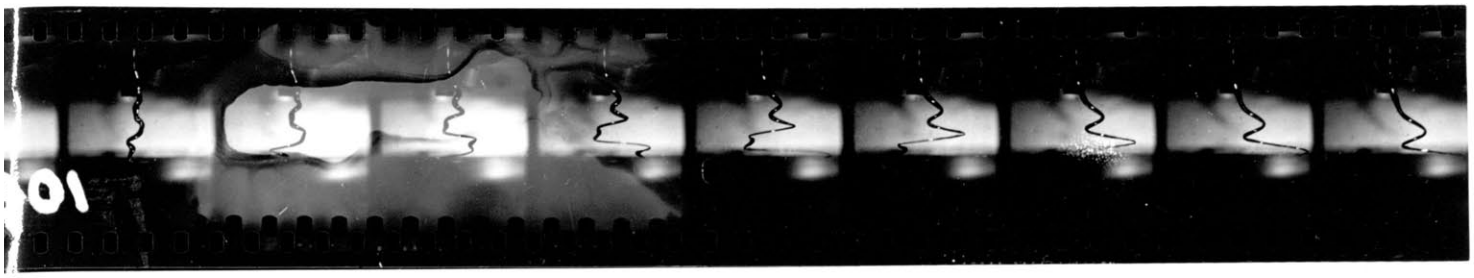

Test 11 A

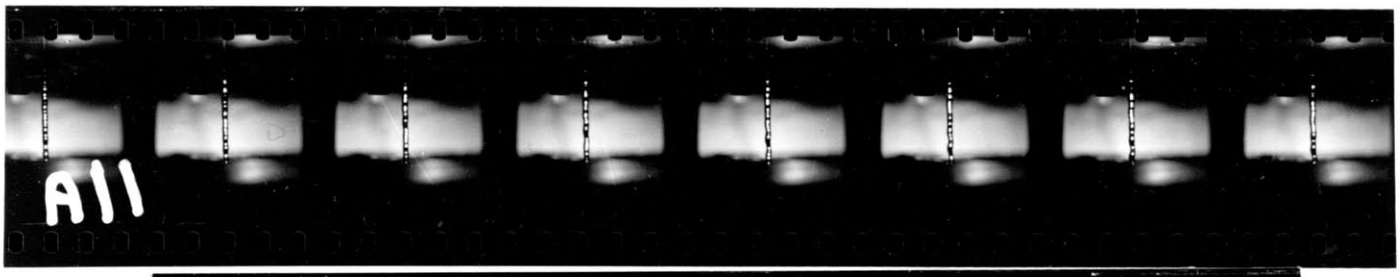

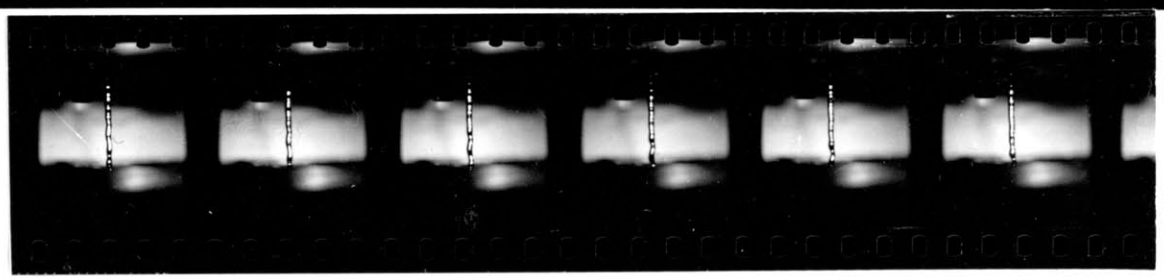

Test 12 B

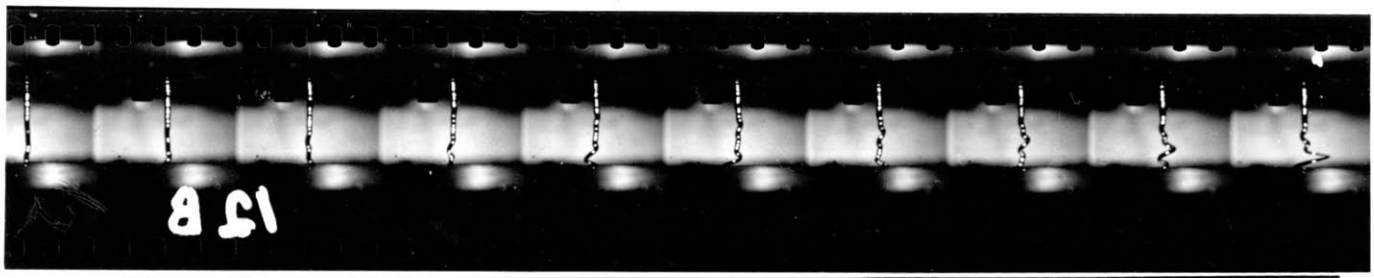

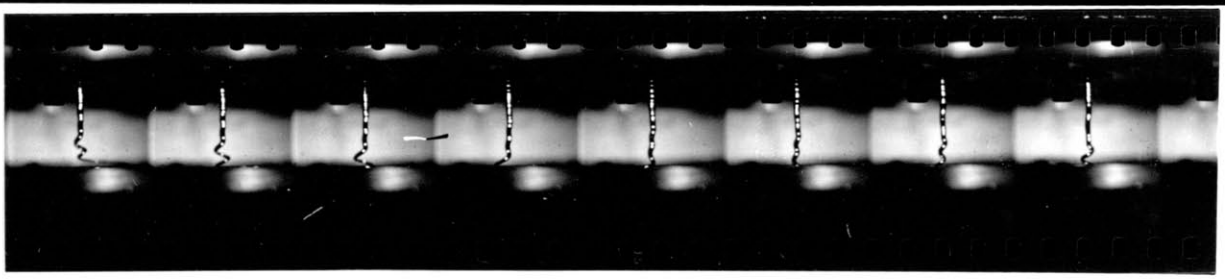

Test 13 A

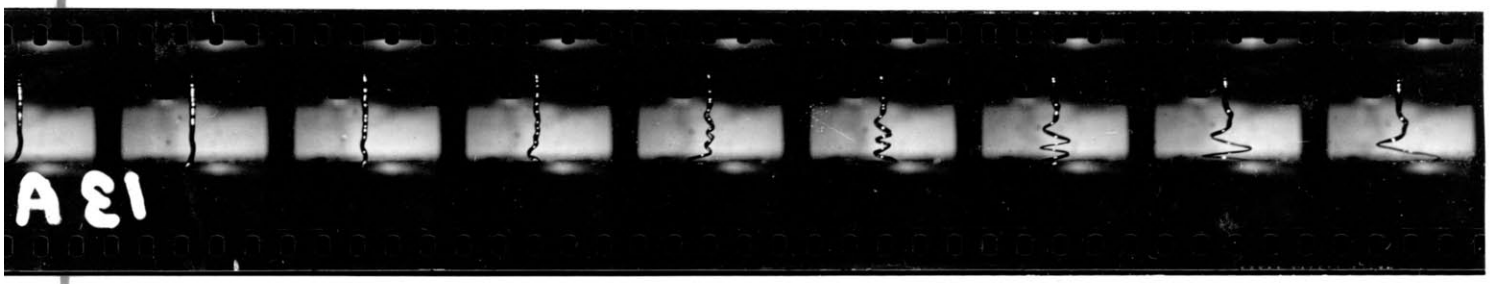

Test 13 B

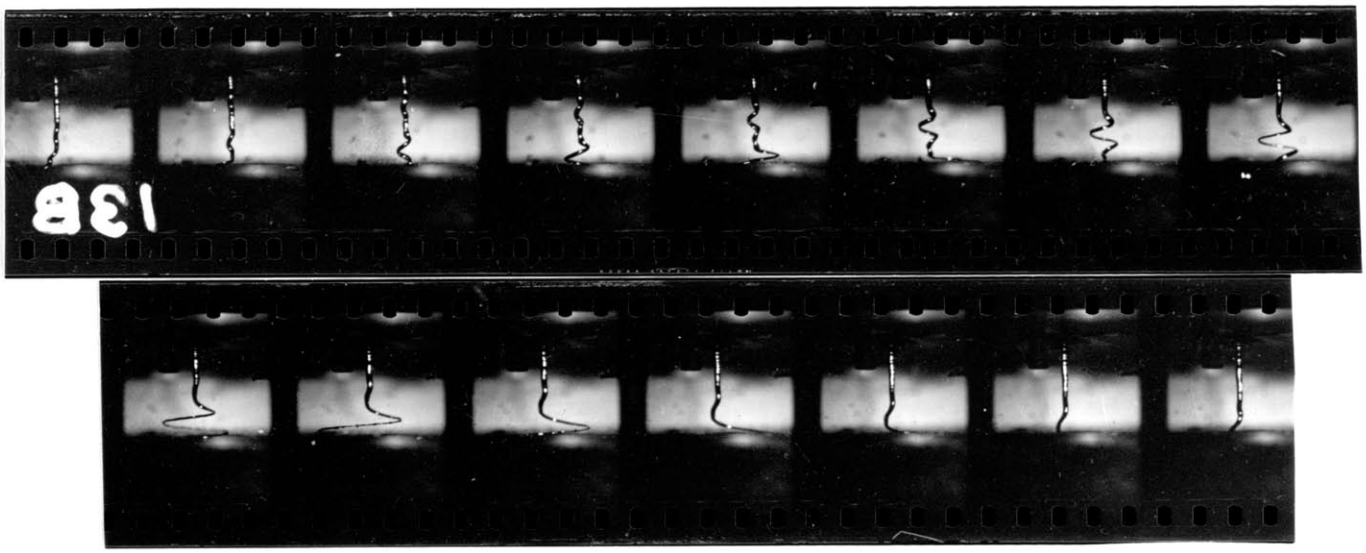

Test 14 A

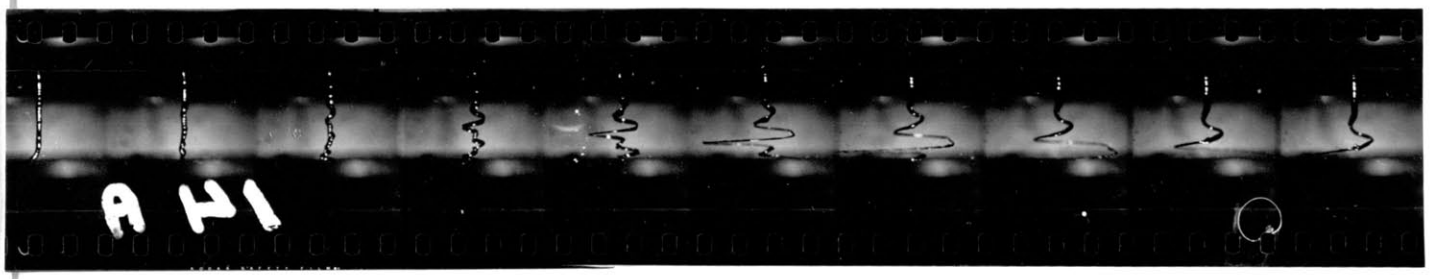

Test 14 D

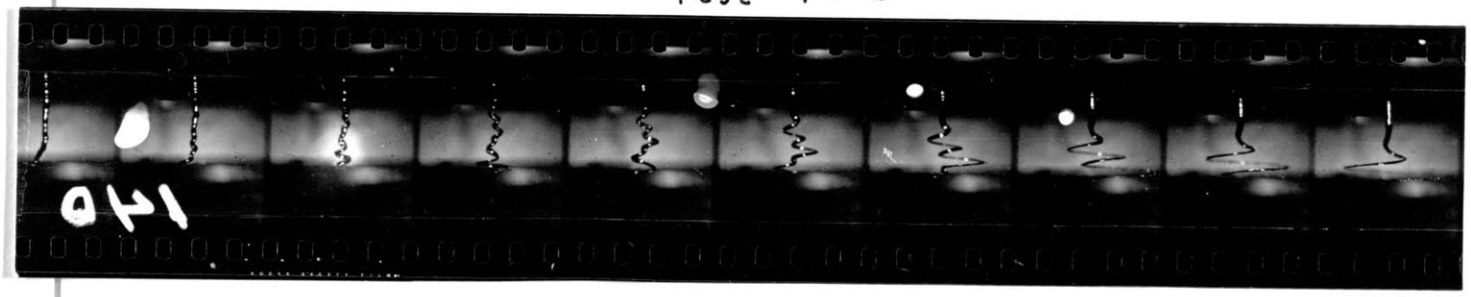

Test 14 C

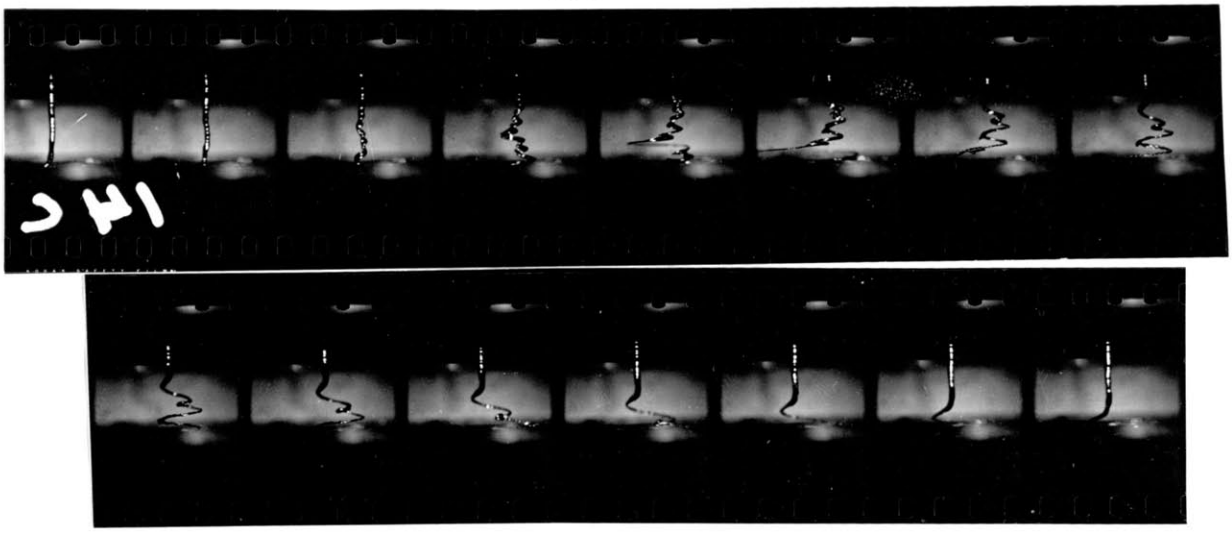

Test 15 A

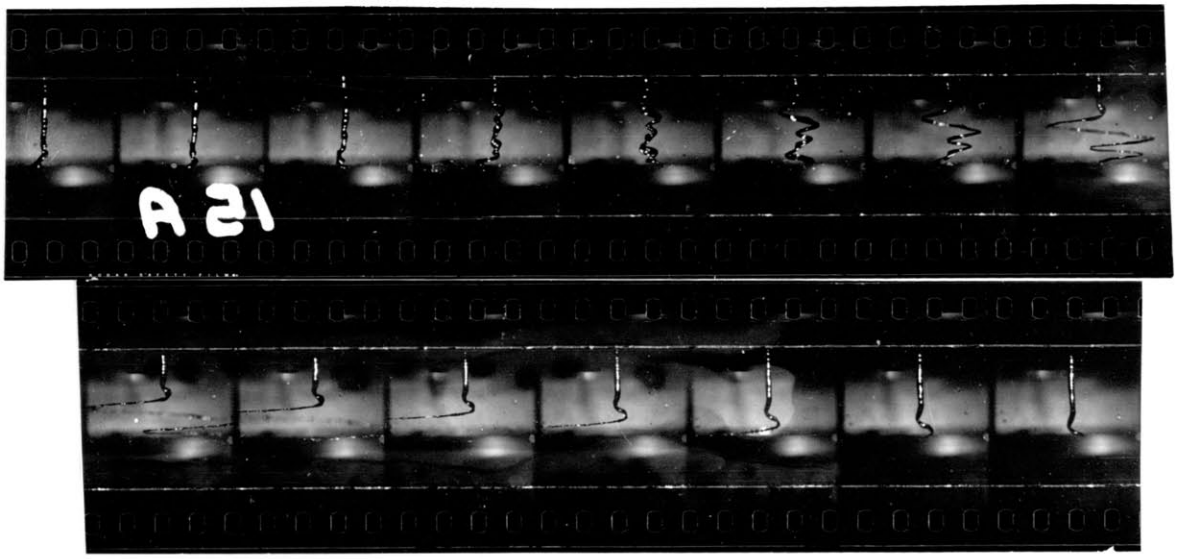

Test 15 B

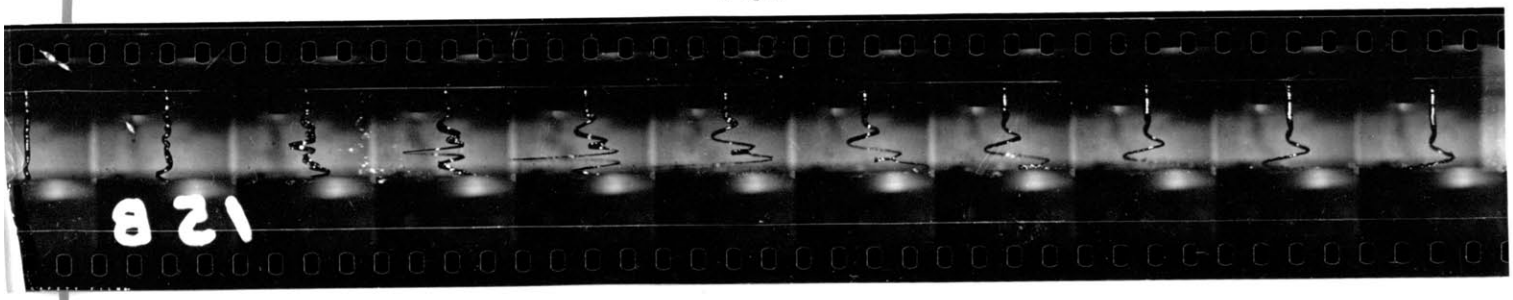

Test 15 C

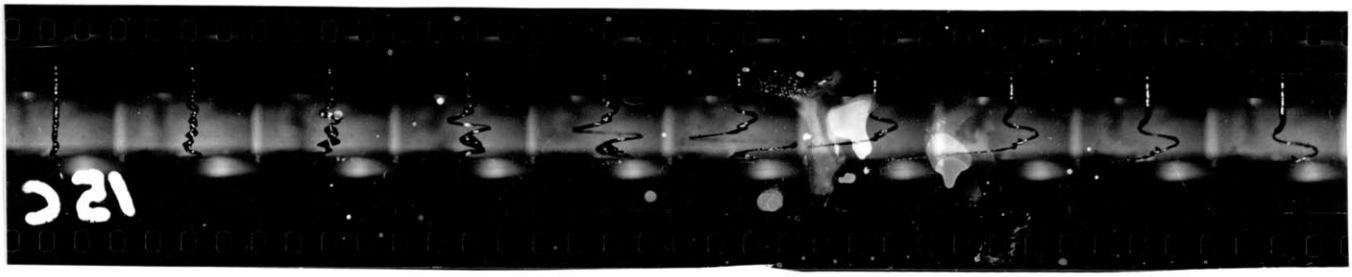

Test 15 D

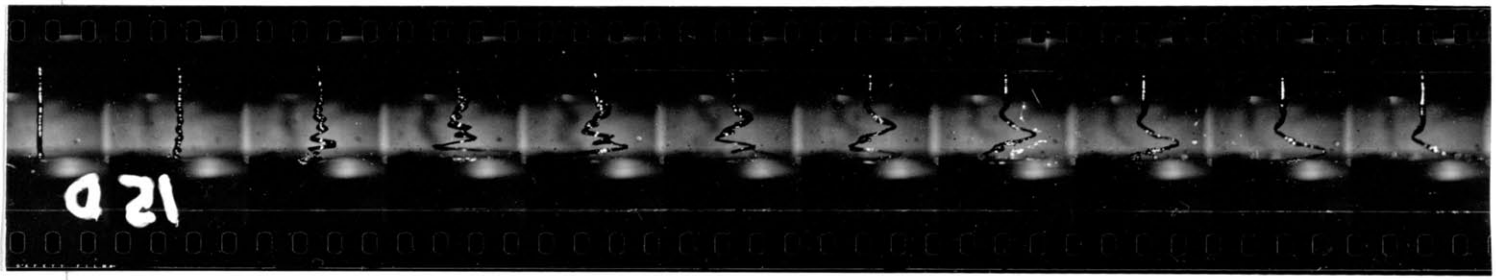

Test 15 E

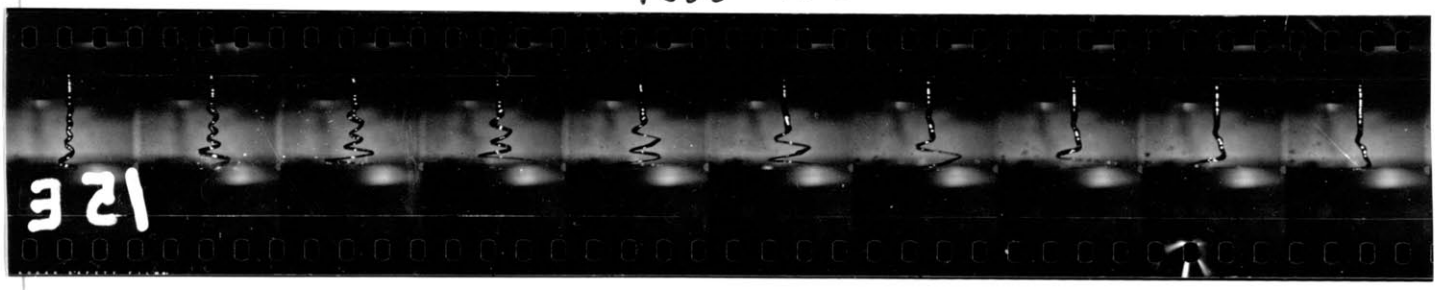

Test 15 F

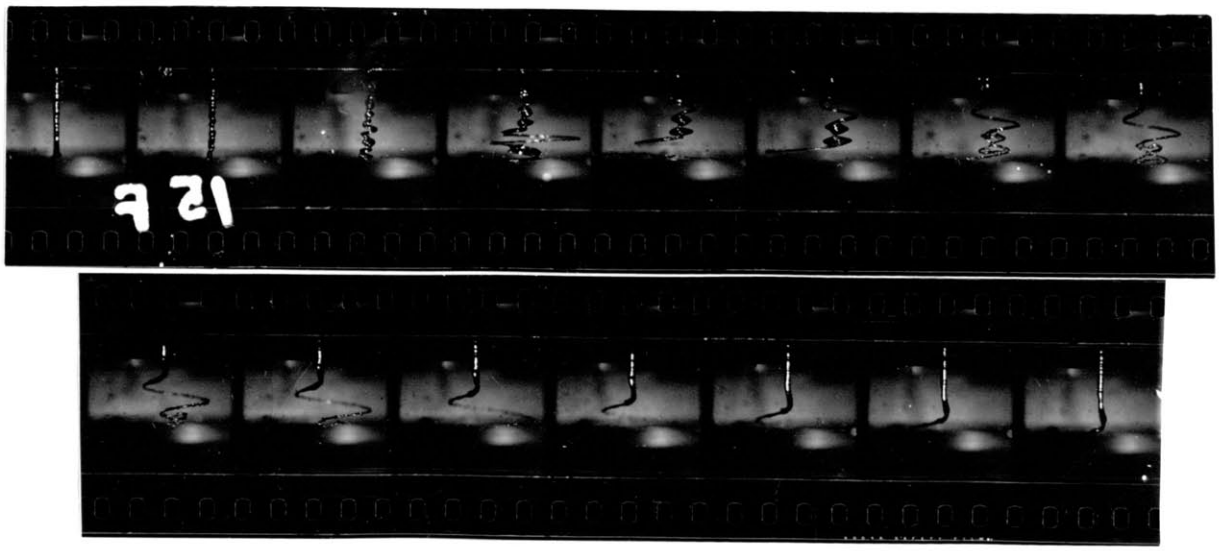

Test 15 B

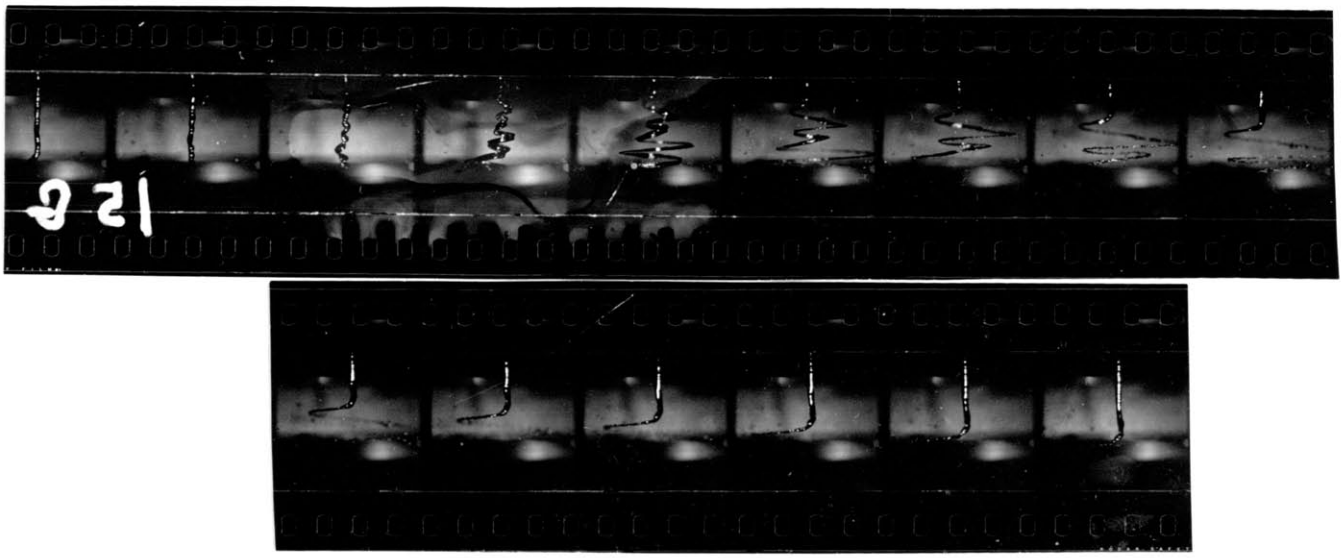

Test 16

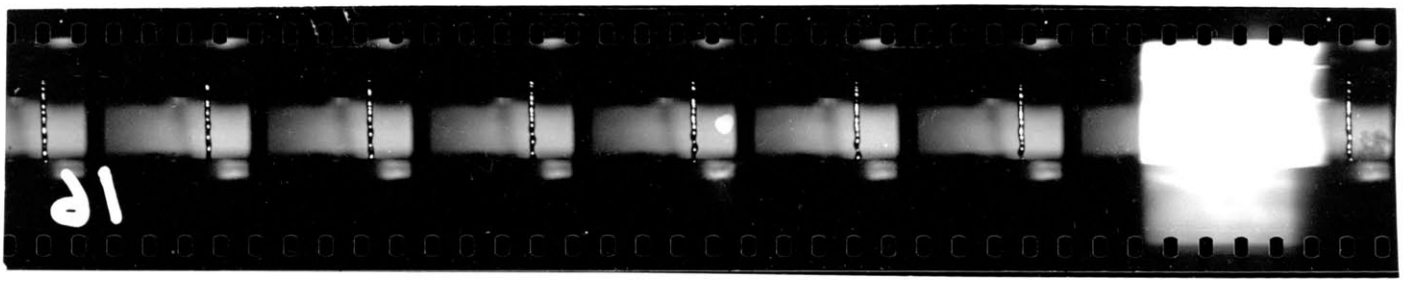

Test 17 B

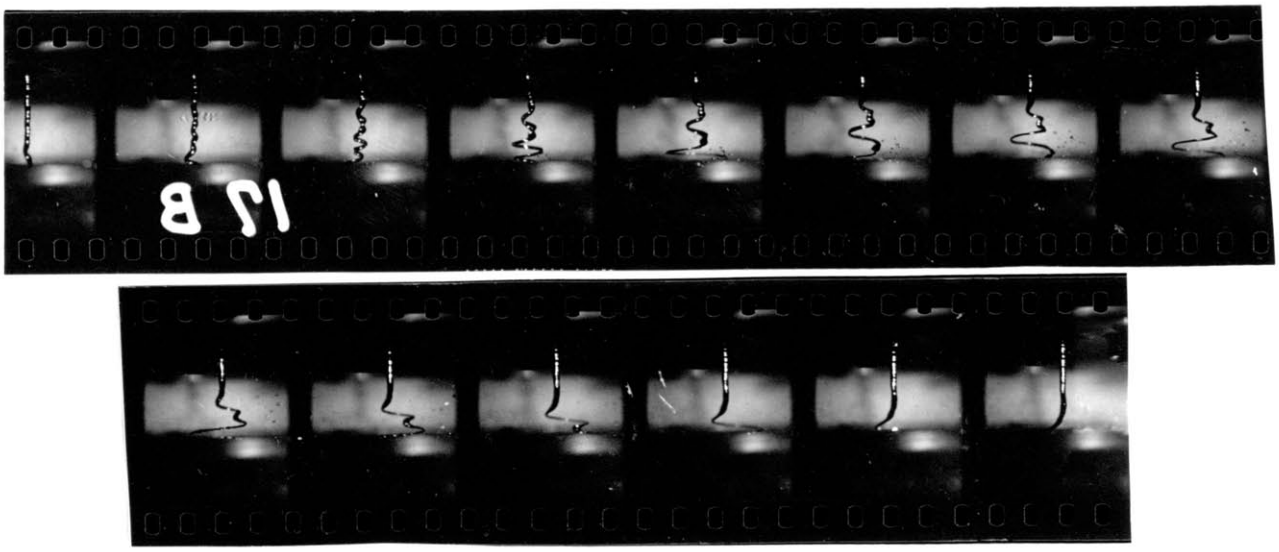

Test 17 A

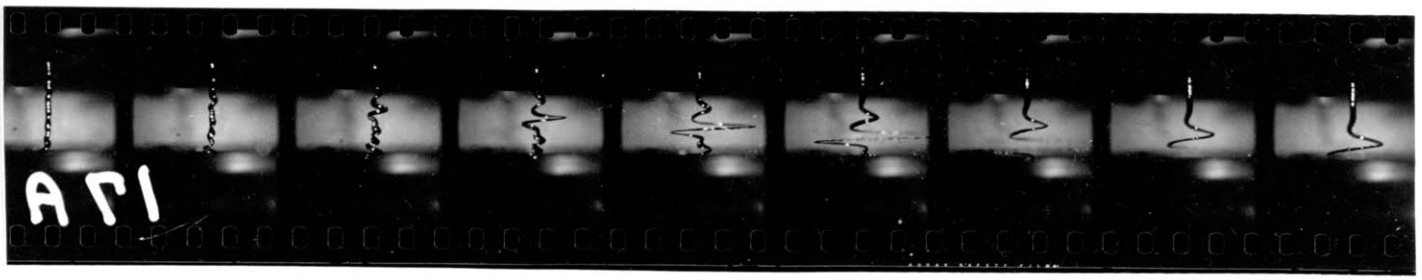

Test 18 A

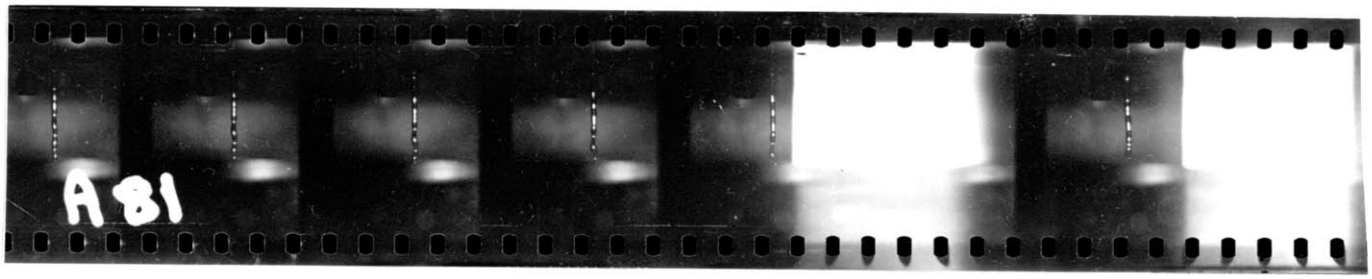

Test 18 B

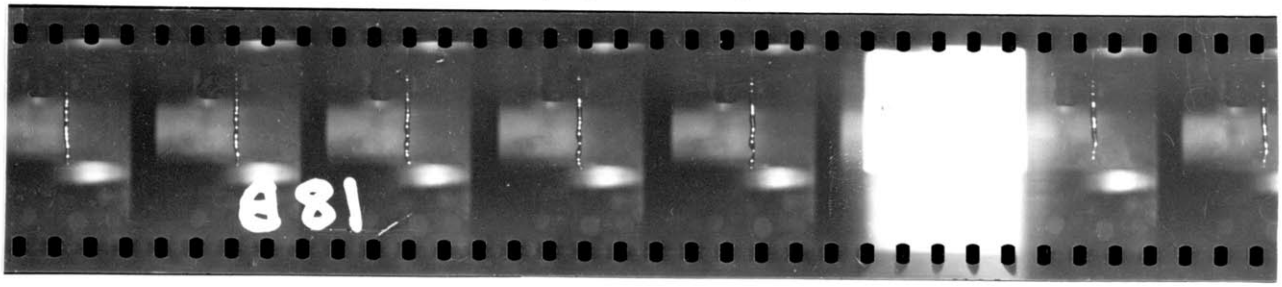

Test 18 C

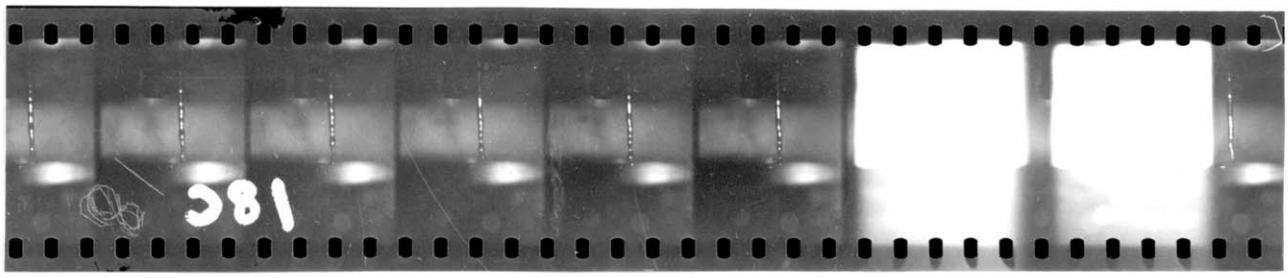

Test 19 B

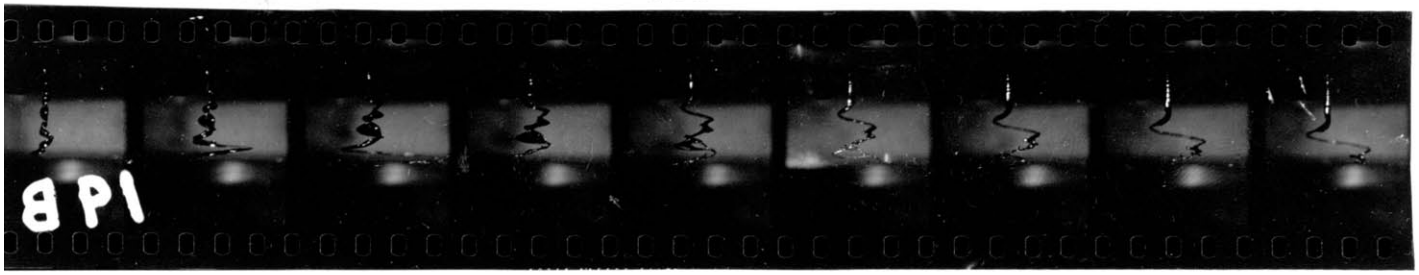

Test 19 C

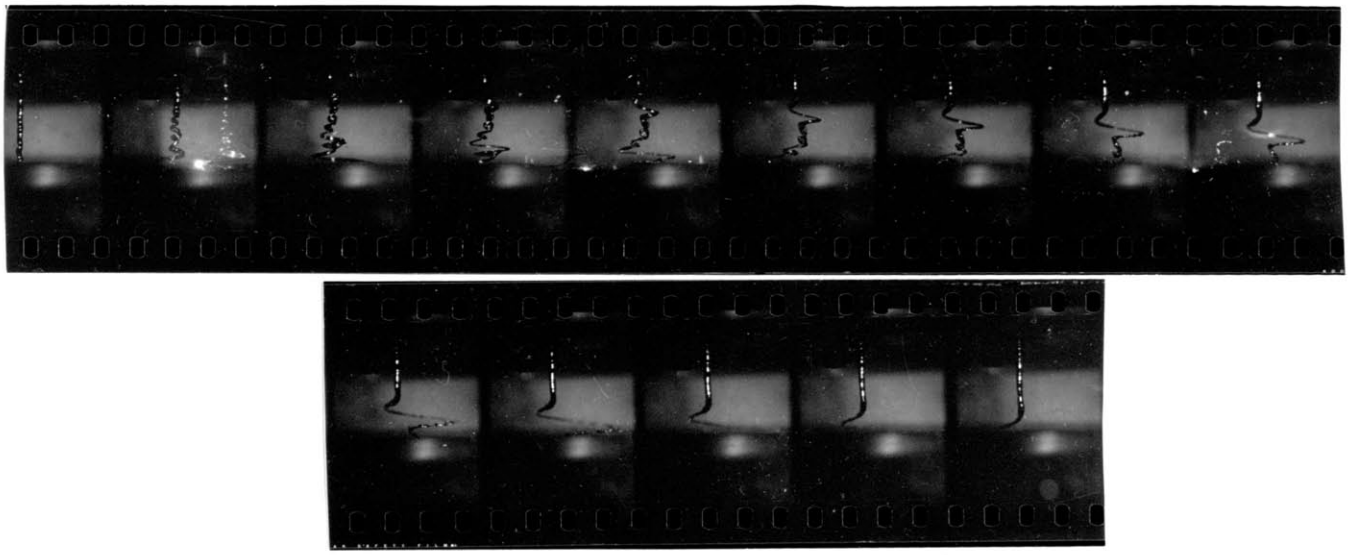

Test 19 D

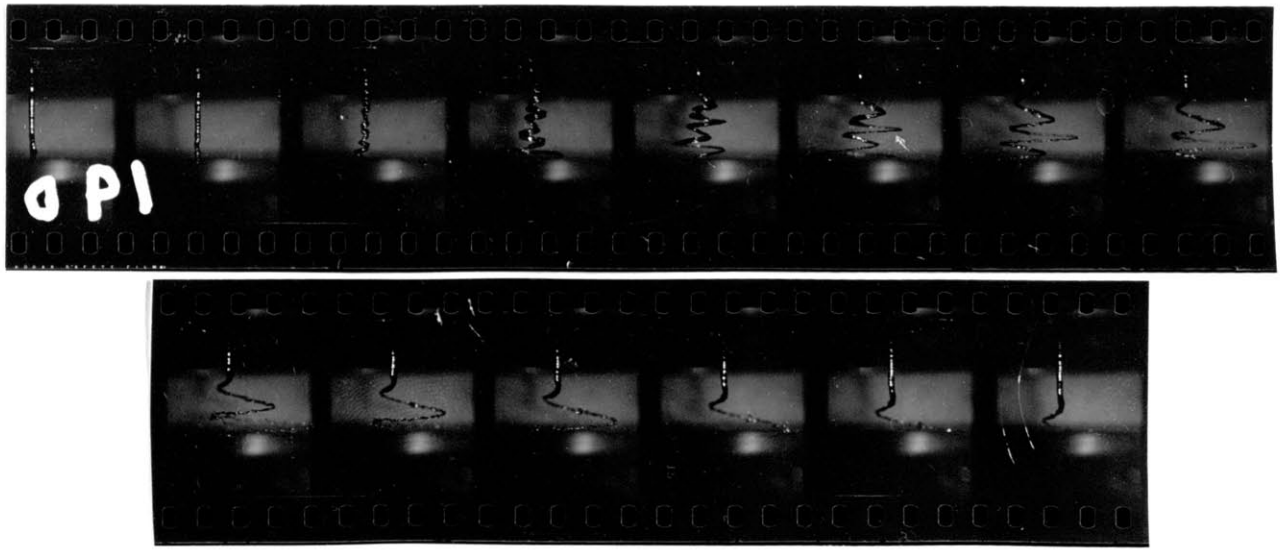

Test 21 A

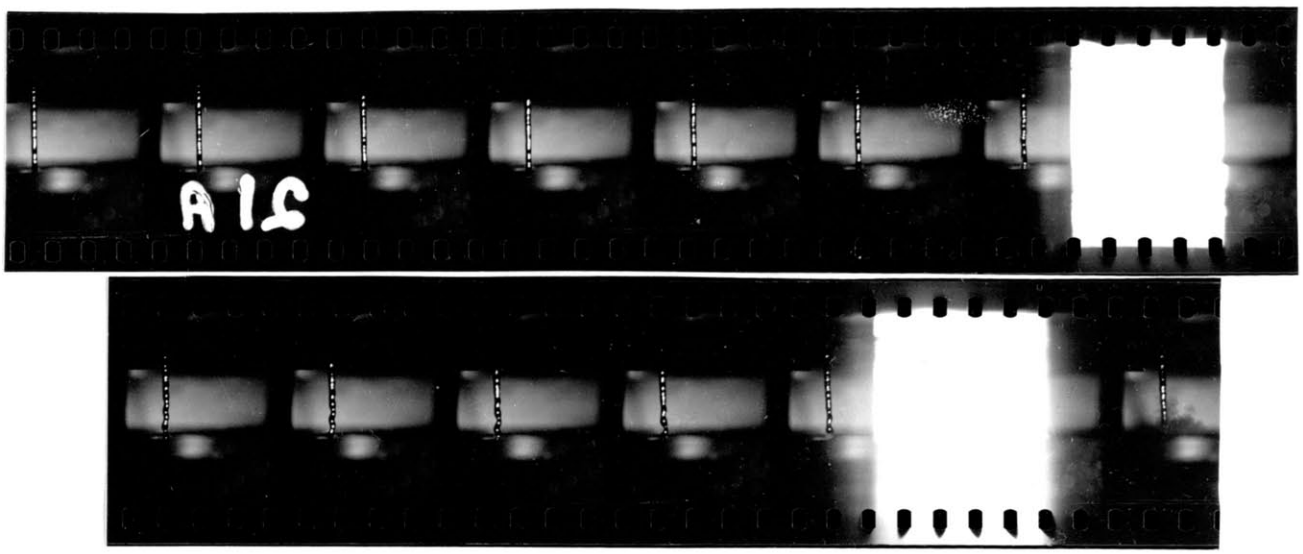

Test 21 B

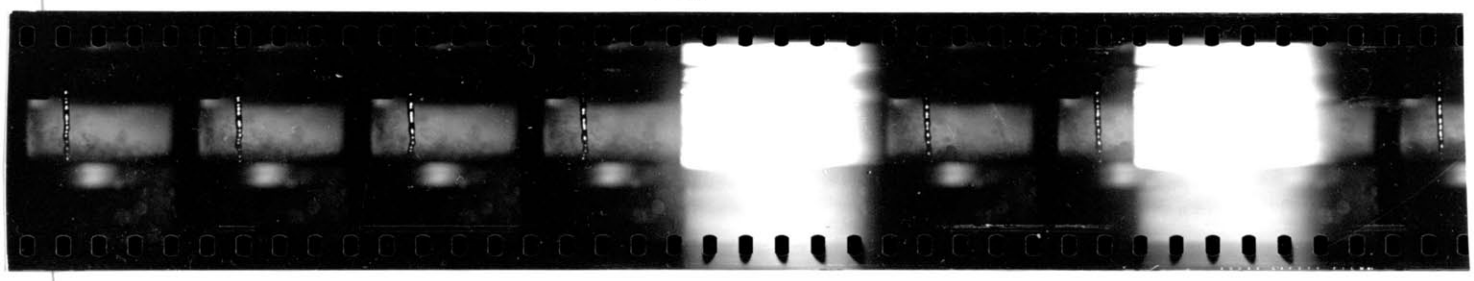

Test 22 A

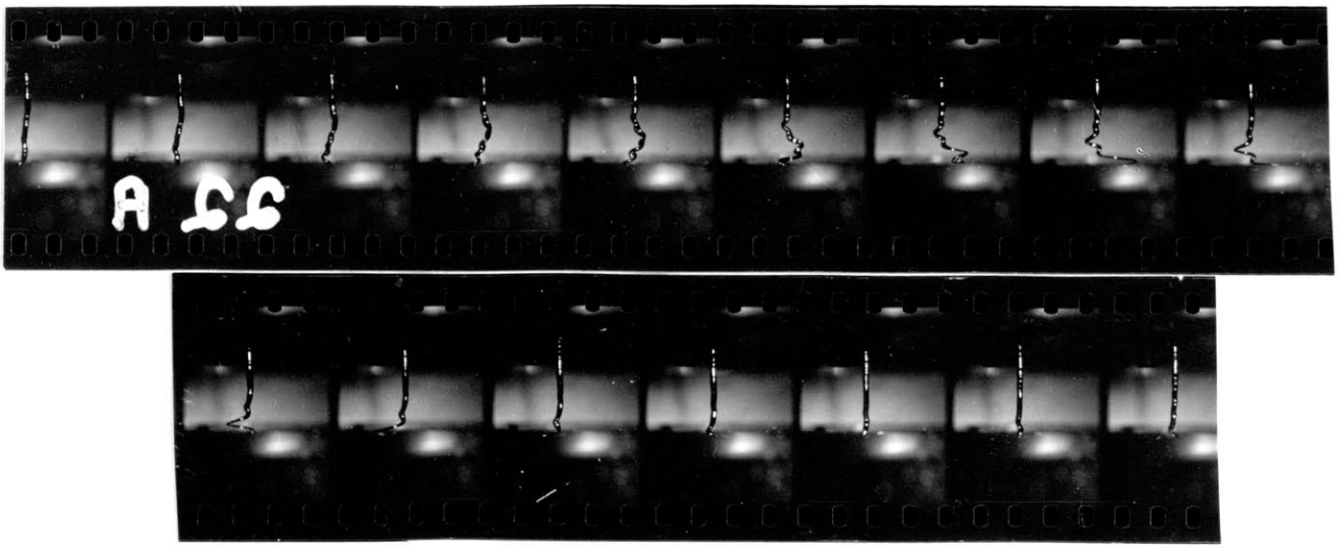

DISCLAIMER

Page has been ommitted due to a pagination error by the author.

Test 22 B

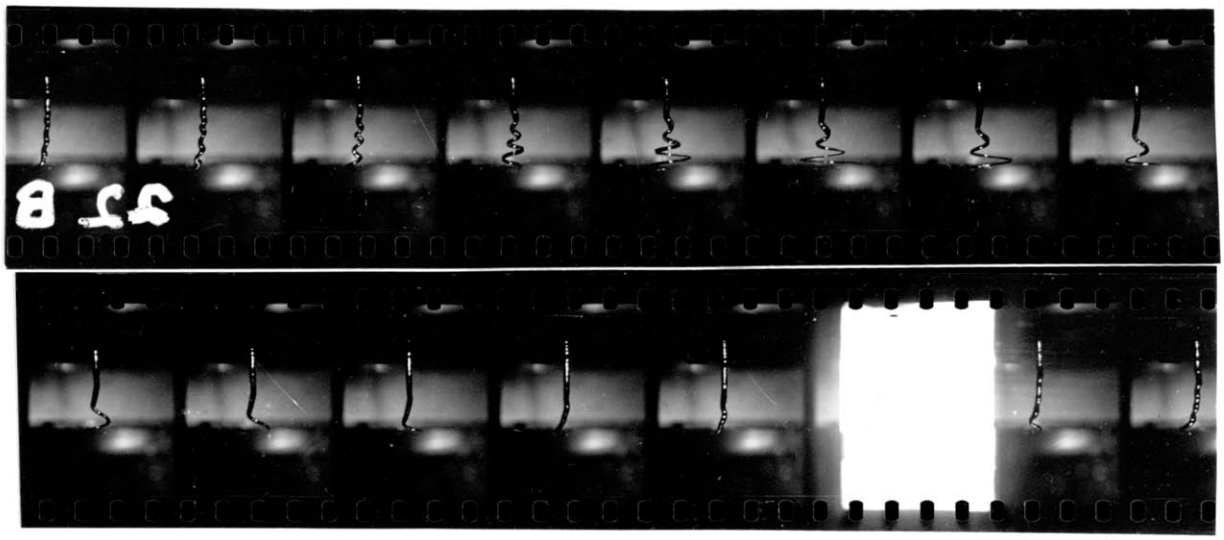

Test 23 A

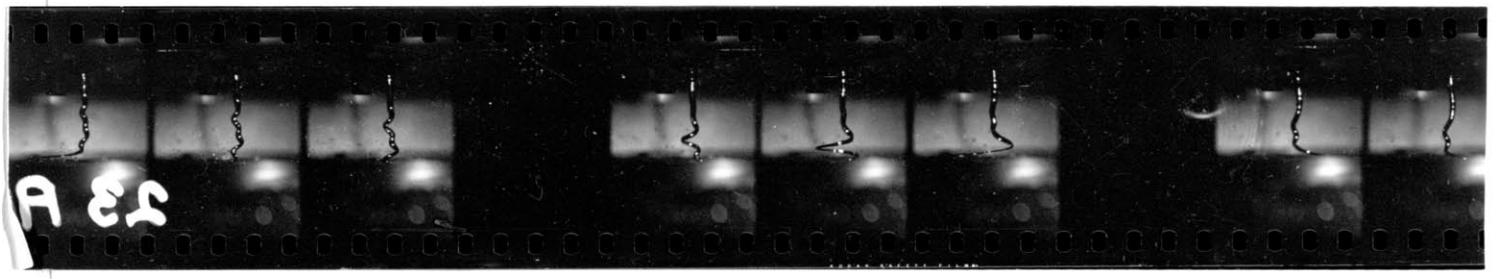

Test 24 A

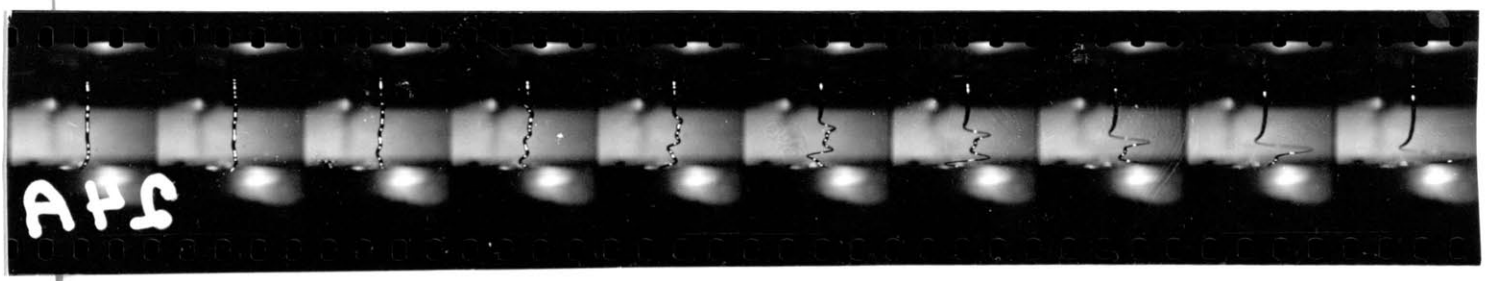

Test 24 B

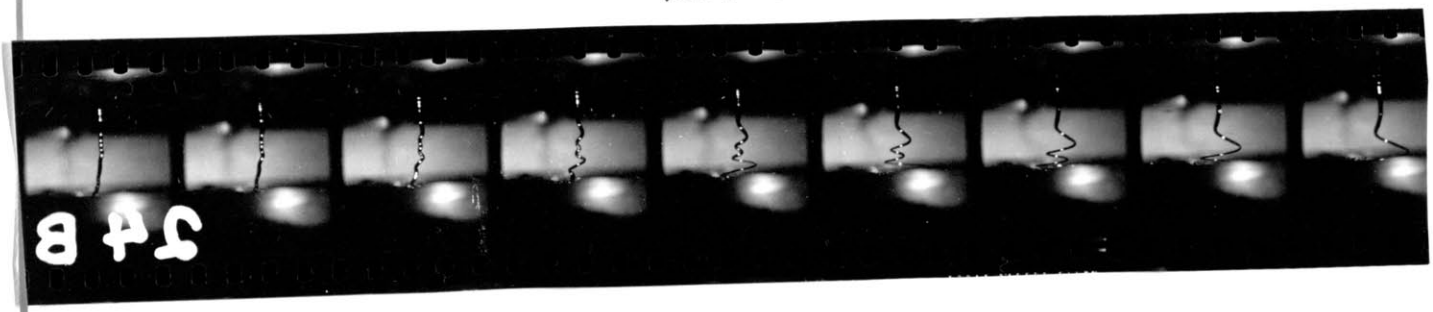

Test 25 A

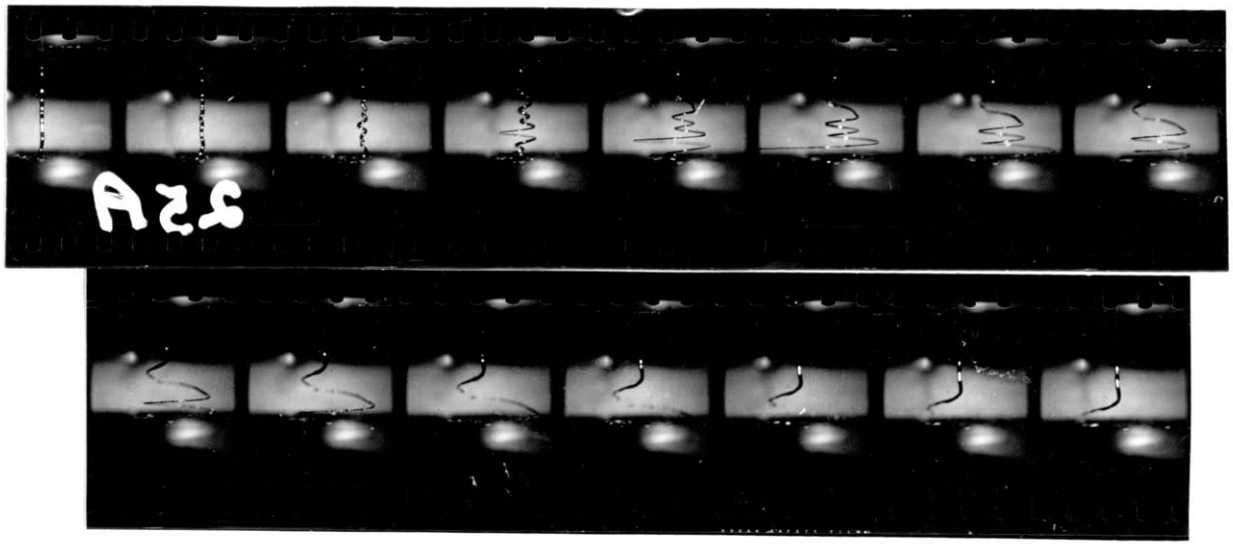

Test 25 B

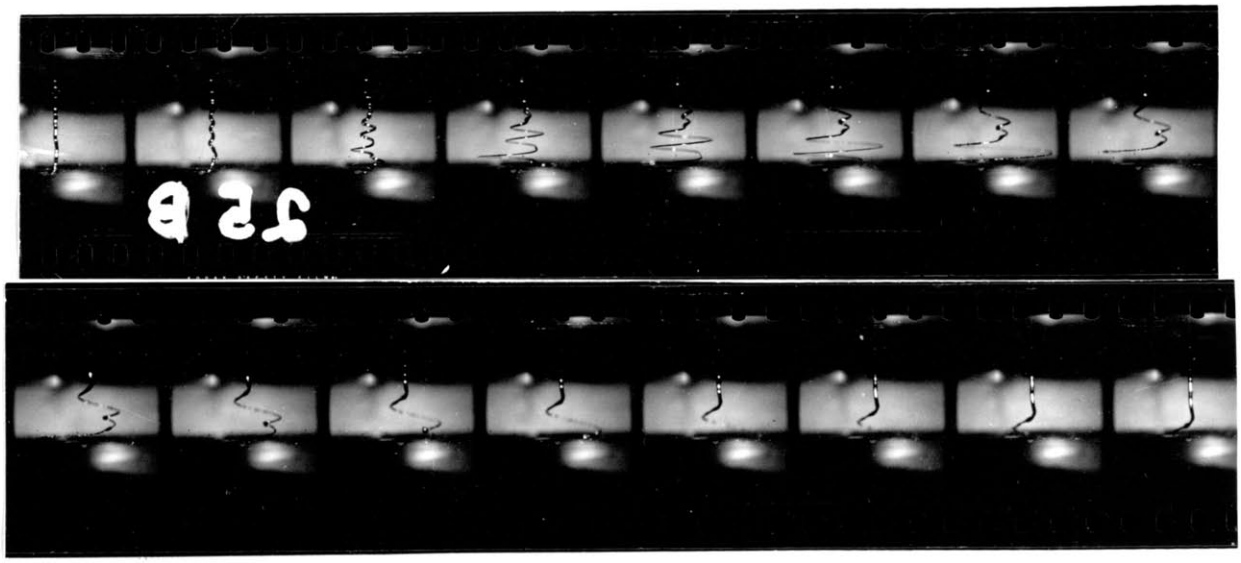

Test 25 C

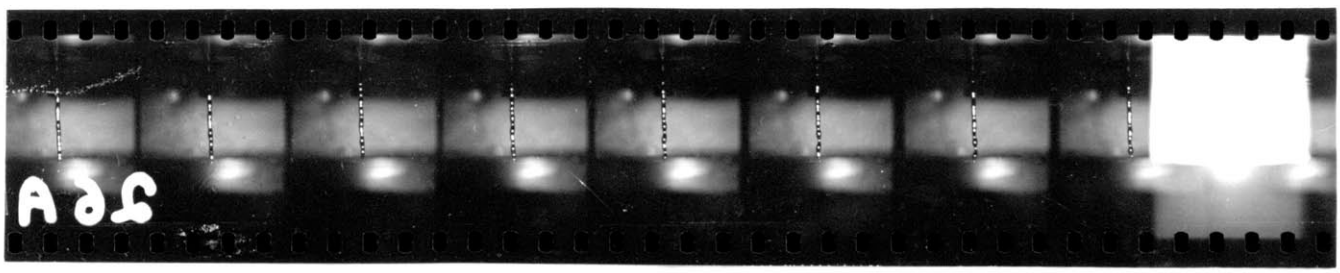

Test 26 B

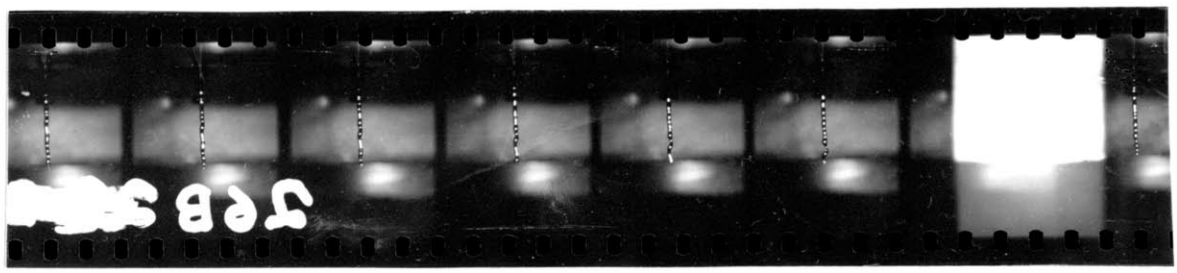

Test 26 C

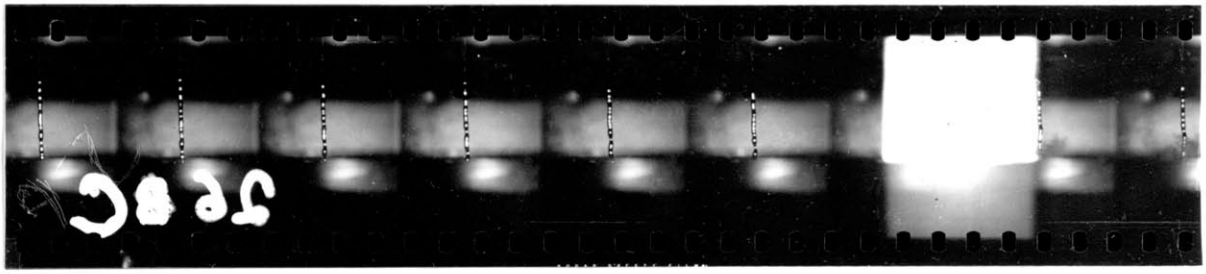

Test 27 A

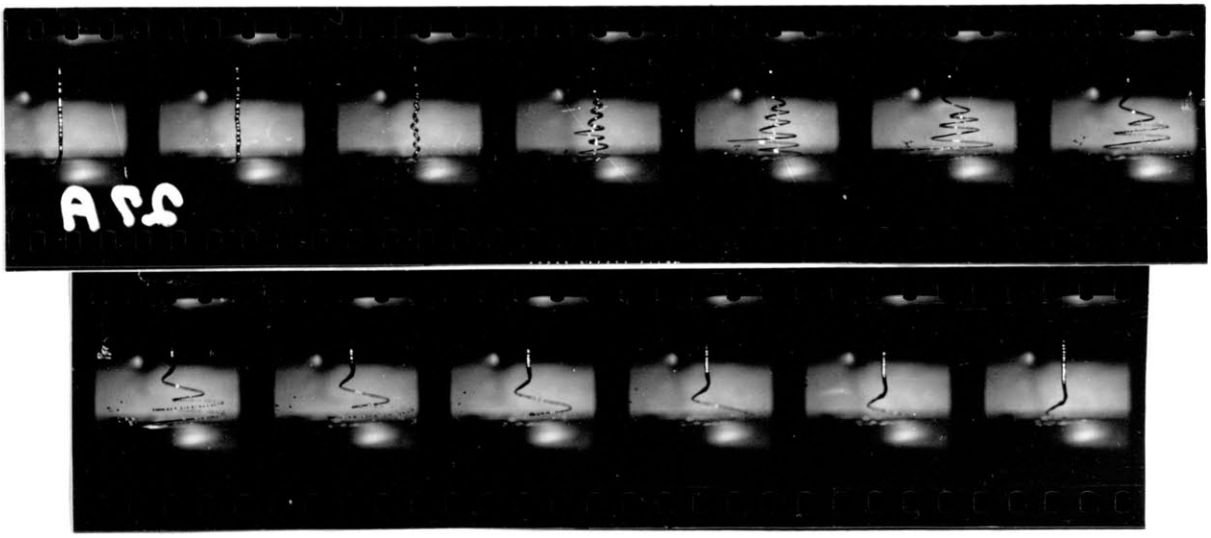

Test 27 B

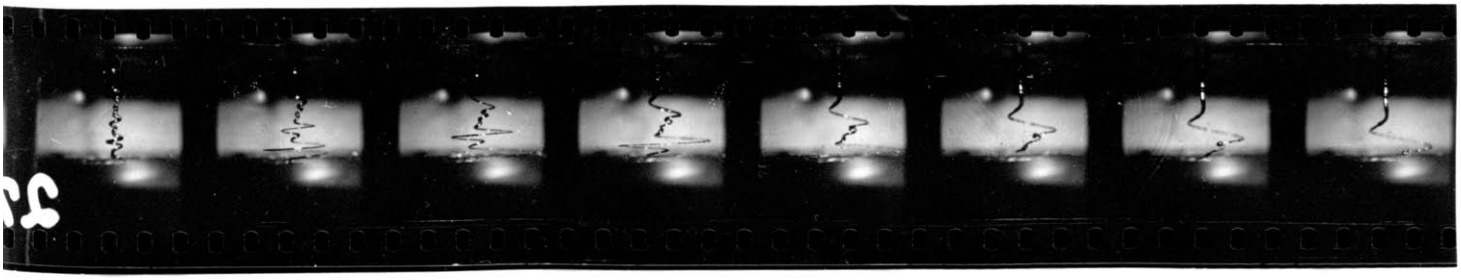

Test 28 A

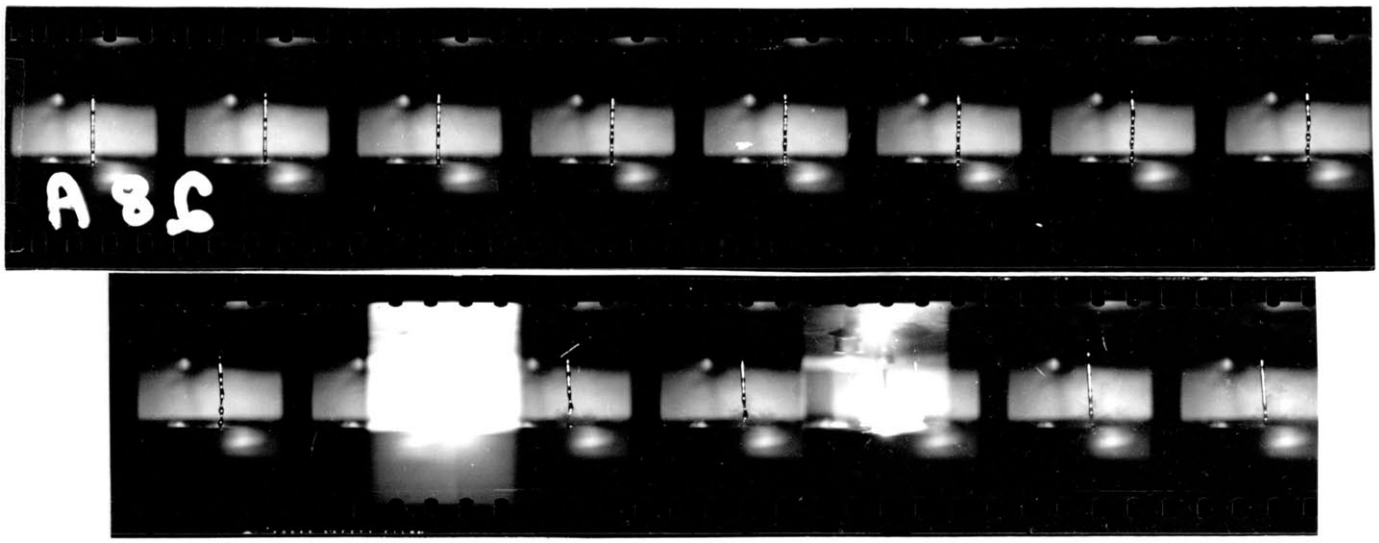

Test 28 B

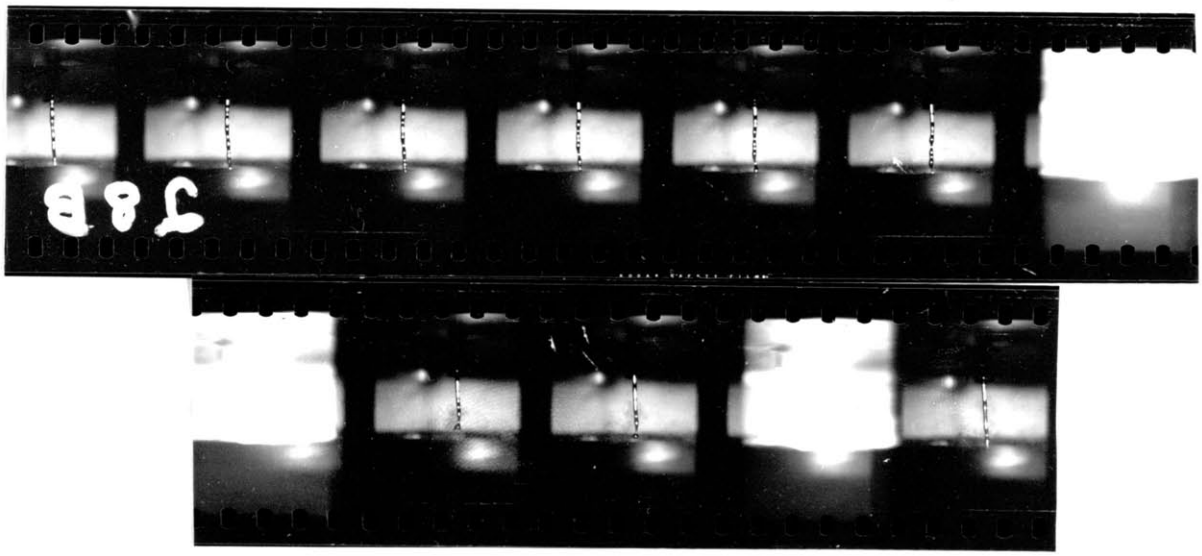

Test 29 A

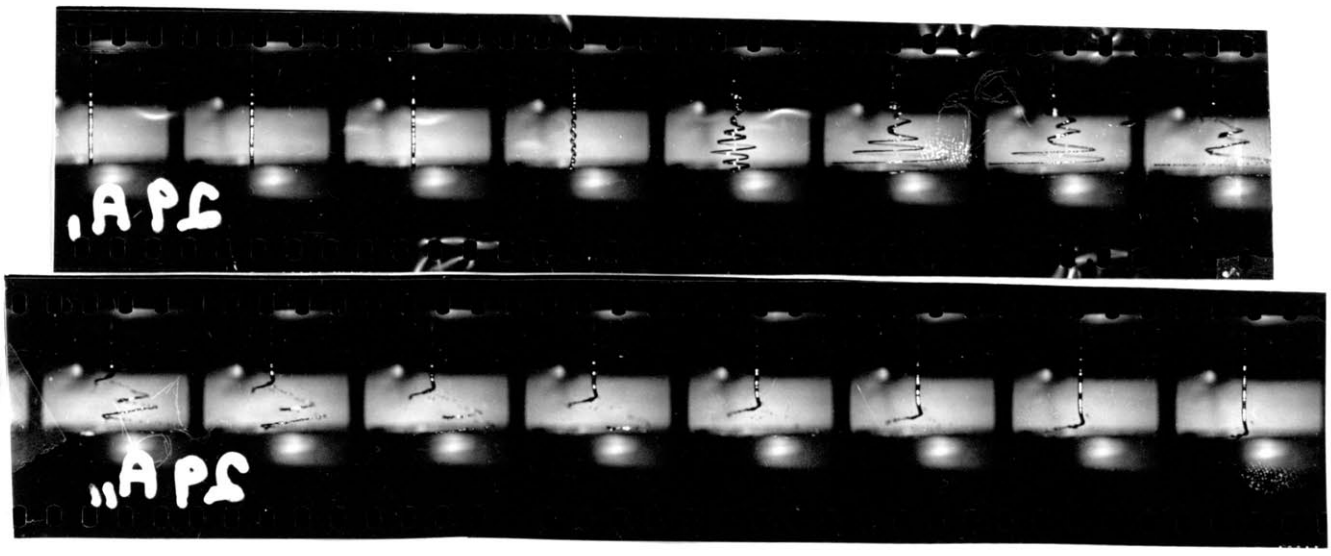

Test 29 C

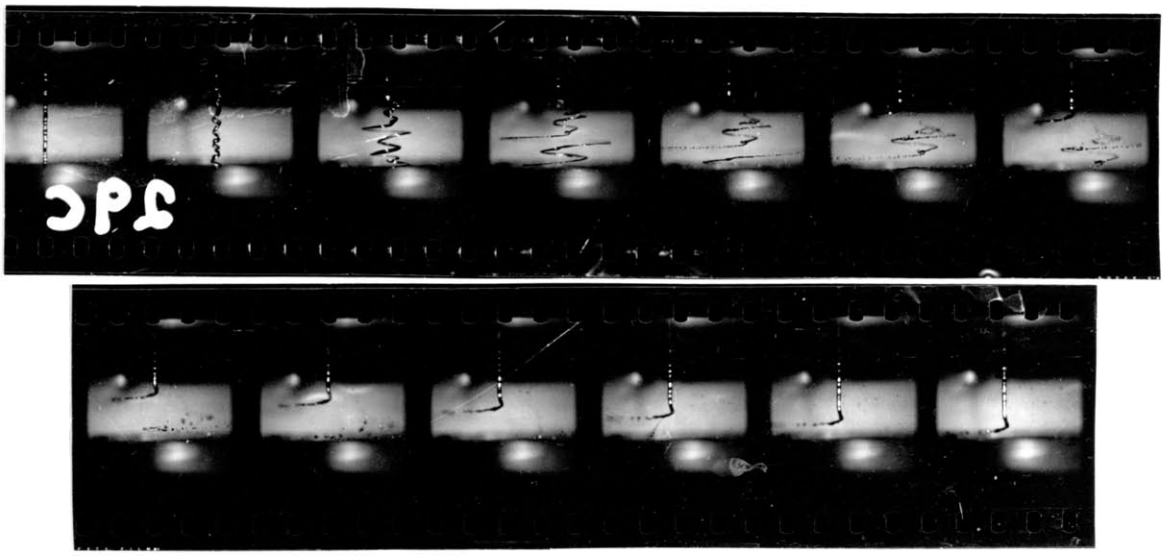

Test 30 A

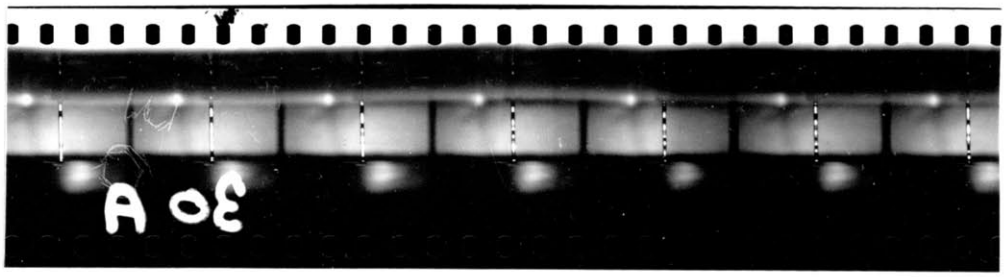

Test 31 A

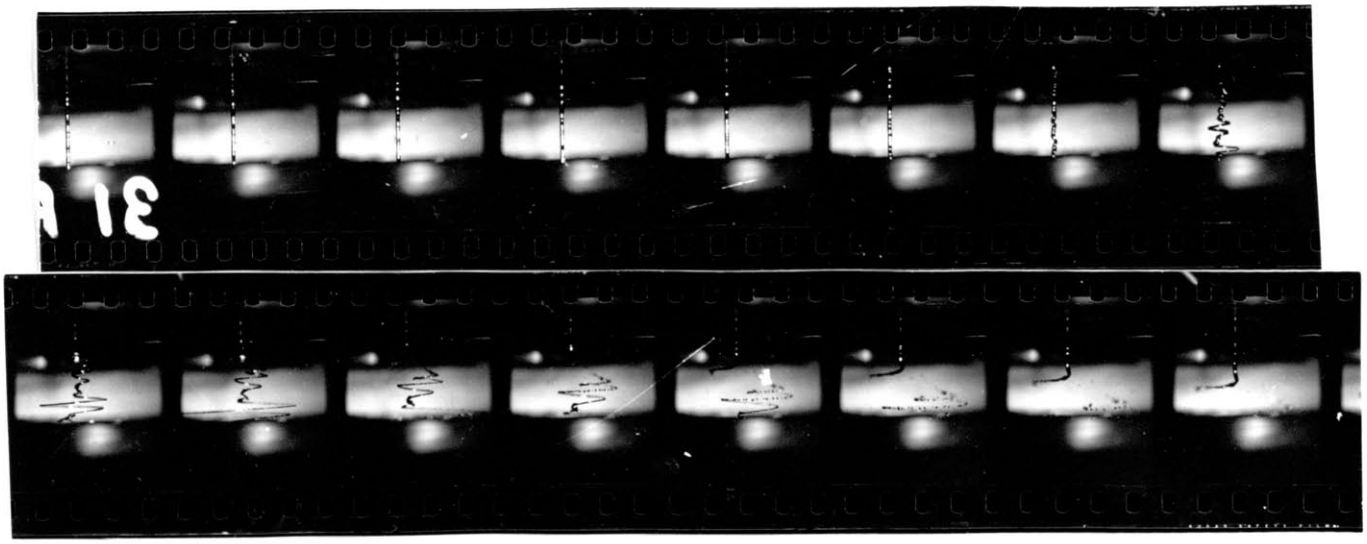

Test 31 B

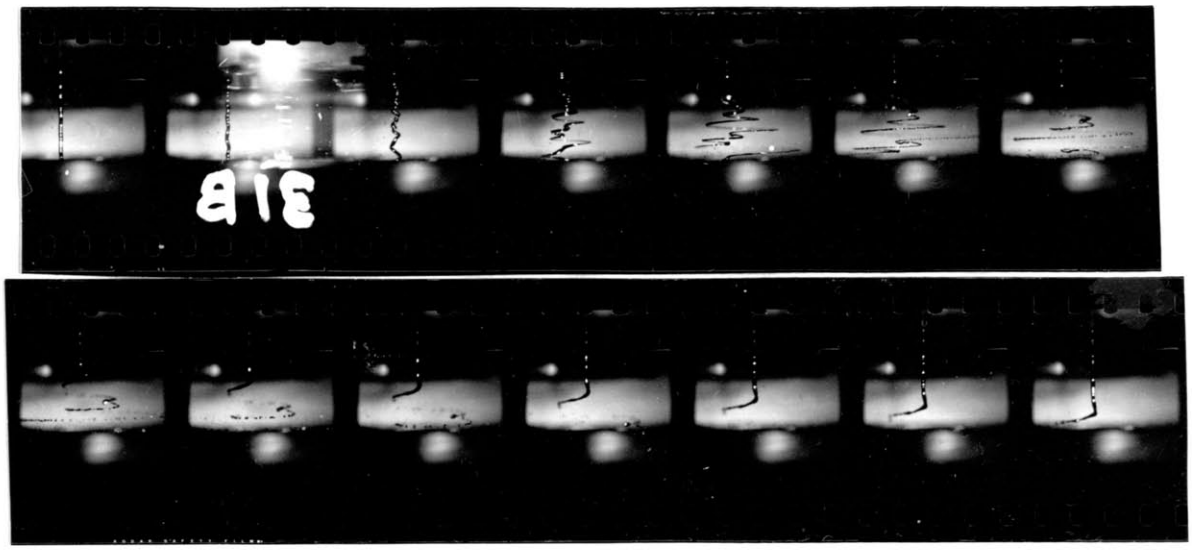

Test 32

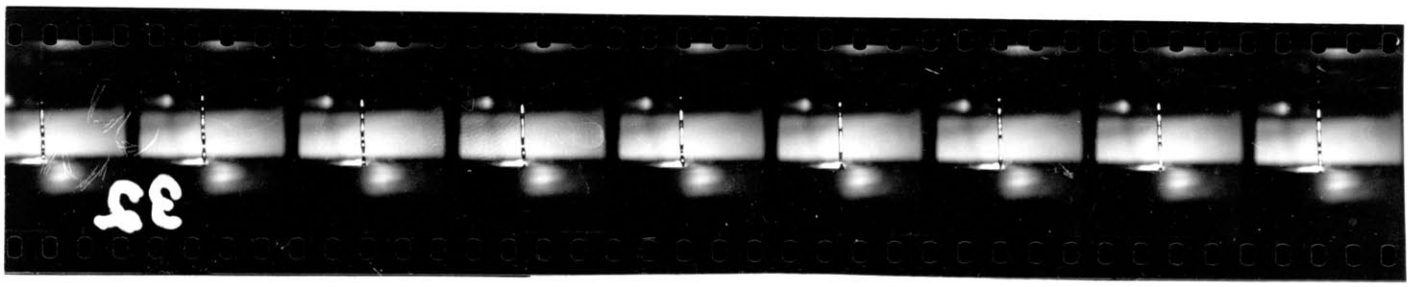

Test 33 A

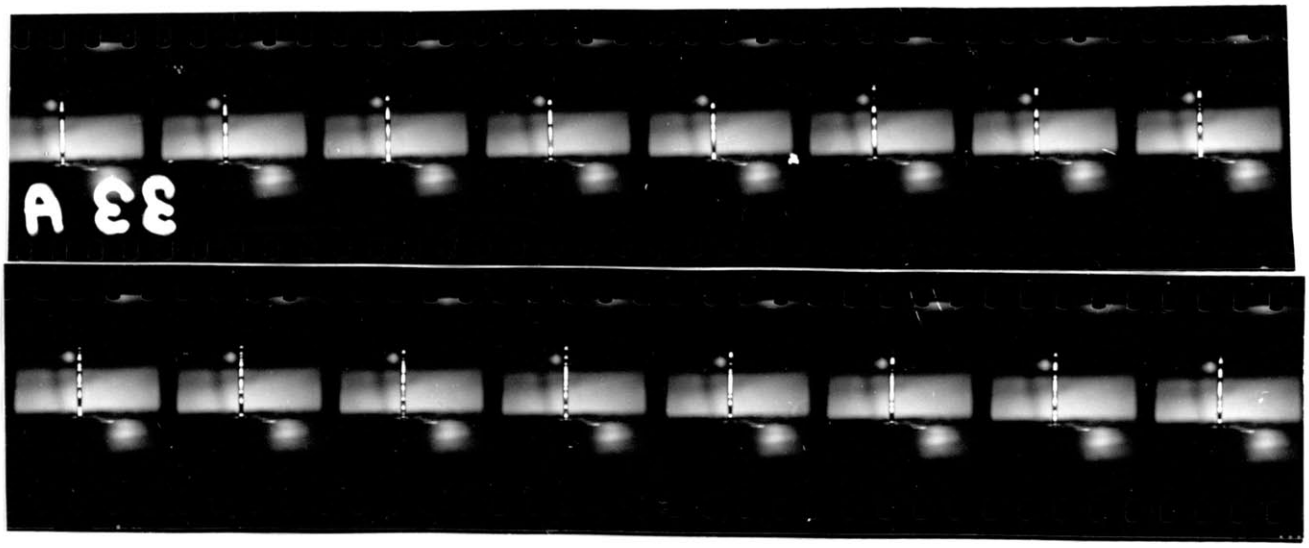

Test 34 A

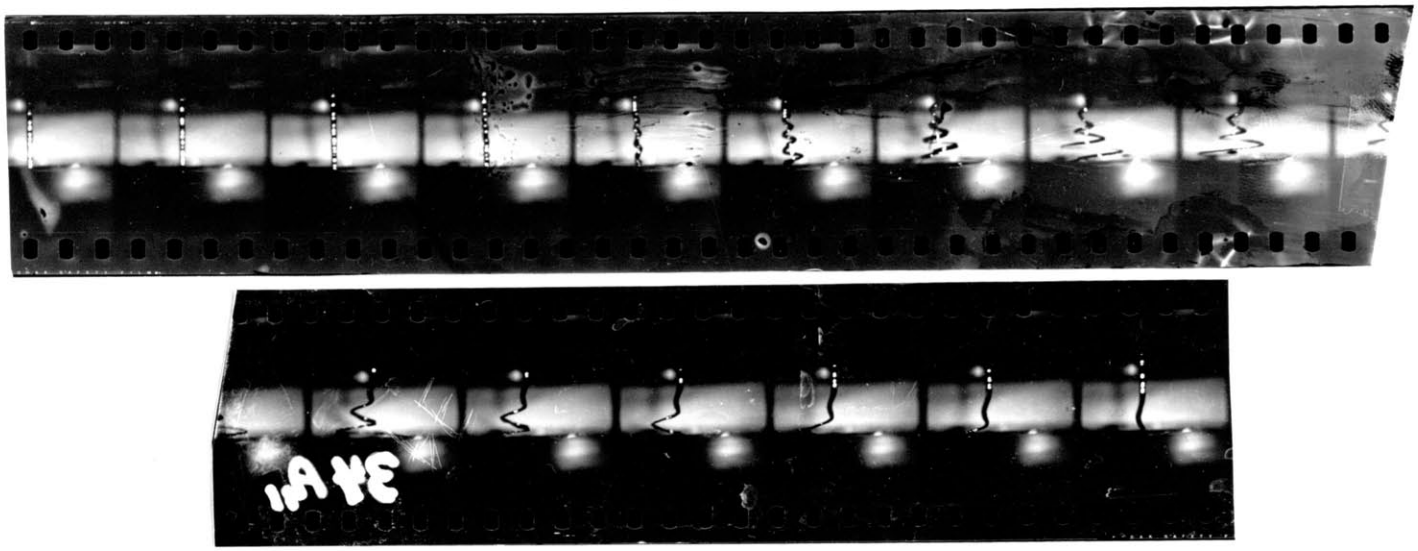

Test 34 B

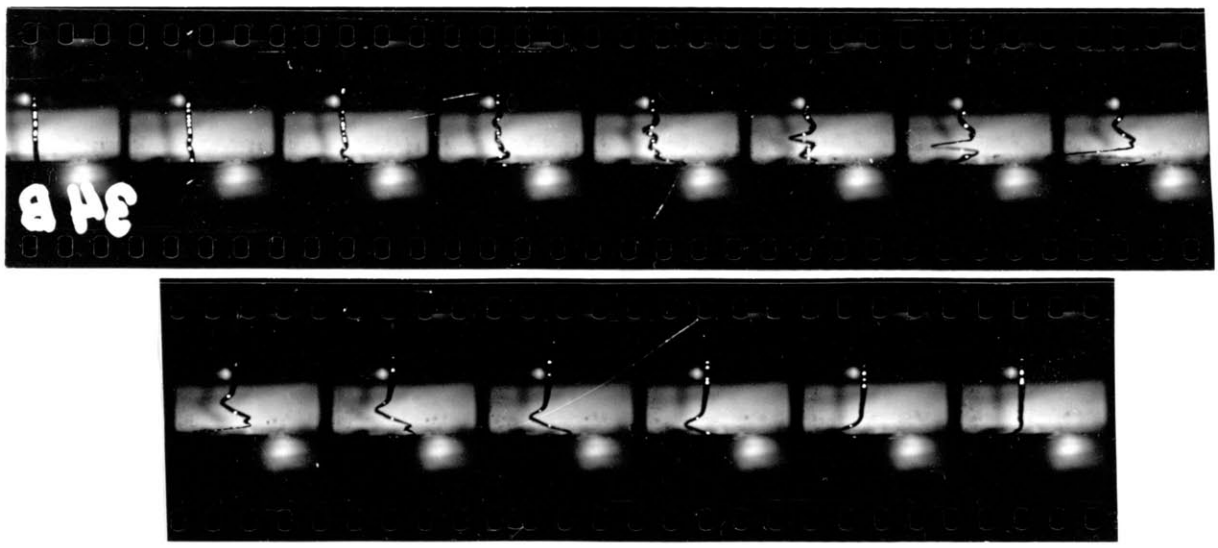

From a general perusal of the photographs, one clearly sees the pinch and spiral instabilities predicted in the theory.

Each film strip represents a section taken from the 14 feet of film used in each test. Often several sections are presented from each test (a test number between 1 and 34 was assigned to each test; capital letters designate sections within a test, e.g., 22C, etc.). It was found that within a test the phenomena observed were periodic. This is due to the current "cut-off" nature of the instabilities. For a pinch, the mercury begins in what appears to be equilibrium, pinches off (the current therefore going to zero), and then returns to equilibrium (that is, looks like a smooth stream flow with no perturbations). The process repeats itself when the current begins flowing through the mercury again. In an exactly analogously manner the spiral instabilities exhibit a periodic nature. Therefore, in the data presented, each strip represents one cycle from equilibrium to instability to equilibrium. It was also observed that all of the cycles of instabilities within a test fall into one or two classes. Therefore, we present only the typical examples of each of these types from each test, instead of presenting here all 14 feet of each of the 34 tests. From looking at the total 14 feet of film, there apparently is no time ordering of the types, which gives us the freedom to choose our examples randomly in time.

Each frame represents $\approx .004$ sec. Therefore, a complete cycle takes place in less than 1/10 sec; no wonder the instabilities could not be observed visually.

Some of the frames are "white" due to sparking in the mercury. When the mercury pinches down so far, apparently the current approaches zero so rapidly that $L \frac{dI}{dt}$ is much greater than the ionization potential of mercury and therefore causes the current to arc. The open circuit voltage is not large enough to cause such a breakdown. We shall say more about this later.

In general, we see that for $B_o = 0$, the current pinches and then sparks. For $B_o > 0$, the mercury spirals outward, and then apparently breaks electrical contact so that the spiral stops growing and simply falls into the reservoir below. Therefore, the last 4-6 frames of a test are usually uninteresting. We show a complete cycle in the No. 9C and No. 10A tests but because of space limitation have chopped off the uninteresting end section of the rest of the cycles. Any exceptions, though, are presented in their entirety.

In addition to the photographic data of the mercury stream, we have the current characteristics taken from the Sanborn recorder. The recorder was used to obtain the qualitative nature of the current behavior. However, we now feel that new information may be obtained if we could correlate the film with the pulses on the recorder. Future experiments will be designed with an electronic synchronization device. As a first approximation, the recorder and film were synchronized by mechanically synchronizing an extra flash of light on the camera lens with a mechanical timer in the recorder. The results were generally unsatisfactory because

of mechanical lag and of difficulty in distinguishing the flash from the mercury sparks. However, at present the film and recorder data cannot be uniquely correlated. This will not bother us, because for pinches, the sparks correlate the current and the film, and for spirals the current pattern was cyclic in the same way that the spirals on the film were cyclic (later we present results showing that the cycles are of identical duration).

The results of the oscillograms of the current for the 34 tests show that the current obeys one of the five typical types displayed on the next page. Later we shall describe the other tests in terms of these. In each of our examples, we take about 1 sec of paper from each of the 5 tests. Note in particular the time scale on the Sanborn data in comparison with the time scale on the films ($\approx$.004 sec/frame). For example, each major peak represents a <u>whole cycle</u> of a spiral instability.

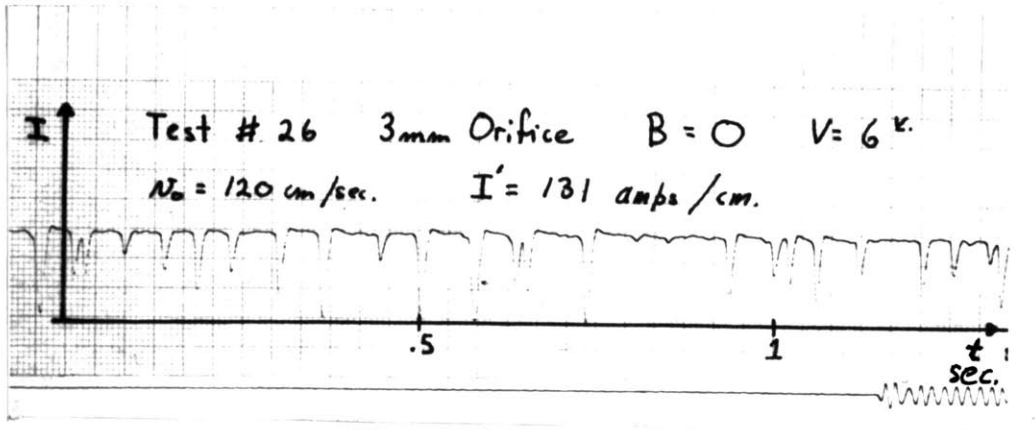

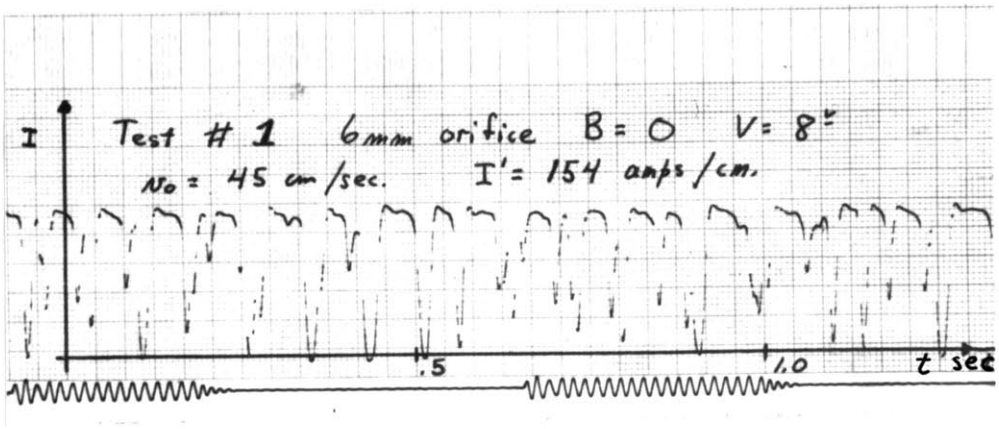
I
Test # 1 6mm orifice B = 0 V = 8v
N_0 = 45 cm/sec. I' = 154 amps/cm.
.5
1.0
t sec

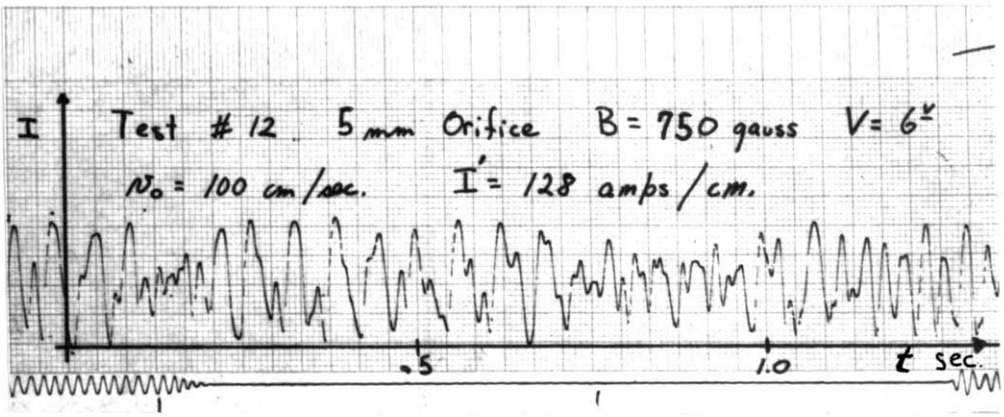
I
Test # 12 5 mm Orifice B = 750 gauss V = 6v
N_0 = 100 cm/sec. I' = 128 amps/cm.
.5
1.0
t sec.

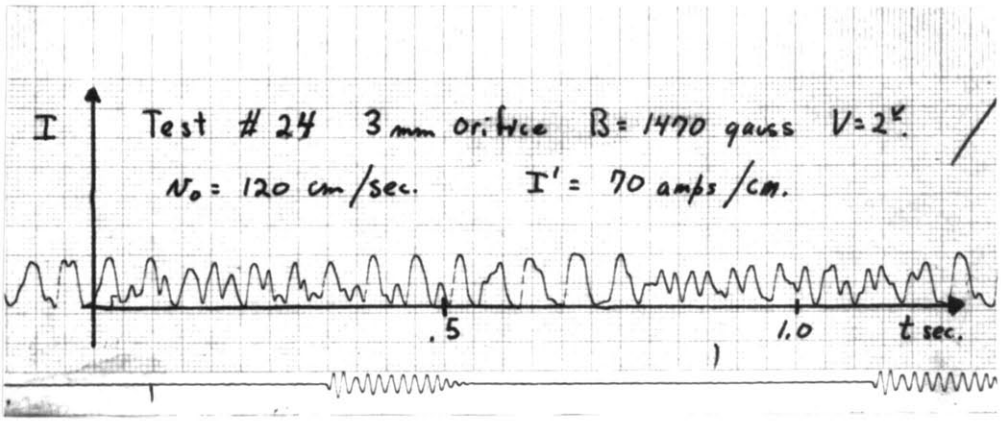
I
Test # 24 3 mm orifice B = 1470 gauss V = 2v
N_0 = 120 cm/sec. I' = 70 amps/cm.
.5
1.0
t sec.

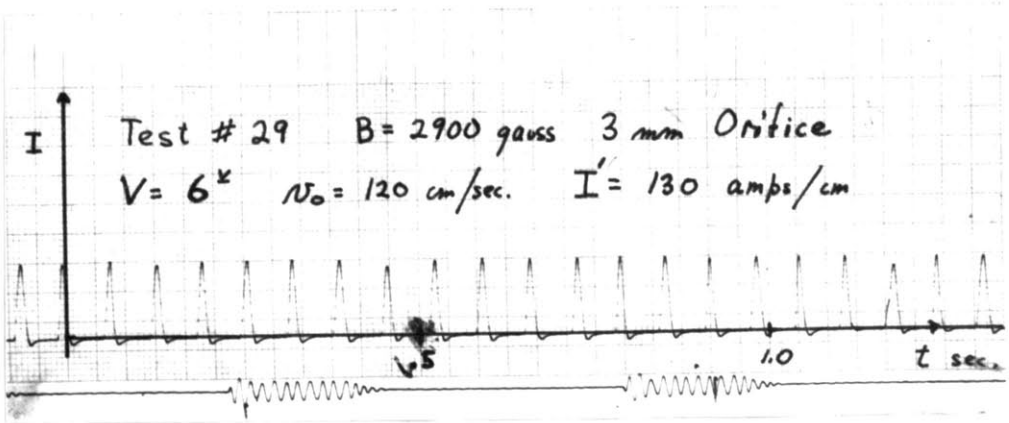
I
Test # 29 B = 2900 gauss 3 mm Orifice
V = 6v N_0 = 120 cm/sec. I' = 130 amps/cm
.5
1.0
t sec.

For the tests No. 26 and No. 1 (for $B_o = 0$), the current is on most of the time -- but the pinches intermittently cut the current down (often to zero). The number of pinches is greater for high currents than low currents.

For tests Nos. 12, 24 and 29 the current is off more time than it is on -- characterized by major peaks separated by a few minor peaks. The minor peaks disappear as the magnetic field increases, the mercury stream acting as a "noise-free pulse generator" in No. 29 (for the highest magnetic field shown).

In tests Nos. 12 and 24 on the Sanborn data, we note a somewhat periodic nature of the major peak heights (tests Nos. 24 and 12 exhibit spiral instabilities), that is the maximum current of the spiral cycles seems to be a function of time. Reason: If we start with a smooth stream so that the current is the maximum possible, then the forces causing the spiral are very large and cause the mercury to spiral very widely and quickly, hence violently. The stream becomes thinner, and the current goes down very close to zero. The stream breaks into droplets because of the violent disturbance. Therefore, the main stream loses most of the mercury which went into the spiral except for a small tail (most of the spiral breaking away in droplets). The stream will then remake contact on the lower plate via the "tail." Therefore, the current surge for the next cycle will be almost, but not quite, the same as the smooth stream's initial surge of current

because the tail has a higher resistance. But if the current is less, we should expect the violence of the spiral to be less. Therefore, again the mercury spirals and breaks up, but the "tail" left on the main stream is now longer because the forces were less violent. Therefore, since the tail is longer, when the mercury makes contact the third time the current is even smaller. Repeating the above process several times, the current peak should drop to a minimum value. The minimum is determined by surface tension -- the "tail" can only be so long and thin. Therefore, the "tail" breaks off and the initial contact is made again by the main stream thus giving a large surge of current, etc., etc. The "tail" can clearly be seen in the last five or six pictures of Nos. 9C and 10A. Note that it <u>is</u> thinner than the main stream.

For the most part, the periodic variations of the amplitude of the major peaks are small. We shall note the cases where they are large, because they could change our value of I_o by as much as 20%. One can note such variations on two of the 14-foot lengths of film (Nos. 12 and 17). Other films show differences in cycles but <u>not</u> of a periodic nature as described above. Care was taken for the most part to select tests which give us current at the maxima so that we know approximately what the value of the current is. However, the possibility of an error of as much as 20% in I_o is possible. This is the main reason why we desire to synchronize $I_o(t)$ with the film so that we have <u>all</u> the currents of all

the cycles as a function of time. Clearly, the study of the periodic nature of the current would be an interesting problem in itself. However, for the present we are interested mainly in the over-all picture of the instabilities; such details can be investigated later.

Here it might be mentioned that on tests Nos. 28, 29, 31, and 34 the current was turned on after the camera was running (a very delicate operation since the film ran out in $\sim$1 1/2 seconds). Unfortunately none of these four tests exhibit the periodicity of the amplitude of the major peaks of the current near enough to the beginning of the test to be of any value, i.e., the current peaks are all approximately the same height at the start of each of these runs.

Before comparing the results of the various runs to obtain the I_o, B_o, v_o, and R_o dependence, let us first point out certain qualitative aspects of some of the more unusual photographs.

Test 1. We note the side pinch as described in the theoretical predictions. Also, a mercury spark provides light to photograph itself, revealing a well-defined pinch with the mercury pinched down to almost a thread.

Test 2B. Side pinch.

Tests 3 and 4 represent the 6 mm stream with $B_o = 0$, $I_o = 0$. We note that the stream is fairly nonuniform, which gives us very large initial perturbations. The asymmetry probably leads to the excellent side pinches in Tests 1 and 2.

DISCLAIMER

Page has been ommitted due to a pagination error by the author.

However, because of this, we ran most of the tests on the 5 and 3 mm streams, which are extremely smooth for $I_o = B_o = 0$ (see Tests 5, 6, and 8).

Test 7B reveals two side pinches forming, culminating in two sparks.

Test 10B, frame 4. A globule of mercury forms at a bend of the stream at the expense of thinning the stream.

Test 13B, frame 10. Beads form along the stream. (This is probably due more to surface tension than to the current.)

Test 15A through G. The stream has a tendency to broaden and flatten out(this appears as a globule in the photographs) at the bends of the spiral. This is especially true in Test 15F, frame 8, where the globule actually splits, the two halves then spiralling around one another. A blow-up of this phenomenon appears on the next page. Note that the radius of the spirals of the bifurcated streams is approximately one-half that of the original stream. The current divides; therefore, the magnetic force should be approximately half. Note also the pinches which appear on the stream. Such a bifurcated stream was theoretically explained earlier (though probably inadequately).

This is probably the first time such an instability has been observed; indeed, such an instability invites a great deal of further study.

Other cycles in Test 15 show signs of splitting; Test 15C, frame 6, splits but it is almost out of the range of the

camera. The bifurcation phenomena appear to occur only for very high fields.

Note the pinches along and the very wide radius of the spiral in Test 15A.

Test 17B. A globule of mercury travels along the stream.

Test 18A, B, C. Nice symmetrical pinches.

Test 19B. A globule again forms and bifurcates as in Test 15F.

From these pictures it is clear that the globule is more nearly a thin sheet of mercury rather than cylindrically solid. Under such conditions surface tension is probably responsible for the split. Such a phenomenon may suggest experiments with rectangular streams of mercury where, in particular, one side of the rectangle is much greater than the other, and with elliptically shaped streams.

Test 22B. A very symmetrical spiral.

Test 25A and B. Very wide, symmetrical spirals with many loops.

Test 27A. Wide, many looped spiral with whole loops breaking into droplets.

Test 28A. Three pinches in a row -- magnificent.

Test 29C. Note how small the tail is after a violent spiral (tending to support a previous hypothesis).

In addition to their scientific beauty, of course, one cannot fail to appreciate the aesthetically pleasing nature of some of the photographs.

Before going further, we should discuss briefly B_o, h_o, R_o, and v_o. The magnetic field was calibrated for h_o = 4 inches and 6 inches. Previous work has shown it homogeneous to 2% in direction and magnitude, and to within .5% linear in current (for $I > 4^a$). Throughout the paper we shall refer to the magnetic field in terms of the amperage. Since we are seeking only comparison, such a reference is satisfactory. However, the conversion to gauss is given by

$$B_o = (142.4 \cdot I + 50) \pm 2\% \quad \text{for } h_o = 4"$$
$$B_o = (107.5 \cdot I + 30) \pm 2\% \quad \text{for } h_o = 6"$$

The initial stream speed v_o was measured (see the "Experiment" section). The results are shown in Fig. 1 for the three orifice diameters, 3mm, 5 mm, and 6 mm. In these graphs the dotted line extrapolates to the average value of time for 500 cc of mercury to leave the reservoir. All experiments were run with 500 cc but the total times varied from those on the chart by ± 2-3%. Therefore, our speeds v_o are valid by a corresponding amount. The shape of v_o vs t is due to baffles placed in reservoir A to support the copper rod.

The apparatus is constructed with five nozzles (ranging from 2-6 mm in diameter), four of which were corked during a test. Time permitted us to run tests on the 3 mm, 5 mm, and 6 mm streams. (Although we shall continue to refer to them as 3, 5, and 6, the actual diameters are 3.32, 4.70, and 5.75 mm, respectively.)

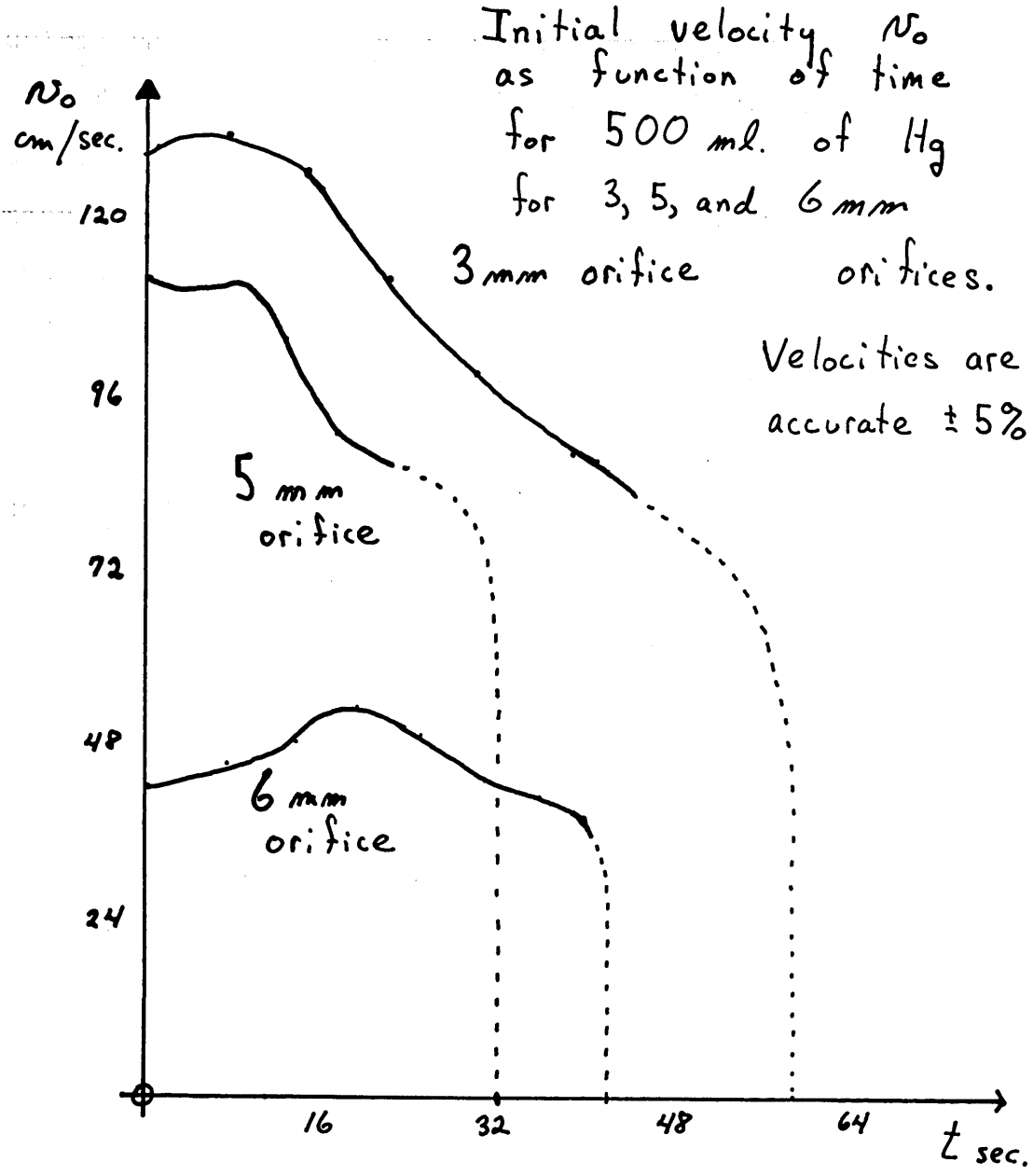
Initial velocity v_o as function of time for 500 ml. of Hg for 3, 5, and 6 mm orifices.
Velocities are accurate ± 5%
v_o cm/sec.
120
96
72
48
24
3 mm orifice
5 mm orifice
6 mm orifice
16
32
48
64
t sec.

Fig. 1.

Measurements of pinch size, spiral radius, rate of change of spiral radius, and stream speed were made by projecting the film on a piece of graph paper calibrated such that one unit equals .05 cm.

A summary of the details of each test follows. All tests were run at h_o = 4 inches, where h_o is the pole separation of the magnet.

Test	V volts	$2R_o$ mm	B_o amps	v_o cm/sec	I_{max} amps	I_{av} amps	Osc sec	ν amps
1	8	6	0	45	370	320	--	--
2	6	6	0	45	290	260	--	--
3	0	6	0	45	0	0	--	--
4	0	6	0	40	0	0	--	--
5	0	5	0	100	0	0	--	--
6	0	3	0	120	0	0	--	--
7	6	6	0	40	260	--	--	--
8	0	3	0	85	0	0	--	--
9	6	6	4	45	270	90	--	80
10	6	6	8	45	250	60	--	100
11	6	5	0	100	270	270	--	--
12	6	5	5	100	275	135	.6	20
13	6	5	10	100	265	70	1.1	60
14	6	5	15	100	270	35	1.5	100

Test	C	S	Type	$\tau \times 10^3$ sec.	T_1
1	.04	.17	1	6.7	--
2	.02	.05	26--Fewer but deeper peaks	6.7	
3	--	--	--	5.7	--
4	--	--	--	5.0	--
5	--	--	--	5.45	--
6	--	--	--	5.45	--
7	--	--	Wrong recorder speed--Sanborn data no good	5.45	--
8	--	--	--	5.45	--
9	.04	.2	12 and 24--Not as rough as 24 and I_{av}/I_{max} for 9 is less than for 24	5.45	13 ± 3
10	.04	.23	24--But some peaks 10% higher than the average peak height, and the peaks are more pointed	5.45	17 ± 1
11	0	0	No fluctuations--I = constant	4.3	--
12	.08	.25	12	4.0	16 ± 1
13	.08	.25	12--But I_{av}/I_{max} for 13 is less than for 12	4.0	16 ± 2
14	.06	.20	29--But more secondary peaks (but of small amplitude) between the main peaks; also, high amplitude periodicity in the major peak heights	4.0	16 ± 3

Test	V volts	$2R_o$ mm	B_o amps	v_o cm/sec	I_{max} amps	I_{av} amps	Osc sec	ν amps
15	6	5	25	100	265	18	.8	100
16	8	5	0	100	340	340	--	--
17	8	5	10	100	340	34	.6	120
18	8	5	0	85	325	310	--	--
19	8	5	20	100	300	150	1.1	60
21	10	5	0	100	415	370	--	--
22	2	5	15	100	84	40	--	15
23	2	5	30	100	77	20	.8	10
24	2	3	10	120	66	30	.8	15
25	2	3	25	120	62	10	--	0
26	6	3	0	120	190	180	--	--
27	6	3	10	120	190	40	--	10
28	6	3	0	90	184	140	--	--
29	6	3	20	120	182	30	--	0
30	2	3	0	85	65	65	--	--
31	10	3	10	120	270	20	1.0	10
32	4	3	0	85	130	130	--	--
33	4	5	0	80	170	170	--	--
34	4	5	15	100	170	50	--	40

Test	C	S	Type	$\tau \times 10^3$	T_1
15	.08	.13	29--But very high amplitude periodicity of major peaks--and more low amplitude peaks between the major peaks	4.0	16 ± 3
16	0	.025	26--But see S and C	4.0	--
17	.06	.25	12--But compare I_{av}/I_{max} and ν	4.0	16 ± 4
18	.02	.2	1--Compare C	4.0	--
19	--	--	29--Compare ν	4.0	16 ± 2
21	0	.17	1	4.0	--
22	.1	.25	24	4.0	16 ± 1
23	.1	.25	24 and 12	4.0	--
24	.08	.25	24	4.0	15 ± 1
25	.08	.08	29	4.0	18 ± 1
26	0	.17	26	4.0	--
27	.1	.1	29	4.0	16 ± 1
28	.06	.20	26 and 1	4.0	--
29	.11	.11	29	4.0	16 ± 1
30	0	0	No fluctuations--I = constant	4.0	--
31	.12	.12	29--But very high, sharp peaks	4.0	16 ± 1
32	0	.017	Almost no fluctuations--see C and S	4.0	--
33	0	0	No fluctuations--I = constant	4.0	--
34	.08	.42	12	4.0	15 ± 2

In the above chart, V is the voltage of the batteries supplying current to the mercury stream, R_o is the stream radius in mm, B_o is the applied external magnetic field in amps $B_o = (142.4 \cdot I + 50) \pm 2\%$, v_o is the outlet speed of the stream from the nozzle taken from Fig. 1 , I_{max} is the peak current of the major peaks as recorded by the Sanborn recorder, I_{av} is the approximate ($\pm$ 10%) time average of the current and is a measure of how long the current was actually flowing, osc is the average period of the fluctuations of the amplitude of the major peaks (about which we have spoken before), ν is a measure of the total maximum amplitude of the fluctuations of the amplitude of the major peaks (and is also a measure of the maximum uncertainty in I_o), C is a measure of the cut-off (for pinches) and cut-on (for spirals) of the current, i.e., the number of times per second the current cuts completely off or on, S is a measure of the total number of peaks/second (of all amplitudes) in the current pattern, type is a comparison with one of the five typical oscillograms presented earlier -- we note that I_{max}, I_{av}, osc, ν, S, C, and type almost completely characterize an oscillogram -- τ corresponds to the time between successive frames on

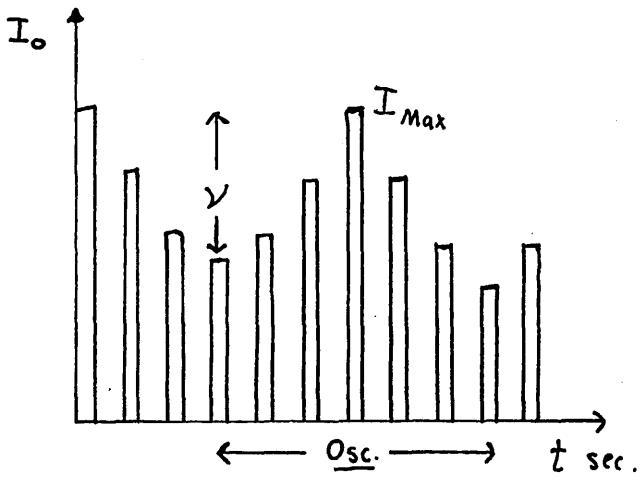

the film, and T_1 represents the number of frames for a spiral instability to complete its cycle.

We observe that $T_1 \approx$ constant for <u>all</u> V, v_o, and B_o, which means it is only a function of the apparatus or is a slowly varying function over the range of values we used. The approximate average uncertainty given for T_1 is a measure of the relative magnitude of ν. (These were measured independently.) This should be the case because longer cycles would imply smaller current pulses and short cycles larger current pulses. If one checks the cycles we are using, we find that they all are either average length or shorter implying that they represent the higher currents, i.e., $\approx I_{max}$.

In order to compare pinches and spirals from one set of parameters to the next, it is necessary obviously to find a basis of comparison. After viewing many feet of film, the following quantities were chosen: (1) v_r: the average of the rate of change of the radius of the largest loop of the fourth and sixth frames of a spiral instability. The zero frame is defined to be the most <u>unperturbed</u> frame of the cycle. It was found that most spirals develop between the fourth and sixth frames. For a pinch, v_r is the average rate of change of the radius of a pinch at its smallest point averaged over the four frames before it pinches off. (2) N: For a spiral, N is the average number of loops in the spiral of the fourth and sixth frames. For a pinch, N is the average number of

pinches along the total length of the stream at any instant of time. (3) R is the average of the radius of the largest loop of the fourth and sixth frames for a spiral instability. Its analog for a pinch is relatively meaningless. We did not use the stream speed v_z because it is very dependent on the distance of fall and we cannot make <u>all</u> our measurements at the same z (it takes a stable point of reference to make a measurement). Measurements were not taken on all the cycles. Only the most typical were measured. The results are as follows:

Test	v_r (arbitrary units)	N	R (arbitrary units)	Pinch P Spiral S
1	9	4		P
2A	7 1/2	2		P
2B	10 1/2	2		P
7B	9	3		P
9C	12	2 1/2	37	S
10A	22	2 1/2	41	S
11A	11 1/2	1		P
12B	8	1 1/2	9	S
13A	9 1/2	2 3/4	13 1/2	S
14A	21	3 1/4	50	S
15A	21	3 1/4	31	S
16	12 1/2	2		P
17A	23	3 1/2	46	S
18B	12 1/2	2 +		P
19D	25	4 1/2	36	S
21A	13	2 1/2		P
22B	20	2 1/2	23	S
23A	10	2	13	S
24B	8	2 3/4	15	S
25A	45	4 1/2	75	S
26A	12 1/2	2		P
27A	30	6	65	S
28A	10	3		P
29A	60	5	75	S
30A	--	1		P
31	50	5	60	S
32	6	1		P
33A	--	1		P
34A	16	3 1/2	27	S

In order to systematically review the data, we must first define correlation groups. Clearly, voltage cannot be used to correlate the data. However, the currents resulting from the voltage are distributed over wide ranges. Therefore, to make any sense out of the data, we shall group the tests into five "current groups" which cover the densest regions in "current space." (Tests which are circled belong half way between the <u>two</u> groups in which they appear.)

Group	Current (amps)	Tests
I	60-80	22, 23, 24, 25, 30, (32)
II	180-220	26, 27, 28, 29, 33, 34, (15), (32)
III	250-280	2, 7, 9, 10, 11, 12, 13, 14, 31, (15), (19)
IV	320-340	16, 17, 18, (19)
V	370-415	1, 21

Using these current groups, we can now arrange our results in terms of the following correlation groups:
A_i -- vary B_o, B_i -- vary I_o, C_i -- vary v_o, D_i -- vary R_o.

Group	I_o	$2R_o$	B_o	v_o	Tests
A_1	III	6	0, 4, 8	45	2, 9, 10
A_2	III,(II)	5	0, 5, 10, 15, (25)	100	11, 12, 13, 14, (15)
A_3	IV,(III)	5	0, 10, (20)	100	16,17,(19)
A_4	I	5	15, 30	100	22, 23
A_5	II	5	(0), 15	(80),100	(33), 34
A_6	II	3	0, 10, 20	120	26, 27, 29
A_7	I	3	(0), 10, 25	(85),120	(30),24,25
B_1	III,V	6	0	45	2, 1
B_2	V, IV, III, (II)	5	0	100,(80)	21, 16, 11, (33)
B_3	IV, (IV and III), III, II	5	15	100	(17 and 19), 14, 34
B_4	(II),(II and I),I	3	0	(120),85	(26), (32), 30
C_1	III	6	0	45, 40	2, 7
C_2	IV	5	0	100, 85	16, 18
C_3	II	3	0	120, 90	26, 28
D_1	V	6, 5	0	(45),(100)	(1), (21)
D_2	III	6, 5	0	(45),(100)	(2), (11)
D_3	III	6, 5, 3	10	(45),(100), (120)	(10), (13), (31)
D_4	II	3, 5	0	(120), (80)	(26), (33)
D_5	II	5, 3	15	(100),(120)	(34), (27 and 29)
D_6	I	5, 3	(15),(10)	(100),(120)	(22), (24)
D_7	I	5, 3	(30),(25)	(100),(120)	(23), (25)

In the table, order has been preserved horizontally and symbolically. These are the only possible group correlations. Parentheses refer to elements which strictly do not belong to the group, but probably will give some positive indication of a trend. Note that the D_i groups really have no v_o correlation because we could not control v_o. The above groups will be discussed by systematically considering: (1) the films, (2) the Sanborn recorder oscillograms, and (3) the summary chart of the tests given on page

Results

(1) There is no correlation between tests run with B = 0 and B greater than zero except that pinches often form along the spiral instabilities. Such a correlation would be attained by letting B approach zero in small steps.

(2) Define $I_{av}/I_{max} = \delta$, a measure of the average relative time the current flows during a test. We will then correlate the data by plotting the dependence of changes in B_o or v_o or I_o or R_o in terms of δ, I_{av}, ν, osc, C, S, v_r (pinch or spiral), N(pinch or spiral), and R. We shall also judge each correlation as to whether we feel the relative numbers fit the over-all physical phenomena (+++ good, ++ fair, + poor).

B_o Dependence -- Group A:

Test	Subgroup	B_o	δ	I_{max}	ν	Osc	C	S	T_1	v_r	N	R
9	A_1	8	.24	250	100	--	.04	.23	17	22	2 1/2	41
10	(++)	4	.33	270	80	--	.04	.2	13	12	2 1/2	37
(15)	A_2	(25)	.05	265	100	.8	.08	.13	16	21	3 1/4	31
14	(+++)	15	.1	270	100	1.5	.06	.2	16	21	3 1/4	50
13		10	.25	265	60	1.1	.08	.2	16	9 1/2	2 3/4	13 1/2
12		5	.5	275	30	.6	.08	.25	16	8	1 1/2	9
(19)	A_3	(20)	.1	300	60	1.1	--	--	16	25	4 1/2	36
17	(+++)	10	.5	340	120	.6	.06	.25	16	23	3 1/2	46
23	A_4	30	.25	77	40	--	.1	.25	16	10	2	13
22	(+)	15	.5	84	15	.8	.1	.25	--	20	2 1/2	23
34	A_5	15		No correlation								
(33)		0										
29	A_6	20	.15	182	0	--	.1	.1	16	60	5	75
27	(++)	10	.2	190	10	--	.1	.1	16	30	5	65
25	A_7	25	.16	62	0	--	.08	.08	18	45	4 1/2	75
24	(+++)	10	.5	66	15	.8	.08	.25	25	8	2 3/4	15

I_o Dependence -- Group B:

Test	Subgroup	I_o	δ	I_{max}	ν	Osc	C	S	T_1	v_r	N	R
1	B_1	V	.85	370	--	--	.04	.17	--	9	4	--
2	(+++) (pinch)	III	.90	290	--	--	.02	.05	--	9	2	--
21	B_2	V	.9	415	--	--	0	.17	--	13	2 1/2	--
16	(+++)	IV	1.	340	--	--	0	.025	--	12 1/2	1 1/2	--
11	pinch	III	1.	270	--	--	0	0	--	11 1/2	1	--
33		(II)	1.	170	--	--	0	0	--	--	1	--
(17 and 19)	B_3	IV and (IV and III)	(.3)	(320)	(90)	(.8)	(.06)	(.25)	16	(24)	(4)	(41)
14	(+)	III	.11	270	100	1.5	.06	.2	16	21	3 1/4	50
34	(spiral)	II	.45	170	40	--	.08	.42	--	16	3 1/2	27
26	B_4	II	.95	190	--	--	0	.17	--	12 1/2	2	--
32	(+++)	II and I	1.0	130	--	--	0	.017	--	6	1	--
30	pinch	I	1.0	65	--	--	0	0	--	--	1	--

Speed v_o Dependence -- C Group:

Test	Subgroup	v_o	δ	I_{max}	ν	Osc	C	S	T_1	v_r	N	R
2	C_1	45	.9	290	--	--	.02	.05	--	9	3	--
7	(+++) (pinch)	40	--	260	--	--	--	--	--	9	3	--
16	C_2	100	1	340	--	--	0	.025	--	12 1/2	2	--
18	(+++) (pinch)	85	1	325	--	--	.02	.2	--	12 1/2	2+	--
26	C_3	120	1	190	--	--	0	.17	--	12 1/2	2	--
28	(+++)	90	.8	184	--	--	.06	.2	--	10	3	--

Stream Radius R_o Dependence -- D Group:

Test	Subgroup	$2R_o$	v_o	δ	I_{max}	ν	Osc	C	S	T_1	v_r	N	R
1	D_1	6	45	.9	370	--	--	.04	.017	--	9	4	--
21	(+++) (pinch)	5	100	.9	415	--	--	0	.17	--	13	2 1/2	--
2	D_2	6	45	.9	290	--	--	.02	.05	--	9	3	--
11	(+++) (pinch)	5	100	1	270	--	--	0	0	--	11 1/2	1	--
10	D_3	6	45	.24	250	100	--	.04	.23	17	22	2 1/2	37
13	(+++)	5	100	.25	265	60	1.1	.08	.25	16	9 1/2	2 3/4	13 1/2
31	(spiral)	3	120	.07	270	10	1.0	.12	.12	16	50	5	60
33	D_4	5	80	1	170	--	--	0	0	--	--	1	--
26	(+) (pinch)	3	120	1	190	--	--	0	.17	--	12 1/2	2	--
34	D_5	5	100	.45	170	40	--	.08	.42	--	16	3 1/2	27
27 and 29	(++) (spiral)	3	120	--	186	--	--	.1	.1	--	60	5 1/2	70
22	D_6	5	100	.5	84	15	--	.1	.25	16	20	2 1/2	23
24	(+) (spiral)	3	120	.5	66	15	.8	.08	.25	15	8	2 3/4	15
23	D_7	5	100	.26	77	10	.8	.1	.25	--	10	2	13
25	(++) (spiral)	3	120	.16	62	--	--	.08	.08	18	45	4 1/2	75

Group A Generalizations:

(1) As the magnetic field increases the relative time average of the current decreases. Also the number of secondary peaks decreases, indicating a more violent, but very fast interaction. For the very highest fields (as in test 29) the current output looks like the output of a "noiseless" pulse generator. (2) As B_o increases, the I_{max} decreases, for a given voltage and radius. For higher B_o, we have a more violent spiralling; therefore the stream which makes contact with the copper electrodes is thinner, resulting in an average decrease in current. (3) There appears to be no correlation between ν and B_o (for half the tests ν increases and for half the tests ν decreases, as B increases). (4) A small amount of evidence indicates that Osc increases almost linearly with magnetic field. (5) T_1 usually is approximately 16, but for those cases where it appears to change, the cycles become larger as B_o increases. This is due to the fact for large B_o, small perturbations are amplified quickly and often to sustain a cycle. (6) The rate of change of spiral radius v_r very definitely increases as B_o increases as does also the average spiral radius R. (7) The number of loops in the spiral also very definitely increases as B_o increases. The force for higher fields is so great that the mercury travels almost horizontally, thus allowing many more loops to form within a given space.

Group B Generalizations:

(1) As I_o increases, the relative time average of the current decreases very slightly. (2) There is a slight indication that ν increases as I_o increases. (3) For $B_o = 0$, there are more peaks and more cut-offs as I_o increases, i.e., for high currents, the pinch has time to pinch off where even the smallest perturbations occur, perturbations which the lower currents do not have time to pinch. A detailed study of this could be made if we were able to induce known perturbations. From our $B_o = I_o = 0$ photographs we can say, though, that the initial perturbations are smaller than the eye can detect. For $B_o > 0$ apparently the trend reverses, i.e., the number of peaks decreases as I_o increases (though this conclusion is borne out by "poor" evidence). (4) For $B_o = 0$, the pinches pinch faster and there are more of them along the stream, i.e., even the smaller initial perturbations are amplified at the higher currents. For $B_o > 0$ the spiral radius, the number of loops, and v_r all increase as I_o increases.

Group C Generalizations:

(1) As v_o increases the I_{max} increases because the faster stream makes better contact with the lower reservoir. (2) As v_o increases C decreases and S decreases. E.g., in C_2 we have a real cut-off in S; in going from $v_o = 85$ to 100, S goes from .2 to .025, i.e., the pinch time for most of the

perturbations on the 5 mm stream is greater than .042 sec and less than .046 sec, the order of magnitude of our theoretical prediction. (3) As v_o increases, v_r of a pinch increases slightly -- an important assumption in our theory is then borne out. (4) As v_o increases the average number of pinches along the stream decreases.

Unfortunately we do not have any elements of group C with $B_o > 0$.

Group D Generalizations:

Because we had no control over the accessible ranges of v_o for the various stream radii, we note that our correlations for R_o dependence also depend upon a speed v_o correlation. We must therefore consider the correlation operator X defined as R_o increasing and v_o decreasing. The results of D have meaning only for X rather than R_o or v_o. The results of group C will be needed to find any R_o dependence. (1) For X and $B_o = 0$, C increases and S decreases indicating that pinches are taken more to completion for X. Since as v_o decreases, S increases (from group C) then as R_o increases, S decreases, a fact which probably just describes the geometry of our system (i.e., the smoothness of outlet nozzles, etc.). For $B_o > 0$, for X, S increases and we can say nothing about R_o. (2) We have insufficient data to discuss the effect of X on pinching. For $B_o > 0$, for X, v_r decreases, N decreases, and R decreases. From this most probably, as R_o increases,

v_r, N, and R decrease, i.e., a thinner stream spirals more violently, other conditions being equal.

Of course, the above generalizations are no better than our sampling of the data -- data which depend very much on unknown initial conditions. Certainly, though, we have noted definite trends, and obvious experiments suggest themselves to more thoroughly support them. A more analytical comparison may be interesting, but not justified from the nature of the tabulated data. When an accurately synchronized apparatus with a mechanically flexible design (so that we can vary v_o and I_o) is built, then a more detailed study may be justified. Also, in the same spirit we cannot possibly expect to correlate our data analytically with our theoretical results. However, our group correlations yield qualitatively the identical results that we predicted earlier.

In experimenting to find the best lighting, type of film, etc., we took many random single pictures. Those that lead to new or interesting comparative results will be presented here.

E_5

E_6

F

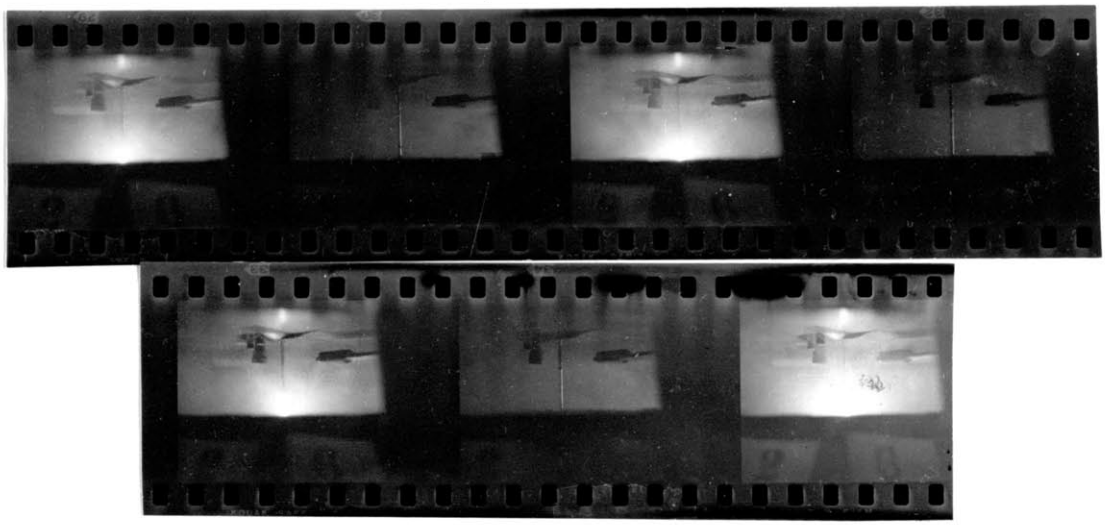

H

M_1

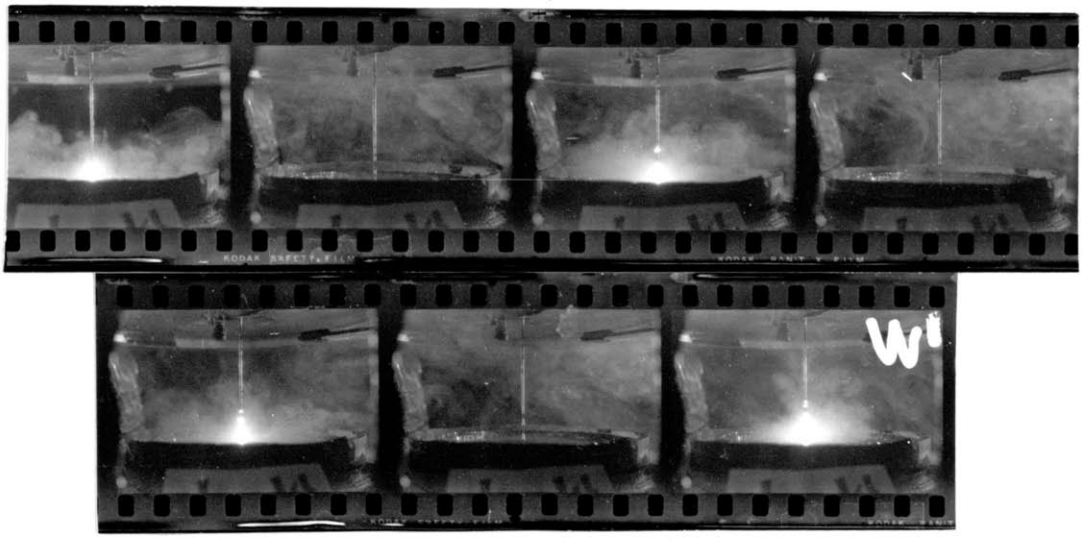

N_1

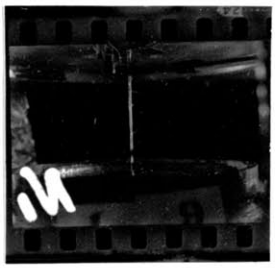

N_2

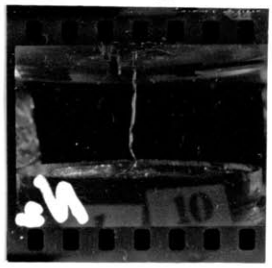

N_3

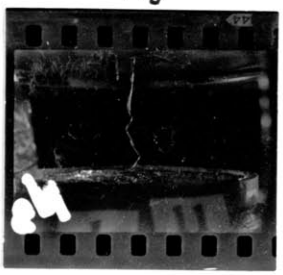

N_4

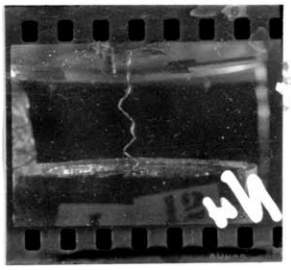

O

P

E_5 and E_6 are good pictures of spirals after breaking into droplets (R_o = 3 mm, h_o = 4 in., $B_o = 8^a$-12^a, $I_o \approx 160^a$).

F is a series of frames showing sparks rising on the stream as the speed v_o decreases. Each frame represents $\sim$5 sec. The alternate frames are $I_o = B_o = 0$. This series of shots hints very strongly that the pinch time is <u>not</u> random, but depends very strongly on the initial perturbation (the pinch rises <u>linearly</u> as v_o decreases linearly). Therefore, experiments done by inducing <u>known</u> perturbations and measuring the effects may yield a great deal of information. (F: B = 0, V = 8 volts, R_o = 5 mm, h_o = 6 in.)

H is a spiral for R_o = 3 mm, V = 6 volts, $B_o = 4^a$, h_o = 6 in.

M_1 is a series of 5 sec apart frames showing sparks rising as v_o decreases for R_o = 3 mm, V = 6 volts, h_o = 6 in., B_o = 0. The dense cloud is mercury vapor resulting from the heat of the spark. We note that the alternate pictures with $I_o = B_o = 0$ show nice pinches due <u>just</u> to surface tension. It is for this reason that measurements were not taken at h_o = 6 in. -- because the effects of surface tension and the current-field interactions cannot be separated.

N is a series of four photographs at h_o = 6 in., V = 2 volts, R_o = 6 mm, N_1 at B_o = 0, N_2 at $B_o = 4^a$, N_3 at $B_o = 8^a$, N_4 at $B_o = 16^a$. Qualitatively this series is in agreement with our previous discussion for B_o dependence.

O shows the line-up of the stream with the direction of magnetic field (the edge of the tape) to within 2^{o}.

P is the 3 mm stream, V = 2 volts, $B_o = 0$, $h_o = 6$ in., exhibiting a pinch.

Clearly, the above series of pictures exhibit qualitatively the same characteristics (where applicable) as in our previous discussion. Clearly, changing h_o to 6 in. does not change qualitatively the results, except that surface tension then plays a greater role.

Having discussed the main body of our data, let us look now at several relatively minor questions which may be of interest to an over-all interpretation of the experiment.

Does a large majority of the spirals always begin in the same direction? No. If they <u>did</u>, the spiral instability might be strongly a function of our geometry.

Tests were run reversing the direction of the magnetic field and/or reversing the current direction. Qualitatively, no difference was noted.

What are the limits on V and B_o such that the stream is stable? From our charts we can see that the 3 mm stream has no pinches for $I_o < 70$ to 100 amps and the 5 mm stream for $I_o < 200$-240 amps. Correcting for the differences in v_o we see that the cut-off current goes approximately as the area of the stream. (If v_o of the 3 mm stream equals 120 cm/sec and v_o of the 5 mm stream equals 100 cm/sec, then

$$\left.\frac{I_o(3)}{I_o(5)}\right|_{\substack{\text{lower limit}\\ \text{for pinching}}} = \frac{85 \cdot 120}{220 \cdot 100} = .47$$

The ratio of the areas is .50.) This relationship may be accidental; we certainly do not have conclusive evidence. Of course, more experimental work should be done on this point. Clearly the value of the current below which there are no pinches is velocity dependent, i.e., if one waits long enough, pinches will probably form <u>for all</u> currents (even if there is no surface tension). The apparatus broke before we were able to test the lower limit of B_o for instability.

It is found that for most pinches, the mercury arcs when the pinch gets to a very small radius. We can explain this on the grounds of two phenomena: (1) We calculated theoretically that the mercury at the narrowest point of a pinch should heat to thousands of degrees C. This is sufficient to vaporize the mercury and create thermal electrons. (2) The self-inductance of the circuit is approximately given by $L = \ell 2\mu_o \ln d/a$ (where we are using rationalized mks units), d is the average separation of the wire, a is the radius of the wire, and ℓ is the length of the wire. $L \simeq .3\ 10^{-4}$ henries ($d \simeq 6$ in., $a \simeq 1/4$ in., $\ell \simeq 20$ meters).

$\frac{dI}{dt} \geq 1.2\ 10^5$ amps/sec (using the test No. 1 oscillogram).

Therefore, $V \geq 4$ volts, i.e., the added voltage must take us

over the first excitation potential of mercury, 13.6 volts. The high electric fields cause a cascade of the thermal electrons formed from the heating, the whole process resulting in a cascade of photons, i.e., the spark. The spectrum of the spark was recorded and found to have the normal mercury spectral lines 4047, 4078, 4358, 4916, 5461, 5770, and 5790 Å. In addition, two relatively weak (but as yet unidentified) lines were found at 4960 and 5360 . (They are not in the air spectrum or mercury spectrum.)

The arcing resulting from the pinch causes great difficulty in photographing the stream because the cloud of mercury vapor hides the stream. A capacitor across the stream was considered, but to have any effect, it must be $\approx$ .1 farad. Possibly by rewiring the circuit (and decreasing the inductance) we can eliminate a great deal of the arcing.

As we stated earlier, the present work is to investigate the instability phenomena in such a way as to understand the physical mechanisms involved in order to suggest further detailed work. For the experiments done and presented in this paper we did <u>not</u> have <u>enough</u> mechanical control of the variables v_o, I_o, and the initial perturbations to conduct meaningful functional dependence experiments; we had <u>too many</u> mechanical operations for recording the data. We therefore suggest the following improvements and new experiments in order to understand the instabilities in a more detailed

manner. We should, of course, keep these suggestions in mind in the light of our data and previous discussion. (1) We should change the external resistance R (which includes the resistance of the batteries and line) to see how this influences the current vs time plot. In particular, we should let R be large enough so that I_o stays constant (i.e., we eliminate our periodicity of the major peaks phenomenon) and we should be able to vary R so that we can adjust I_o, i.e., so that we can obtain a definite current dependence of the instabilities. (We now know what voltages correspond to a given I_{max}.) (2) It would be advantageous to have control over v_o by using a pressure device in reservoir A to either keep v_o at a constant value over a test or to let v_o vary continuously over a wider range than we had in our experiment. (3) It is vital that the Sanborn recorder be correlated with the film by either turning the current on in the middle of the film and/or correlating a flash on the camera lens with a spark burning a hole in the recorder paper (no mechanical parts!). Also, the Sanborn recorder should be redesigned to run faster to spread out the peaks in order to study in detail the time dependence of I_o. (4) The voltage across the stream should also be recorded. This will give us some indication about the sparking and also will allow us to plot the conductivity of the stream as a function of time. Probably the variations of the conductivity of the mercury in the vicinity of a pinch

are very interesting. (5) The upper limit of the B_o and I_o for stability should be found as a function of R_o and v_o. (6) Many extensive experiments can be done by varying the height h_o and the radius R_o (say from 10 mm down to 1 mm). (7) A more homogeneous magnet should be found. Even though 2% is fairly homogeneous, it could be much better. Then we could show conclusively that the instabilities arise from our other considerations and are not due just to an inhomogeneous field. (8) Experiments should be done on elliptical, annular, and rectangular streams. These could be related to our bifurcation phenomenon, in an attempt to better understand it. We should also test <u>two</u> streams of mercury falling parallel to each other. (9) In order to understand the role the initial perturbation plays, we could induce perturbations -- by oscillating the nozzle (which would give MHD waves on the surface of the mercury), by varying the angle between $\vec{B}_o$ and the flow, by letting the mercury rotate, by letting the mercury run over a small wedge as it falls, by having an external low amplitude oscillating field B_x, or by heating the mercury locally for a very short time with a carbon arc -- and then measuring the functional dependences of the resulting disturbances. (10) We can extend our work to exploding wires and in particular exploding wires in an external magnetic field (a problem which has not as yet been investigated). A fundamental understanding of the above problems will probably lead to a fundamental understanding of magnetohydrodynamics.

From the results of the experiment there can be no doubt that a mercury stream with current and in an external magnetic field along the direction of flow is unstable both with respect to its diameter (the pinch) and to its direction along the direction of the magnetic field (the spiral). We have seen, recorded, and are able to reproduce the instabilities. We have presented charts showing approximate relative magnitudes of the instabilities and have made generalizations upon these charts. In general, we found that the instabilities depend very strongly and nonlinearly on the current and magnetic field (spirals and pinches growing faster and being more numerous for the higher fields and currents). We have a first order theory which predicts qualitatively the phenomena we have observed: the symmetrical pinch, the side pinch, the spiral instability, and the new bifurcation instability. Our qualitative results agree with Lehnert's.[1] On the basis of our results we have been able to suggest improvements and new experiments which should lead to a more detailed and fundamental understanding of magnetohydrodynamic instabilities.

Acknowledgment

A major portion of the satisfaction one receives from doing a thesis results from the friendships and acquaintanceships one develops in the process. The objective research certainly could never have been completed without the subjective guidance and inspiration of a great number of people.

Many people went a great deal out of their way in helping in some phase of the work. To say "thank you" sincerely and meaningfully is always difficult to express on paper. Let this be my feeble attempt to express my sincerest appreciation:

To Larry and Bill Ryan (R.L.E. glass blowing); John Keefe, John, Chuck, Paul, ... (R.L.E. Shop); Ben Divers (R.L.E. photography); Steve (Spectroscopy Lab); "Beans" and Bill Mosher (Magnet Lab); and Miss Hill, Ann, and Patience in the Graduate Physics Office.

Also, to Professor Bitter and Professor Stroke for the loan of their magnet and lab; Professor Bradley whose advice and help in the optics and photography were invaluable; and Professor Edgerton whose advice and equipment helped us to find the appropriate photographic techniques.

To Miss Carolyn Shang Ed Martens, Ray Lewis, Al Ferry, and Dave Weitzler, who unselfishly spent many hours helping to collect and tabulate the data.

To Professor Ingard who, as my thesis advisor, has contributed a great portion of his time and energy the past year. For his invaluable technical experience, guidance, and help in the experimental work, and for his creative thought and inspiration in the theoretical work, I express my deepest appreciation.

Bibliography

1. Lehnert, B and Sjorögren, G., "A Liquid Conductor Model of the Hollow Pinch," Journal of Nuclear Energy: Part C, Vol. 1, No. 3, March 1960.

2. Hering, Carl, "A Practical Limitation of Resistance Furnaces, the Pinch Phenomenon," Trans. of American Electrochem. Society, Vol. XI, p. 329, 1907.

3. Northrup, E. E., "Some Newly Observed Manifestations of Forces in the Interior of an Electric Conductor," Physical Review, Vol. XXIV, No. 6, p. 474, 1907.

4. Longmire, C. L. and Rosenbluth, M., "Stability of Plasmas Confined by Magnetic Fields," Annals of Physics, 1, 120 (1957).

   and

   Karr, Hugh J., "The Plasma in a Magnetic Field," p. 40, edited by Rolf K. Landshoff, Stanford University Press, Stanford, California, 1958.

5. Chace, William G., "A Bibliography of the Electrically Exploded Wire Phenomenon," GRD Research Notes, No. 2, November 1958.

6. Alfven, Hannes, "Cosmical Electrodynamics," Oxford, Clarendon Press, 1950.

   and

   Alfven, Hannes, "On the Origin of the Solar System," Oxford, Clarendon Press, 1954.